

*Republic of Iraq  
Ministry of Higher Education  
And Scientific Research  
Kerbala University  
Collage of Engineering  
Department of mechanical engineering*



# *Study The Effect of (Gas-Solid) Fluidized Flow on Heat Pipe Performance*

*A Thesis  
Submitted to the  
Mechanical Engineering Department  
of the University of Kerbala in a Partial Fulfillment of  
the Requirements for the Degree of Master of Science in  
Mechanical Engineering*

*By*

*Taher Habeeb Hussein Al-Kharasani*

*(BSc. Mechanical Eng. 1997)*

*Supervisors*

*Assist. Prof. Dr. Mohammed Wahhab AL-Jibory*

*Assist. Prof. Dr. Hafidh Hassan Mohammed Al-Ghazali*

بِسْمِ اللَّهِ الرَّحْمَنِ الرَّحِيمِ

قَالُوا سُبْحَانَكَ لَا عِلْمَ لَنَا إِلَّا مَا

عَلَّمْتَنَا إِنَّكَ

أَنْتَ الْعَلِيمُ الْحَكِيمُ

صدق الله العلي العظيم

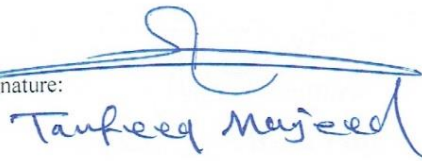
سورة البقرة (الآية ٣٢)

## *Linguistic Certification*

---

I certify that this thesis entitled "**Study the effect of(Gas-Solid) fluidize flow on heat pipe performance** " was prepared by (**Taher Habeeb Hussein**) under my linguistic supervision. Its language was amended to meet the English style.

Signature:



Taufeeq Majeed

Name:

Title: Linguistic Supervisor

Collage of education for human sciences

University of Karbala

Date: / /2019

## *Supervisors Certification*

We certify that this dissertation entitled "**Study The Effect of (Gas-Particle) Fluidized Flow on Heat Pipe Performance**" was prepared by engineer (**Taher Habeeb Hussein**) and had been carried out completely under my supervision at the University of Kerbala, Mechanical Engineering Department in partial fulfillment of the requirements for the degree of Master Science in Mechanical Engineering.



*Signature:*

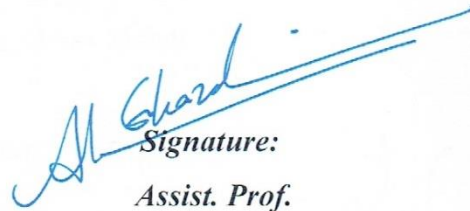
*Assist. Prof.*

**Dr. Mohammed Wahhab AL-Jibory**

*Mech. Eng. Dept.*

*University of kerbala*

*Date: / /2019*



*Signature:*

*Assist. Prof.*

**Dr. Hafidh.H.Mohammed Al-Ghazali**

*Mech. Eng. Dept.*

*University of Kufa*

*Date: 13/2/2019*

## EXAMINING COMMITTEE CERTIFICATION

We certify that we have read this thesis entitled "**Study The Effect of (Gas-Solid) Fluidized Flow On Heat Pipe Performance**" and as an examining committee examined the student (**Taher Habeeb Hussein Al-Kharasani**) in its content and that in our opinion it meets the standard of a thesis and is adequate for the award of the Degree of *Master of Science in Mechanical Engineering*.

Signature: 

Name: Assist. Prof. Dr  
Mohammed Wahhab Aljibory

Date: / / 2019

(Supervisor)

Signature: 

Name: Assist Prof. Dr. Hafidh  
Hassan Mohammed Al-Ghazali

Date: 13 / 2 / 2019

(Supervisor)

Signature: 

Name: Prof. Dr. Alaa Abbas Mahdi

Date: 13 / 2 / 2019

(Chairman)

Signature: 

Name : Assist. Prof. Dr Mohammed  
Idrees Mohsin

Date: / / 2019

(Member)

Signature: 

Name: Assist Prof. Dr. Mohammed  
Hasan Abbood

Date: 13 / 2 / 2019

(Member)

Approval of deanery of the College of  
Engineering / University of Kerbala

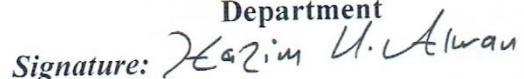
Signature: 

Name: Assist. Prof. Dr. Laith Shakir Rasheed

(Acting Dean of the College of Engineering)

Date: 13 / 2 / 2019

Approval of Mechanical Engineering  
Department

Signature: 

Name: Lect. Dr. Hazim Umran Alwan

(Head of mechanical engineering  
department)

Date: 13 / 2 / 2019

## *Dedication*

---

*To my dear father*

*The symbol of affection*

*To my dear mother*

*The symbol of sincerity*

*To my friends*

*To everyone I had learned from my life.*

*I dedicate this modest effort*

*Taher*

2019

## *Acknowledgments*

---

Full achievement of any project cannot be achieved without thanking those who made it possible. First and foremost, I thank Allah for where I am and for giving me the strength to keep going.

I would like to express my deep thanks and sincere gratitude to my supervisors **Assist. Prof. Dr. Mohammed Wahab AL-Jibory** and **Assist. Prof. Dr. Hafidh Hassan Al-Ghazali** for their assistance, guidance, encouragement and endless help throughout the steps of this work.

I am grateful to my cousin **Assist. Prof. Dr. Tawfeeq Majeed Al-Kharasani** for the help he gave me during my studies.

My sincere thanks also go to my friends **Abad Al-Ameer** and **Anwer.f.faraj** at the Iraqi Drilling Company who encouraged me to complete my studies

I sincerely thank all the staff of the Mechanical Engineering Department of the University of Kerbela and kufa for their support and teaching.

I am also thankful to all who helped me directly or indirectly to complete this work.

## ***ABSTRACT***

This work presents an experimental and numerical study to investigate enhancement the heat transfer values to heat pipe by using fluidize bed. Using cement fly ash as a fluidize material that was heated to simulate cement factory chimney, the air interred to manufacturing model and heated by electrical heater. Air interring with superficial velocity (0.8739,1.1236, and 1.377) m/s. The cement fly ash particle putting in air flows way at evaporator part with different height (2.5,5,7.5and10) cm.

The experimental system (test rig) which includes: flowmeters, thermocouples, U-tube manometer, valves, heat pipes, wooden box, connected airlines, and cyclone, was fabricated to calculate enhancement in heat pipes heat gain. Manufacturing three wick heat pipes was the first step the outer and inner pipe diameter was (22.25 and 19.80) mm respectively, five stainless steel layers fixed inside each pipe. Distilled water was used as working fluid with amount (65.5) ml, and all heat pipes was arranging horizontally in test rig.

All the tests were carried out with a Reynolds number range ( $Re = 2400 - 318728$ ) and uniform inlet velocity conditions, the experimental study also includes preparation of particles and measurement its properties such as density, thermal conductivity, and particles diameter. The flow rate, domain and heat pipes surface temperature and pressure drop, were measured.

ANSYS FLUENT bundle-(18) soft program was used to solve the governing differential equations in two and three dimensions to study the effect and focus on heat transfer improvement and particles behavior inside domain.



This study found that The maximum Nusselt number was (35.2) which is occurred at ( $Re = 318728$ ), increasing Reynolds number from (2400 to 318728) gives increased in heat gain at heat pipes evaporator part by (72.5) %, also the results show that increase solid particle degreased porosity by (9%),also Increasing superficial velocity for (0.8739 to 1.337) m/s increased the heat gained at evaporator part to (21) % , The comparison between the experimental and numerical (Nusselt number) shows acceptable agreement, and the maximum and minimum differences were  $\pm(18.6, 4)$  % respectively.

## Table of Content

Subject	Page
Abstract.....	I
Contents .....	III
Nomenclature .....	IX
<b>Chapter One-Introduction .....</b>	<b>1-11</b>
1.1 Overview .....	1
1-2 Effective parameter on heat transfer in heat pipe.....	3
1- 3Heat pipe components .....	4
1-3-1 Container .....	4
1-3-2 Wick .....	5
1-3-3 Working fluid.....	5
1- 4Fluidization .....	7
1.5 Fluidization Phenomenon.....	7
1.6 Particle Size .....	9
1.7 Pressure drop in fluidized bed .....	9
1.8 Particle influent in heat exchanger .....	10
1-9 The aim of present study.....	11
<b>Chapter Two – Literature review.....</b>	<b>12-28</b>
2.1 Theoretical Studies .....	12
2.2 Experimental Studies .....	15
2.3 Experimental and Theoretical Studies .....	21
2.4. The scope of This Work .....	23
2.5. Summery.....	24
<b>Chapter Three –Mathematical Model and numerical analysis.....</b>	<b>29-50</b>
Mathematical Model and numerical analysis .....	29

3.1 basic design of heat pipe.....	29
3.2 Particle motion model.....	30
3.3 Effective thermal conductivity.....	31
3.4 Modal and correlation.....	31
3.5 Gas-Solid Separator.....	32
3.6 Basic Calculation.....	35
3.6.1 Rate of heat transfer.....	35
3.6.2 Mixture specific heat.....	35
3.6.3 Heat transfer coefficient.....	35
3.6.4 Nusselt Number.....	36
3.6.5 Reynolds Number.....	36
<b>Numerical Method.....</b>	<b>36</b>
3.7 Problem Assumption.....	37
3.8 Simulation Models .....	38
3.8.1 Governing Equation.....	38
1-Continuity equation.....	39
2-Momentum equation.....	39
3- Energy Equation.....	40
4-Turbulence Model.....	40
3.9 Geometry Model.....	41
3.9.1 The Geometry.....	43
3.10 The mesh.....	44
3.11 Boundary Conditions.....	46
3.12 Under Relaxation Factor.....	48
3.13 Steps To Simulation model .....	48
3.14 Demonstrating the Results.....	50

<b>Chapter four – Experimental Work.....</b>	<b>51-77</b>
4.1 fabricated rig body and the main component .....	51
4.1.1 Main box body.....	54
4.1.2 Distributed plate.....	55
4.1.3 Heating source.....	56
4.1.4 Connected line.....	56
4.1.5 Air supply source.....	57
4.1.6 Particle separator device (cyclone).....	58
4.2 Heat pipe design and manufacture.....	58
4.2.1 Heat pipe structure.....	58
4.2.2 The wick .....	61
4.2.3 Working fluid.....	62
4.2.4 cleaning Heat pipe before charging.....	63
4.2.5 Heat pipe evacuated and charging with working fluid.....	64
4.2.6 Heat pipe limitation.....	65
4.3 Heat pipe tested.....	65
4.4 Choosing particle and its properties.....	67
4.4.1 Particle density.....	67
4.4.2 Thermal conductivity.....	67
4.4.3 Particle diameter.....	68
4.5 Instrument device and calibration.....	70
4.5.1 Air flow measurement.....	70
4.5.2 Pressure drop measurement.....	70
4.5.3 Temperatures recorder.....	71
4.5.4 Thermocouples.....	72
4.6 The error analysis.....	72

4.7 experimental procedure.....	72
4.7.1 Calculation procedure.....	74
1-heat pipe surface area.....	75
2-Air flow rate.....	75
3- Particle porosity $\epsilon$ .....	75
4- Equivalent density of (gas- particle) mixture.....	75
5- Specific Heat of (gas- particle) mixture.....	75
6- Superficial velocity $U_{sup}$ .....	76
7- Effective Thermal Conductivity.....	76
8- heat gain.....	76
9- Heat Transfer Coefficient.....	76
10- Nusselt Number.....	77
11-Reynolds Number.....	77
12- heat transfer to condenser part.....	77
<b>Chapter Five – Results and discussion .....</b>	<b>78-114</b>
5.1 Experimental Conditions.....	78
5.2 Experimental Results.....	79
5.2.1 Evaporator temperature distribution .....	79
5.2.2 The Influence of heat pipes locations.....	79
5.2.3 Influence of particle bed thickness.....	80
5.2.4 porosity variation.....	82
5.2.5 Influence of Air velocity.....	83
5.2.6 pressure drop.....	85
5.2.7 influence of particle bed on heat transfer coefficient.....	86
5.2.8 Nusselt Number. variation with Reynolds Numbers.....	88
5.3 Numerical condition .....	89

5.3.1 Program Validation .....	89
5.3.2 The Influence of heat pipe location.....	90
5.3.3 Influence of particle bed thickness.....	93
5.3.4 pressure drop.....	95
5.3.5 porosity.....	95
5.3.6 Influence of Air velocity.....	97
5.3.7 heat pipe surface temperature.....	100
5.3.8 heat distributed inside condensers part.....	101
5.3.9 Influence of particle bed on heat transfer coefficient.....	104
5.3.10 Nusselt number variation with Reynolds Numbers.....	105
5.4 comparison between experimental and numerical results.....	107
5.4.1 comparison of heat pipe location.....	107
5.4.2 Influence of particle bed thickness.....	109
5.4.3 pressure drop comparison.....	109
5.4.4 porosity comparison.....	110
5.4.5compression of superficial velocity effect.....	112
5.4.6 compression of heat transfer coefficient.....	113
5.4.7 compression experiential and numerical Nusselt number.....	114
<b>Chapter six – Conclusions and Recommendation.....</b>	<b>116-117</b>
6.1 Conclusions.....	116
6.2 Recommendations.....	117
References.....	118-125
Appendix A .....	A1-A8
Appendix B .....	B1-B4
Appendix C .....	C1-C2
Appendix D.....	D1-D2

## NOMENCLATURE

SYMBOL	DESCRIPTION	UNITS
$A$	Surface area of the tube	$m^2$
$A_{hpev}$	Heat pipe surface area at evaporator part	$m^2$
$A_{hpco}$	Heat pipe surface area at condenser part	$m^2$
$A_{ev}$	Cross section area of evaporator air line	$m^2$
$A_{con}$	Cross section area of condenser air line	$m^2$
$A_v$	Cross section area for vapor core inside pipe	$m^2$
$A_{hole}$	Area for one hole in distributed blot	$m^2$
$A_{eva.}$	cross-section area of the box in evaporator part	$m^2$
$C_f$	Specific Heat of (gas- particle) mixture	J/Kg .C
$C_s$	Specific Heat of particle	J/Kg .C
$C_g$	Specific Heat of gas	J/Kg .C
$D_o$	Heat pipe outer diameter	m
$D_w$	Wick wire diameter	m
$d_i$	Heat pipe inner diameter	m
$d_h$	Hydraulic diameter	m
$d_p$	particle diameter	$\mu m$
$d_{pi}$	sieve diameter	mm
$F_{lift,q}$	lift force	N
$f$	Friction factor	---
$G$	Energy	Joule
$G$	Acceleration of the ground	$m/s^2$
$H$	Box height	m
$h_{pq}$	Interphase enthalpy	J/kg.C
$h_q$	Specific enthalpy of the q phase,	J/kg.C
$h_m$	Height different in water manometer	m

$h$	Heat transfer coefficient	W/m <sup>2</sup> .C
K	Thermal conductivity	W/m.k
K <sub>es</sub>	conductivity of fixed beds of particles	W/m.k
K <sub>ef</sub>	conductivity due to fluid flow	W/m.k
K <sub>eff</sub>	Effective thermal conductivity	W/m.k
K <sub>p</sub>	Particle thermal conductivity	W/m.k
K <sub>g</sub>	Air thermal conductivity	W/m.k
K <sub>ls</sub>	momentum exchange coefficient between liquid or solid phase	Kg/s.m <sup>3</sup>
K <sub>per</sub>	Permeability	---
L	Length	m
L <sub>b</sub>	Box height	m
L <sub>eff</sub>	Effective heat pipe length	m
L <sub>e</sub>	Evaporator length at heat pipe	m
L <sub>c</sub>	Condenser length at heat pipe	m
L <sub>ad</sub>	Adiabatic length at heat pipe	m
$\dot{m}$	Mass flow rate	kg/s
$\dot{m}_{air\ eva}$	Air flow rate at evaporator part	kg/s
$\dot{m}_{air\ con}$	Air flow rate at condenser part	kg/s
$\dot{m}_{pq}$	Mass transfer from p to q phase	Kg /s
$\dot{m}_{qp}$	Mass transfer from q to p phase	Kg/s
N	Number of hole in eva. distributed blat	---
Q <sub>gain</sub>	Power transferred to evaporator part	Watt
Q <sub>pq</sub>	intensity of heat exchange between q and p phase	Watt
Q <sub>v,max</sub>	Viscous limit	Watt
Q <sub>e,max</sub>	Entrainment limit	Watt
Q <sub>c,max</sub>	Capillary limit	Watt
Q <sub>s, max</sub>	Sonic limit	Watt



$\vec{q}$	Heat flux	Watt
$R_{pq}$	Interaction force between phases	N
$R_{vm}$	virtual mass force	N
$r_w$	Wick heat pipe radius	m
$r_v$	Vapor heat pipe radius	m
$r_c$	effective Capillary radius	m
$s_q$	Source term include source of enthalpy	J/kg.C
$T_{bed}$	Bed temperature	°C
$T_{sc}$	Heat pipe average surface temp.at condenser	°C
$T_{se}$	Heat pipe average surface temp.at evaporator	°C
$T_v$	Vapor core temperature	°C
$U_s$	Superficial velocity	m/s
$U_m$	Minimum air velocity passing through particles	m/s
$U_{mf}$	Minimum air velocity create fluidization	m/s
u, v, w	Velocity component in Cartesian coordinate	m/s
$\vec{v}$	Phase velocity	m/s
$V_m$	Virtual mass	kg
$V_l$	Working fluid Volume	m <sup>3</sup>
$V_w$	Wick volume	m <sup>3</sup>
$x_i$	percentage ratio for particle weight on sieve	---

## Greek Symbols

SYMBOL	DESCRIPTION	UNITS
$\alpha$	Under relaxation factor	---
$\alpha_q$	Volume fraction	---
$\epsilon$	dissipation rate for the turbulent flow	---
$\varepsilon$	Porosity	---
$\varepsilon_p$	Wick porosity inside heat pipe	---
$\theta$	Heat pipe Inclination angle	degree
$\lambda$	Bulk viscosity	kg/m.s
$\mu$	Dynamic viscosity	kg/m.s
$\rho_w$	Water Density	kg/m <sup>3</sup>
$\rho_s$	Solid Density	kg/m <sup>3</sup>
$\rho_g$	Air Density	kg/m <sup>3</sup>
$\rho_c$	Gas-solid mixed density	kg/m <sup>3</sup>
$\rho_f$	Air-particle mixture density	kg/m <sup>3</sup>
$\sigma$	surface tension	N/m
$\tau_q$	Stress strain tensor	N/m <sup>2</sup>
$\Phi_i$	sphercity	---

## Subscripts

SYMBOL	MEANING
a	Air
g	Gas
i	Inlet, inner
o	Outlet
p	Particle
s	Solid

W	Water
subscripts q and p	Primary and secondary phase

### Abbreviation

SYMBOL	DESCRIPTION
ANSYS	Analysis System
CFD	Computational fluid dynamic
FLUENT	Fluid And Heat Transfer Code
H.T.C.	Heat Transfer Coefficient
Nu	Nusselt number
Re	Reynolds number
3D	Three Dimension



# **CHAPTER ONE**

## **INTRODUCTION**

# CHAPTER ONE

## Introduction

### 1.1 Overview

Heat pipe called "super thermal conductors" consists of simple content but it widely used in manufacture devices to dissipate heat from hot components, and can consider it as a kind of heat recovery unit, that leads to fuel monetarism. Since the heat recovery work under severe circumstances (high temp, pollution of gas) that lead to reduce heat pipe efficiency and that evokes researchers to discover new modification to reach a good heat transfer rate with low cost and pollution. The high efficiency of the heat pipe to heat transfer lead researchers to use it in heat recovery and heat dissipation system, figure (1.1) shows the main components of heat pipe [1].

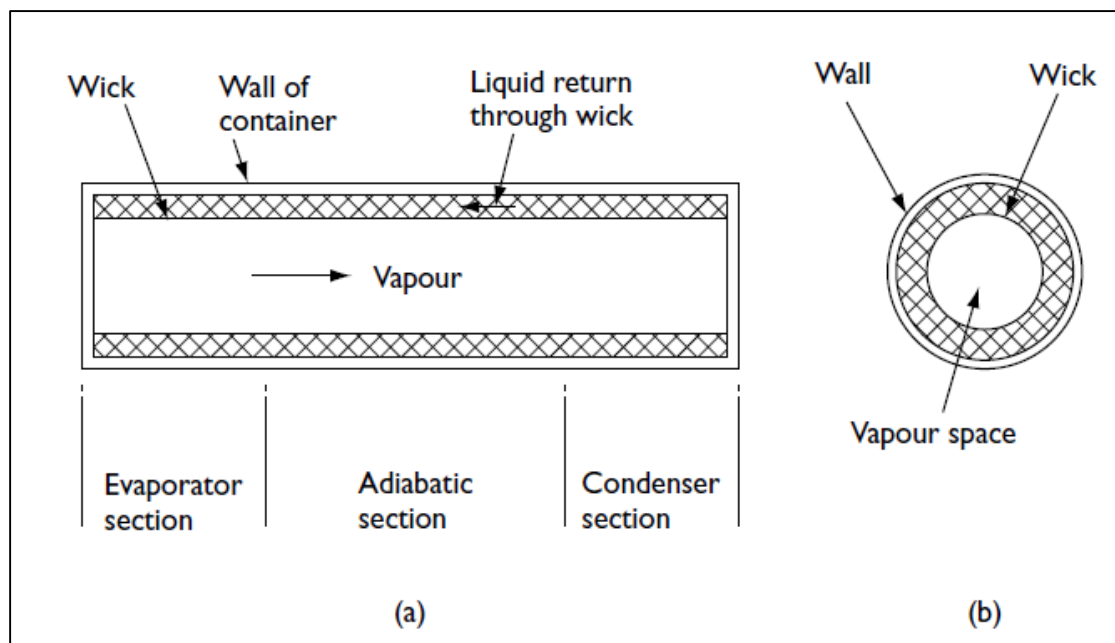


Figure (1.1) main regions and components of heat pipe[2]

Gaugler 1942 discovered the first idea of heat pipes, however, it was not in deal until 1962, when Grove invented it. Thermal siphon and heat pipe work at same principle (evaporating and re-condensing) working fluid, in thermal siphon the working fluid return to evaporator by gravity action; while in heat pipe the condensed working fluid back to evaporator by capillary force during wick. Figure (1.2) shows difference between (wick heat pipe and wickless heat pipe (thermosiphon)) [2].

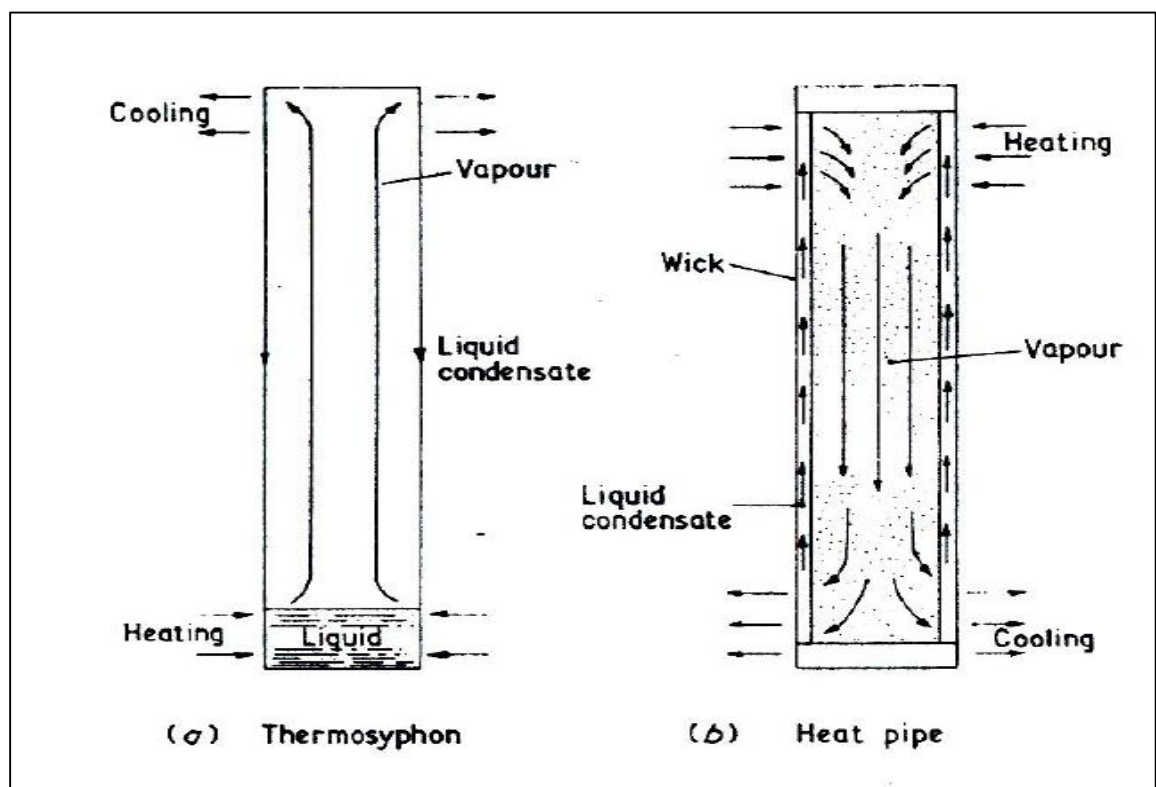


Figure (1.2) heat pipe and thermosiphon [2]

In general, heat pipe is a closed pipe with more than one shape, inside surface was coated with metal with a different form according to working fluid that used and temperature range inquisition in order to increase the capillary force.

Filling that pipe with some kind of working fluid, depends on temperature range, before charging the heat pipe that should be evacuated

from the air. The wick saturated with working fluid while the hole contains working fluid vapor.

The heat adds to heat pipe in evaporator part so it is considered as (source), and losses from it at condenser part, thus, it is regarded as (sink). Heat pipe could transfer a large amount of heat with a small amount of temperature different. Figure (1.1) declares the main heat pipe region. [2]

When using heat pipe in heat exchanger, there are many pipes sort together between two gas flows: one of them is exhaust gas and the other is for fresh air; and that two flows separated from each other. So increasing the amount of heat transfer rate which depends on the area of the pipe can control on it by increasing number of the heat pipes. Certainly, that means more cost and maintenance time, if it is known that the amount of temperature different reaches to the limit and be stable after that.

At that point, the researchers start to think with the best way to increase heat transfer rate with the decreased area and that stimulates them to add fluidize bed from sold particle to hot gas. Under that circumstances, the gas layer has physical properties like liquid because of the heat conduction coefficient for liquid more than the gas.

### **1-2 Effective parameter on heat transfer in heat pipe:**

There are many parameters that have severe effect on heat pipe heat transfer performance as listed below:[3]

- |                                |                            |
|--------------------------------|----------------------------|
| 1: Heat pipe diameter          | 2: Filling ratio           |
| 3: Working fluid kind          | 4: The wick type           |
| 5: Pipe material               | 6: Operation temperature   |
| 7: Heat pipe inclination angle | 8: The nature of out media |



Heat pipe manufacturing equations and calculations are listed in Appendix-A

### **1-3 Heat pipe components**

Heat pipe is sealed container, inside wall there is a wick but in several shapes to increase capillary force and the working fluid putting inside heat pipe with different ratios according to heat temperature limit and rate of heat transfer. The working fluid inside the container works with two phase flows liquid and vapor, the heat transfers to heat pipe in evaporator part then the fluid inside wick starts to heat until evaporating, then the pressure gradient that happened in the evaporator part leads the vapor to the condenser, where the vapor transmit to liquid again and back to evaporator by helping capillary and gravity forces if the pipe inclined, see figure (1.1) [4], [5]

#### **1-3-1 Container**

The main part in the heat pipe is a container which is used to separate the working fluid from outer environment, it should be leak proof. The manufacturing material could be aluminum, stainless steel, copper or sometimes used composite material like carbon composite and sometimes used the refractory material to prevent corrosion. Selecting of the container depends on the following factors: [4]

1-compatibility between working fluid and the external environment.

2- Strength –weight ratio

3- Thermal conductivity

4- Easily fabrication with welding, ductility, machinability

### 1-3-2 Wick

The wick takes the force required to back the working fluid from condenser to evaporator, with increased wick layer means increasing the capillary force that has a severe effect on the return of working fluid. An additional number of wick layer has a great impact on a radial drop in temperature between the heat pipe inner surface and vapor-liquid surface small pores have a great effect on capillary pressure. Figure (1.3) represents some types of wick structure.

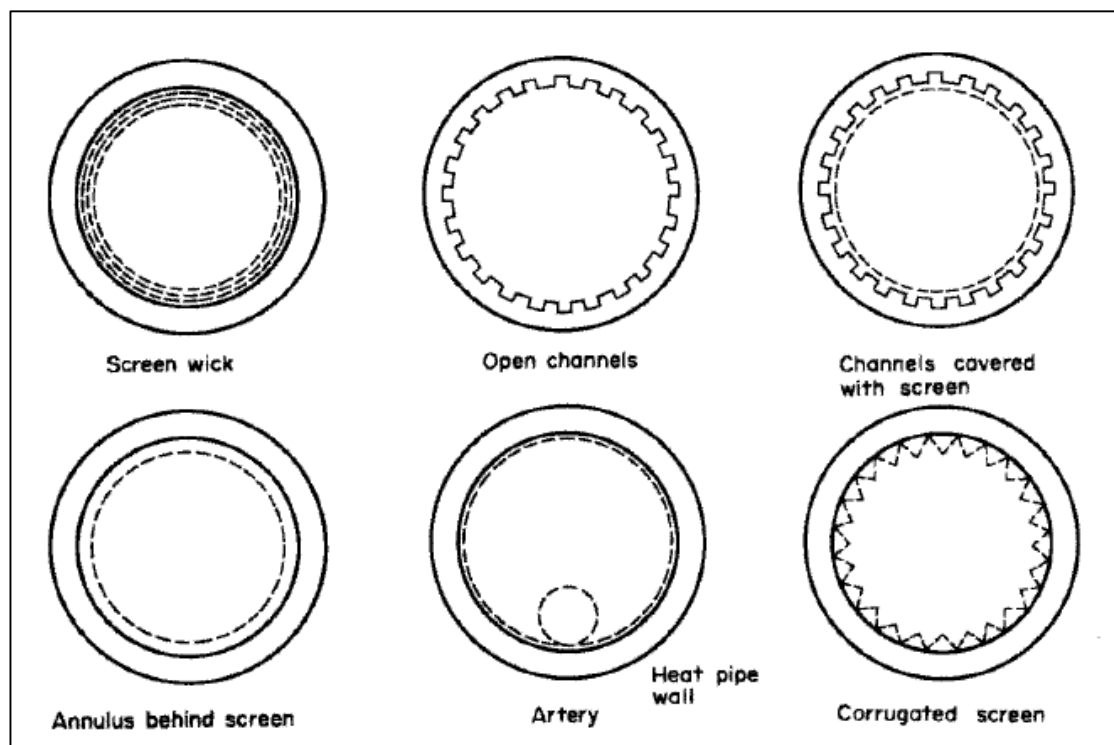


Figure (1-3) some types of wick structure [2]

### 1-3-3 Working fluid

The important consideration in identification is suitable working fluid vapor temperature range under test, and also the thermodynamic consideration that relates to working fluid flow in heat pipe (sonic, viscous, entrainment, capillary and boiling limit).

Choosing the suitable working fluid with specific operation temperature prevents thermal degradation that leads to fluid breaking down to many components, that's why thermal stability is very important under operation range.

On the surface of the liquid, the molecules were pulled due to the attraction that prevents molecules to escape, the temperature and pressure affected directly surface tension but the temperature has more influence. [2]

See appendix-A( Table A-1) represents compatibility data among some kinds of working fluid and wick material [5]

The important features that should be available in working fluid are listed below:[2]

- 1-compatibility with wall material and wick.
- 2- Good thermal constancy.
- 3- Wettability of wall material and wick.
- 4- Latent heat should be high.
- 5- Thermal conductivity should be high.
- 6- Low vapor and liquid viscosity.
- 7- Surface tension should be high.
- 8- Acceptable pour and freezing point.
- 9- Vapor pressure should not have severed fluctuation up and down the operating temperature range.

See appendix-A( Table A-1) represents different types of working fluid with useful temp. Range[2]

## 1-4 Fluidization

When the gas or liquid slowly flow through solid particle, they flow through porous medium, but when the flow speed increased some particle leave solid group, a case between that two speed when the drag force is not enough for solid particles to leave solid group but also it is not stable that case is called [fluidize bed].[6]

The properties of fluidized bed are the same of fluid properties, the particles that are put in the place is call [packed]. when the flow is slow, the air passes through the particles without a change in its position, but when air speed increases the particles start changing it positions, the particles properties like fluid properties at this point, for example its surface will be levelly and also if any object was putting on particle surface it will drown if the object has a high density than particles.

Using liquid to flow through particles then fluidized bed start stretch regularly with increasing flow speed, but when using air, there is instability happened in fluidized bed with increasing flow speed and turbulent flow will appear. The difference between the two cases is coming from differences in density between particles inside and (gas or liquid) at another side.

High motion and good mixer in fluidized bed take good advantage especially in increasing heat transfer coefficient. [6]

## 1.5 Fluidization Phenomenon

It is the process forced the particle to move by attaching it with liquid or air, in that case, the mixture has physical properties liquid- like.

At the start of applied air to the particle container, the air passes through distributor and then reaches particles but air velocity was too slow that the air passes through the particles and goes out without making any change in

particle positions. That is due to the low speed where bed thickness remains without change at that time which is called **Fixed bed or packed bed**.

With increasing of superficial velocity with an amount of minimum velocity ( $U_m$ ), then the particles –air resistance decreased and air drag force increased that lead to increasing the distance between the particles; and all particles were expanded by ( $L_m$ ) and that very clearly can be observed. That process is called **mixed bed**.

With increasing air velocity, the particles continued with expanding in a high size. Bubbles start to be created among particles and to be raised upward that phase is call a **slug**. More air velocity increased that bubbles will be smaller and closer together, that phase is called **turbulent regime**. Additional liquid velocity, fast fluidization appears. Particles moved at this phase as groups where the liquid dissipated the particles , adding more liquid velocity could show pneumatic conveying phase which is a fully fluidization, as shown in figure (1.4) [9]

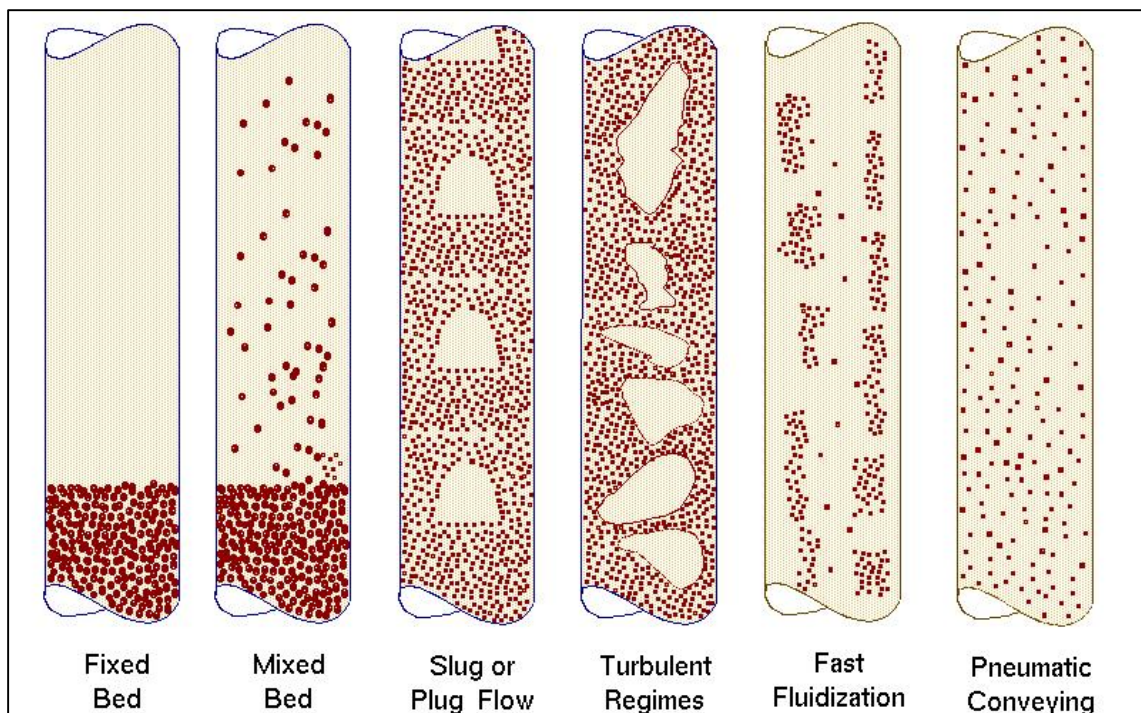


Figure (1.4): Liquid – Solid Fluidize Zones [9]

## 1.6 Particle Size

If the particles diameter is less than (5mm) then it can be considered as big particles, and if it less than (0.4mm) then it can be considered as small particles; for big ones could measure the diameter by micrometer but for small ones, the diameter was measured by sieve. Particle diameter measured was explained in an experimental chapter.

The present calculation considered all particles have spherical shape but in fact, that is not correct because many particles have different shapes so must multiply by the correction factor, called ( sphericity ,  $\emptyset$ ) where.

$$\emptyset = \left( \frac{\text{surface of sphere}}{\text{surface of particle}} \right) \quad \dots(1.1)$$

[Kunji] listed amount of sphericity that we relied on the present work [10].

## 1.7 Pressure drop in fluidized bed

At homogenous particle size, air starts passing during air distributor, there is not any change in  $\Delta p$ , but at  $U_m$  then the  $\Delta p$  increased and also porosity increased, so the  $U_m$  relates directly to  $\Delta p$ .

With increasing velocity to  $U_{mf}$  , the  $\Delta p$  becomes  $\Delta p_{max}$  and porosity decreased  $\epsilon_{mf}$ . If velocity increasing continuously then the bed reaches to air layer, sever decreased in  $\Delta p$  and the relation between  $\Delta p$  and velocity become reverse.[11]. Figure (1.5) shows pressure drop with velocity.

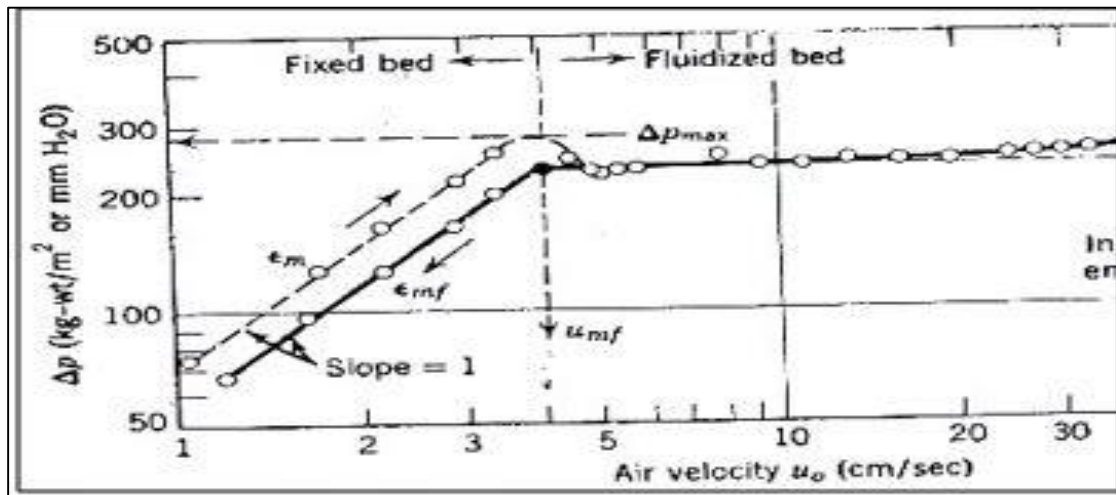


Figure (1.5): Pressure drop a-velocity relation in a fluidized bed[11]

## 1.8 Particle influent in heat exchanger

Heat transfer has an important role in several applications as in vehicles, electronic circle, air condition system, thermal power stations and chemical processes etc. In all previous applications, heat dissipation needs heat exchanger as a device, which depends on convective heat transfer, by using medium to transfer heat; This media (or medium) was pumped inside heat exchanger with calculated values, so need to found suitable media that have a high heat transfer coefficient and low viscosity to reduce consumption. Under that futures size and cost are lowered.

One of the most important method to enhance heat exchanger performance via increased heat transfer coefficient by adding solid particle to mixing. The important knowledge was to use high thermal conductivity of solid particles which can be hundreds or thousand times larger than that of the fluids to increase the mixture thermal conductivity.[10]

## **1-9 The aim of present study**

Heat exchanger is widely used in industrial life and important in the used heat exchanger coming from heat recovery use. The main objectives of the present work are:

- 1- Study the effect of solid particles on heat pipe heat gain.
- 2- Study the effect of air speed on heat pipe heat gain.
- 3- Study the effect of solid particles on heat transfer coefficient.
- 4- Study the relation between solid particles density and pressure drop.
- 5- Study the relation between Nusselt and Renoildes numbers.

and comparing between experiential and numerical values for all previous results.



**CHAPTER TWO**

**LITERATURE**

**REVIEW**

## CHAPTER TWO

### Literature Review

This chapter explains the studying deal with the heat pipe as a tool of heat exchanger with two phase flows (gas –solid) fluidized bed, and many study works in fluidization region.

Since heat pipe has an important role in modifying technology and advances our life, many sciences studied it. Below are some of those studies:

#### 2.1 Theoretical Studies

**Xu and B. Yu (1997) [12]** Studied modelling (gas-solid) flow in a fluidized bed in the three-dimensional central jet fluidized bed of dimensions 0.9 x 0.15 x 0.004 m. by a computational fluid dynamics (CFD), which depends on Newton's third law of motion, The gas-phase equations are solved by the conventional SIMPLE method facilitated with the Crank-Nicolson scheme to give the second order accuracy in the time discretization. at different length and time steps was  $(1.5 \times 10^{-5})$  s. and takes the second order accuracy in the time discretization. Number of particles that used was 2400 with density 2700 kg/m<sup>3</sup>. The aim of this model shows the ability to simulate gas fluidization process, from fixed to fully fluidized bed.

The researcher predicates the fluidization at slow velocity with minimum fluidization velocity, founding a good agreement with experimental results. The researcher has shown that the model could represent the fluidization at largest velocity range and geometry shape.

**Fan et al. (2010) [13]**, studied the solids expansion and segregation in a liquid solid fluidized bed using CFD approach. They modeled two dimensional Eulerian – Eulerian , unsteady laminar flow in fluent 6.3, small size particles in range (1–1.18 mm) were used, the density of the particles were different (1600, 1900 kg/m<sup>3</sup>) which was continuously

fluidized by water. The simulation results showed unsteady agreement with the empirical data of other similar experimental research. The temperature predictions were sensitive strongly due to its influence on liquid viscosity and to the shape of particles. The simulation results also influenced by the mean size of particles and density.

**Ajay and Karnik (2012) [14]**, performed numerical investigation to show how the fluidization minimum velocity affected by the height of the bed. Simulations of the Computational Fluid Dynamics (CFD) were performed by using the commercial, STAR-CCM+ software. Glass beads were used as solid particles with an average diameter of (550  $\mu\text{m}$ ) and density of (2600  $\text{kg}/\text{m}^3$ ). Fluidization minimum velocity was calculated using the bed pressure drop and for various ratios of initial bed heights to base diameter as (0.5, 1, 2, and 3). Simulations showed that the bed height had no influence on the minimum fluidization velocity for cylindrical beds.

**Kumar and Pandey (2012) [15]**, performed a computational fluid analysis using the fluent software for circulating fluidized bed gas–solid combustion mixtures. They offered circulating fluidized bed coal combustion. The gas solid flow for the two phase flow circulating fluidized bed was described by using the turbulence model ( $k$ - $\epsilon$ ). The Discrete Phase Model (DPM) and the non pre mixed combustion species model was used to analyze the coal combustion by taking (5 mm) diameter for the solid particles and (4, 5, and 6 m/s) as the fluidization velocity. It was concluded that the three fluidizing velocities had an insignificant effect of the change in the maximum total temperature. The static and total pressure of the bed increased as the velocity increased.

**Tandon and Karnik (2014) [16]**, studied the dependability of the granular model kinetic theory in expecting the flow of gas – solid hydrodynamics. They used STAR-CCM+ to simulate the granular Euler-

Euler model. The fluidized bed pipe model was rectangular with dimensions of (3" × 9" × 48"). They used Geldert group D particles with density of (1131 kg/m<sup>3</sup>) and air. The results compared with experiments from other research and they found that the KTGF calculated the hydrodynamics successfully.

**Mohammad S.Q. Aldabbagh (2014)[17]** described the optimum design of heat pipe by using matlab (7) to ensure transfer greater amount of heat to heated the water that enter to steam boiler and also puts important point to choose each part of heat pipe (working fluid, container, wick) also tilting of heat pipe since gravity has severe effect on heat pipe performance, the result shows as:

1-Heat pipe performance increased with increasing its diameter and wick cross section area and wick wire diameter and a number of wick layer and specific heat for working fluid. It also increased with increasing heat pipe tilting angle until reached to 90° where maximum heat transfer.

2-working fluid flow rate increased with increasing pipe diameter and wick cross section area, the effective length of the heat pipe, inclination angle and working fluid heat temperature.

**Hou, Z. Y et al(2016)[18]** Studied the effect of fluidize material properties, gas velocity and tube array on heat transfer between fluidize bed and tubes are examined by the two method of computational fluid dynamics, discrete element way. In this work, two significant concerns relevant to gas–solid flows and heat transfer characteristics are addressed by using the combined CFD–DEM approach. To investigate the effect of tube array settings, particle diameter  $d_p$  is set to 0.6mm with a numerically determined minimum fluidization velocity ( $U_{mf}$ ) of 0.36m/s. and particles has a width of  $160d_p$  and height of  $1,000d_p$ . Tube diameter is  $20d_p$ . As the main aim of this part is to examine the effect of tube array settings, all the cases are carried out at a low tube temperature ( $T_s$ ) of 200 °C where radiative heat

transfer is negligible. The inlet gas velocity is set to  $3U_{mf}$ . The results show that if the material has a small cohesive the conductive heat transfers between a fluidized bed and a tube then dominant and the convective heat transfer is dominant for big non-cohesive particles. The gas velocity has sever effect on particle uniformity and heat distributed. The tubes were arranged as a line and staggered type to show that two sorts affect microscopic properties such as porosity and number of contact the surface, due to that comprehend led to choses suitable tubes sort.

## 2.2 Experimental Studies

**GREWAL. N. S. (1980) [19]** experimentally performed suitable correlation, for heat transfer coefficient, between solid-air fluidize bed and single electrical heated horizontal tube.(considering the heat pipe as horizontal heated tube). This correlation is based on the experimental data for heat transfer coefficient between electrically heated horizontal tube bundles (12.7 and 28.6 mm diam.) and square fluidized beds (30.5 x 30.5 cm)\_of alumina ( $d_p = 259 \mu\text{m}$ ) and silica sand ( $d_p = 167$  and  $504 \mu\text{m}$ ). The tubes in the bundle are located at the vertices of equilateral triangles with pitch varying between 1.75 and 9 times the tube diameter. The researcher discusses the effect of size, shape, specific heat, density, air mass fluidize velocity, tube material, tube size, bed high, heat flux and heat transfer rate.

**Udell. K. S. (1985)[20]** studied the effect of porous media saturated with vapor and liquid (single component ). On heat pipe performance taking in consideration, capillarity, gravity force also phase change, amount of heat transfer increased several order of magnitude than pure conduction, because of convection-condensation and evaporation phenomena similar to (conventional heat pipe). Thermal conductivities were calculated for much medium permeability's and gravitational orientation.

Theoretical results give good agreement with experimental results, the results are the following.

- 1- Using counter flow in porous media gives as more efficient for heat transfer.
- 2- With decreasing permeability, the temperature difference between two phase zones increased.
- 3- Thermal conductivity with two-phase zones higher than single phase conductivity with high permeability media.

**Kobro and Brereton (1986) [21]** improved experimentally the heat transfer coefficients in a pipe with 3 m long and 0.2 m diameter using circulation fluidize bed (CFB) technology, using a small (100) mm. heat transfer probe. The researcher found heat transfer coefficients were (70 – 280) W/m<sup>2</sup>.k for heat range (25-850)°C. also found increasing in the heat transfer coefficients with cumulative suspension density.

**Dry et al. (1992) [22]** worked on a thermal technique to calculate the gas residence time, and guess contact efficiency between gas- solids, in a circulation fluidize bed at high-velocity, up flow. Hot air was supplied by passing air on electric furnace which increases air temperature to 550 °C; mixing between air and solid will be done at riser. The thermal reply was computed to obtain the interaction efficiency between the solid and gas.

The study showed the effects of reactor geometry, interring gas method, operating condition. Type and particle density has the important outcome on the(gas-solid) contact efficiency. Fine particles gave more contacting than coarser particles, decreasing overall contact efficiency with decreasing inlet area.

**Ninad, S. (2003)[23]** studied use of a heat pipe to enhance the engine efficiency and net power output where it decreased in summer

because of hot air entering the composition chamber from the turbocharger. The researchers used heat pipe to cool the air entered to turbocharge. Using that method means increasing in air density and that also means increasing the air mass and flow rate. Under these circumstances, the compressor can move high amount from air mass for the same volumetric air flow rate

**Parise. M. R (2006):[24]** experimentally studied tube immersed in gas-solid fluidized bed where cold water inside tube is heated via the particles of fluidizing bed; particles inlet temperature is (450-700) °C. The study deals with the effect of solid particles amount in fluidized bed and distance between baffles in the heat exchanger. The solid particle with 254 µm from silica sand, that sand fluidize in the channel with 0.9 m long and 0.15 m width.

The researcher takes the measurement at study state for solid mass flow rate (10 -100) kg/h, and there are (5- 8) baffles in the heat exchanger.

The temperature taking along the heat exchanger in fluidize bed and heat balance was made for different control volumes in order to obtain the axial profile of (bed to the tube) heat transfer coefficient.

The result is with an increased mass flow rate for a solid particle that leads to increase heat transfer coefficient with the presence of baffles, also the researcher found that when the number of baffles 5-8 there is no observed change happened.

**Ahmad. H. H (2011)[25]** investigated experimentally the effect of working fluid and falling ratio on heat pipe performance by using heat pipe with 600 mm length and evaporator section with 200 mm length and adiabatic section 100 mm. pure water and pure acetone was used , then mixed them with different ratios (30,50,70) % and heated the evaporated part with different powers (125-250) Watt with 25-watt step, and isolated each

evaporate and adiabatic part so loss not exceeds 10%, after sketching the heat transfer coefficient with working fluid and position in heat pipe, the researcher found:

- 1- The evaporator surface temperature increased from the first part of the evaporator until becoming maximum value at the middle of the evaporator and then started to decrease in the residual part of the evaporator and adiabatic section.
- 2- The same result in item 1 can be got when using water and acetone with a falling ratio of 30%.
- 3- Maximum heat transfer coefficient get when using water as working fluid and a minimum of the same factor at 50% mixing ratio, the researcher translates case by changing material properties by mixing.
- 4- Sketch the relation to calculate the heat transfer coefficient at a surface temperature at the pure water and different falling ratio mixture, maximum heat transfer coefficient was found at the pure water.

**Yang et. al. (2012)[26]** studied the way to reduce heat pipe weight, and chose the correct heat pipe metal to prevent: (corrosion, create gas), using light weigh material that reduces weight for more than 80%; but there are many limitations in using like that material, water, for example. Water is the most desirable working fluid but when used with aluminum alloy, magnesium alloy must add more addition to avoid generate non condensable gas that gas blocks vapor line and causes local temperature drop.

The researcher finds that reducing the wick structure can reduce heat pipe weight but more thin wick layer means less capillary force that affect heat pipe efficiency.



Also making heat pipe size small can be an important way to reduce weight. Aluminum has 25% of copper weight and also (50-60) % of copper conductivity but aluminum seldom is used alone so corrosion protection adds to it when water used as working fluid and some time lead adds to internal surface to improve corrosion resistance.

**Salwe. A. M. (2013) [27]** Studied experimentally heat transfer coefficient between heated tube immersed in bubbling (gas-solid) fluidized bed with different angles, air superficial velocities, and particle diameters. The bed was silica sand particles with diameter (200, 350 and 500)  $\mu\text{m}$ , the results showed that maximum and minimum heat transfer coefficient was at tube angle (180, 0)  $^\circ$  respectively. experimental rig consists of fluidizing column is of 59 mm internal diameter and 3 mm thickness and 1 m height, made up of Plexiglas to aid visualization. A fine mesh of copper is used as a distributor plate. A brass tube of external diameter 10 mm and length 50 mm is fitted horizontally inside the column. The axis of brass tube is perpendicular to the axis of fluidizing column. A Cartridge heater of 6 mm outer diameter and 45 mm long is inserted inside the brass tube. Axis of brass tube is at the distance of 185 mm from the distributor plate. Results showed increasing heat transfer coefficient with increasing air superficial velocity, and decreasing by increasing particle diameter. The heat transfer coefficient correlation was a predicate to horizontal tube immersed in a fluidized bed, also correlation for the Nusselt number, comparing heat transfer coefficient and Nusselt number between experimental values and that produced from correlation affect a good agreement.

**Asirvatham. L.G.et.al. (2013)[28]** performed experimentally. how to improved heat pipe heat transfer performance by using silver Nanoparticle with DI-water. That happened by increasing thermal conductivity with power range (20-100) W. And under consideration many

variables such as vapor temperature, volume fraction, and thermal resistance. The researcher used (0.003-0.009) % nanoparticle concentration with average diameter 58.35nm, by using copper heat pipe with length 180 mm, diameter 10 mm, thickness 0.5mm. Evaporator and adiabatic and condensed length (50,50,80)mm respectively. Copper wick used with two layers 100/inch, used thermocouple T type 8 to evaporator and 3 to condenser and an adiabatic section. The water enters to condenser part with rate 260 L/min at constant interring temperature 24 °C.

The researcher uses four pipes. One of them used just distilled water inside and the other mixed Di-water with Nano with different mixing ratio and all pipe tested under same circumstances (flow rate, interring heater power, and water temperature) and the power increased in heater from (20-100) W.

The researcher found 76.2% reduction in thermal resistance and 52.7 enhancement in heat transfer coefficient at used Nano with 0.009% concentration. The dryness increased if evaporator power increased more than 100 W approximately (106 watts at 0.003%), (113 Watts at 0.006%); Thermal conductivity increased for (42.4-56.8-73.5) at (0.003-0.006-0.009)% respectively. and also heat transfer coefficient increased with increasing Nanoparticle concentration .

**Lechner et al 2014 [29]**, examined the heat transfer by fluidized beds when used a cylindrical heater, for just one and also when used many of them. Also study changing fluidize bed material affects heat transfer, but it doesn't take in consideration influence of heater geometry on heat transfer. The heaters are arranged at different vertical and horizontal spacing, alignment also investigated; Tests were done by means of electrical heat transfer probes inside a 0.15 m<sup>2</sup> fluidized bed area. And it used a (lignite) as a solid particle in order to comprehend gas - particles heat convection mechanisms.

Particles that used with diameter range (0– 2) mm, and Superficial velocity is adjusted via a frequency converter typically between (0.1 and 0.5) m/s

The study showed that tube array decreases the heat transfer coefficient because of particle -gas flow turbulences produced via the occupied tubes, and predicates a factored represent the ratio between heat transfer coefficient and a number of the heater. Tube package geometry was successfully applied into beneficial correlations for forecasting heater bundles' heat transfer of (gas-solid) fluidized bed.

### 2.3 Experimental and Theoretical Studies

**Moslemian et. al. (1991) [30]** studied the heat transfer coefficients to the surface immersed in fluidize bed and study the particle speed effect, that experimental done for many locations of a simulated tub, and at the single immersed cylinder. The tube diameter was 184 mm. I.D. The researcher used soda-lime glass with diameter (425-600)  $\mu\text{m}$ , and air superficial velocities 35.6, 54.9, 77.2, and 100.4 cm/s. The results showed the steady relationship between particle motion and heat transfer rate at all locations. The study explains the heat transfer coefficient model, and compare it with another researcher's correlation, and found deprived agreement at low speed, but good agreements at high speed.

**El-baky and Mohamed (2006) [31]** Used a heat pipe as a heat recovery in air conditioner system, putting the heat pipe between return air from the room and fresh air hole, to cool the fresh air before entering to AC, and investigated the thermal performance and effectiveness of heat recovery system. The Ratios of return air mass flow and fresh air are (1, 1.5 and 2.3). Fresh air inlet temperature of (32 – 40)  $^{\circ}\text{C}$  while the return air temperature kept stable at 26  $^{\circ}\text{C}$ . As the results showed. The effectiveness, heat transfer for heat pipe in evaporator and condenser part are enlarged to about 48 % when increasing inlet air temperature to 40  $^{\circ}\text{C}$ . The mass flow rate has

appositive and negative effect at the evaporator and condenser part respectively. The best heat pipes heat exchanger effectiveness is estimated, comparing that effectiveness amount with experimental. Two results are closed together when fresh inlet air temperature close the heat pipes operating temperature.

**Hafidh.H.Mohammed(2011)[32]** performed experimentally and numerically circulation fluidized bed. To explain fluidization effect on heat transfer coefficient. The experimental rig was fabricated from tube with 1500 mm long and inner diameter 76mm ,used cylindrical heater with 28 mm diameter, the power supply changed (50,105 and190)W, air velocity supply at(4.97,5.56,6) m/s ,different particle size used(194-356) $\mu\text{m}$  , with particle bed thickness (15-35)cm. using cyclone as return particle device ,in addition to heat sensor that distributed in region to determine the heat distribution inside tube, also finite different method to measure heat inside domain .a good agreement between experimental and numerical values .The results shows that heat transfer coefficient and heat flux increased with increasing velocity and particle thickness which represent density but that depends inversely on particle size.

**Sahoo. P. and Sahoo. A (2015) [33]** studied properties of fluidized bed in the cylindrical column ID=12 cm with 70 cm high made from Perspex (acrylic), useing cloth as pores of approximately 40 microns tight at bottom with flange help, and also flange covered by cloth .The particle with density of 1300 kg/m<sup>3</sup> and the air passes from bottom of column and uses U tube manometer to determine air flow rate bay this rig. The researcher gets his experimental results and theoretical results getting from CFD to validate with time step=0.001, grid size=0.002 the programming assumption are:

- 1- Unsteady state gas-solid system.
- 2-No mass transfer between gas and solid phase.

3- Neglected viscosity and isothermal.

4- At a bottom uniform velocity.

The research has shown that

Eulerian model with 2D takes close to a real effect, choose correct boundary condition to give as acceptable modeling result inside fluidize bed, CFD could show as bubble path through the particle.

**Pakam Y. et al (2016)[34]** design the analytical model has been fabricated represents 13 heat pipes ,sorted vertical-staggered ,each heat pipe charges with Ethanol as a working fluid ,all heat pipes with 320 mm overall long ,150mm evaporating section,150mm condenser section and 20mm adiabatic section ,at evaporator part hot air with temperature range (100-140)°C .with flow rate (180-230)L/min. while at condenser water passing with constant temperature 30°C, and with flow rate (0.25-0.75)L/min. used MATLAB to simulate outlet water temperature. The result showed differences between experimental and theoretical heat pipe effectiveness which was (4-15) % respectively .and maximum hot air inlet at 140°C getting maximum effectiveness of about 91%.

## **2.5. The scope of This Work**

Many researchers deal with modifying the performance of heat pipe since 1942. All that modification depends on temperature sensor to measure heat temperature fixed on the heat pipe surface. Some of them studied falling ratio effect on heat pipe performance, the other study working fluid effect, wick type and structure also inclination angle have been studied.

In present work. Effect of fluidized bed was studied via applied different level of particles and hot air attack that particles. And calculate the improvement amount at heat pipe performance. Also compared the result

with model design by CFD that was modeled within experimental boundary condition.

## 2.6. Summery

All literature presented in this chapter is listed below

Table (2.1): Summery of the Literatures

Numerical Studies						
No.	Researches	Year	Numerical method	Geometry /flow type	Working range	Results
1	<b>Xu and B. Yu</b>	1997	Conventional SIMPE method	(0.9×0.15 ×0.004)m	Particle number was 2400	Predicate the fluidization at low velocity .
2	<b>Fan et al</b>	2010	FLUENT6.3 two dimensional Eulerian-Eulerian , unsteady laminar flow	studied the solids expansion and segregation in a liquid solid fluidized bed /up flow	Particles di. (1–1.18 mm) Density (1600, 1900 kg/m <sup>3</sup> )	The simulation results showed unsteady agreement with the empirical data of other similar experimental research
3	<b>Ajay and Karnik</b>	2012	(CFD) were performed by using the commercial, STAR-CCM+ software	Cylindrical geometry	initial bed heights to base diameter as (0.5, 1, 2, and 3), particles diameter of (550 μm), and density of (2600 kg/m <sup>3</sup> ).	Simulations showed that the bed height had no influence on the minimum fluidization velocity for cylindrical beds
4	<b>Kumar and Pandey</b>	2012	ANSYS FLUNT turbulence model (k-ε). The Discrete Phase Model (DPM)	circulating fluidized bed gas–solid	fluidization velocity (4, 5, and 6 m/s), Particle diameter (5) mm	the three fluidizing velocities had an insignificant effect of the change in the maximum total temperature. The static and total pressure of the bed increased as the velocity increased.

5	<b>Tandon and Karnik</b>	2014	used STAR-CCM+ to simulate the granular Euler-Euler model	rectangular with dimensions of (3" × 9" × 48")	particles with density of (1131 kg/m <sup>3</sup> )	
6	<b>Mohammad S.Q. Aldabbagh</b>	2014	matlaip (7)	described the optimum design of heat pipe	important point to choose each part of heat pipe (working fluid, container, wick)	Heat pipe performance increased with increasing its diameter and wick cross section area and wick wire diameter and a number of wick layer and specific heat for working fluid
7	<b>Hou, Z. Y et al</b>	2016	CFD–DEM approach	Horizontal tubes	dp is set to 0.6mm (Umf)of 0.36m/s , width of160dp and height of1,000dp. Tube diameter is 20dp	The gas velocity has sever effect on particle uniformity and heat distributed
<b>Experimental study</b>						
No.	Researches	Year	Experimentally method	Geometry /flow type	Working range	Results
8	<b>GREWA L. N. S.</b>	1980	discusses the effect of size, shape, specific heat, density, air mass fluidize velocity, tube material, tube size, bed high, heat flux and heat transfer rate.	square fluidized beds (30.5 x 30.5 cm)	of alumina (dp = 259 μm) and silica sand (dp = 167 and 504 μm)	experimentally performed suitable correlation, for heat transfer coefficient, between solid-air fluidize bed and single electrical heated horizontal tube

9	<b>Udell. K. S</b>	1985	studied the effect of porous media saturated with vapor and liquid (single component). On heat pipe performance	Heat pipe	taking in consideration, capillarity, gravity	Using counter flow in porous media gives as more efficient for heat transfer.
10	<b>Kobro and Brereton</b>	1986	circulation fluidize bed (CFB)	pipe with 3 m long and 0.2 m diameter	heat range (25-850)°C	found heat transfer coefficients were (70 – 280) W/m <sup>2</sup> .k
11	<b>Dry et al.</b>	1992	calculate the gas residence time, and guess contact efficiency between gas-solids	CFB	air temperature to 550 °C	Fine particles gave more contacting than coarser particles,
12	<b>Ninad, S</b>	2003	heat pipe to enhance the engine efficiency	Heat pipe	used heat pipe to cool the air entered to turbocharge	compressor can move high amount from air mass for the same volumetric air flow rate
13	<b>Parise. M. R</b>	2006	tube immersed in gas-solid fluidized bed where cold water inside tube is heated	channel with 0.9 m long and 0.15 m width.	particles inlet temperature is (450-700) °C, flow rate (10 -100) kg/h	increased mass flow rate for solid particles that leads to increase heat transfer coefficient
14	<b>Ahmad. H. H</b>	2011	investigated experimentally the effect of working fluid and falling ratio on heat pipe performance	heat pipe with 600 mm length	Mixed ratios (30,50,70) %, powers (125-250) Watt	Maximum heat transfer coefficient get when using water as working fluid and a minimum of the same factor at 50% mixing ratio,
15	<b>Yang et. al</b>	2012	studied the way to reduce heat pipe weight	Heat pipe	Heat pipe limitations	reducing the wick structure can reduce heat pipe weight but more thin wick layer means less capillary force that affect heat pipe efficiency.



16	<b>Salwe. A. M</b>	2013	Studied experimentally heat transfer coefficient between heated tube immersed in bubbling (gas-solid) fluidize bed	rig consists of fluidizing column is of 59 mm internal diameter and 3 mm thickness and 1 m height, made up of Plexiglas	particles with diameter (200, 350 and 500) $\mu\text{m}$ ,	. Results showed increasing heat transfer coefficient with increasing air superficial velocity, and decreasing by increasing particle diameter
17	<b>Asirvatham. L.G.et.al</b>	2013	performed experimentally. how to improved heat pipe heat transfer performance by using silver Nanoparticle with DI-water	Heat pipe with using copper heat pipe with length 180 mm, diameter 10 mm, thickness 0.5mm.	power range (20-100) W, used (0.003-0.009) % nanoparticle concentration	76.2% reduction in thermal resistance and 52.7 enhancement in heat transfer coefficient at used Nano with 0.009% concentration.
18	<b>Lechner et al</b>	2014	examined the heat transfer by fluidized beds when used a cylindrical heater		Particles diameter range (0– 2) mm, Superficial velocity (0.1 and 0.5) m/s	The study showed that tube array decreases the heat transfer coefficient because of particle -gas flow turbulences produced via the occupied tubes
<b>Experimental and numerical studies</b>						
No.	Researches	Year	Experimental numerical method	Geometry /flow type	Working range	Results
19	<b>Moslemian et. al</b>	1991	studied the heat transfer coefficients to the surface immersed in fluidize bed and study the particle speed effect	tube diameter was 184 mm. I.D	Particles diameter (425-600) $\mu\text{m}$ superficial velocities 35.6, 54.9, 77.2, and 100.4 cm/s.	explains the heat transfer coefficient model, and compare it with another researcher's correlation
20	<b>El-baky and</b>	2006	Used a heat pipe as a heat recovery in air	Horizontal heat pipe	Fresh air inlet temperature of (32 – 40) $^{\circ}\text{C}$	The effectiveness, heat transfer for heat pipe in evaporator and condenser part are

	<b>Mohamed</b>		conditioner system			enlarged to about 48 % when increasing inlet air temperature to 40 °C
21	<b>Hafidh.H .Mohammed</b>	2011	circulation fluidized bed and used finite element method	tube with 1500 mm long and inner diameter 76mm ,used cylindrical heater with 28 mm diameter,	power supply (50,105 and190)W air velocity supply at(4.97,5.56,6) m/s ,different particle size used(194-356) $\mu$ m , with particle bed thickness (15-35)cm	heat transfer coefficient and heat flux increased with increasing velocity and particle thickness which represent density but that depends inversely on particle size.
22	<b>Sahoo. P. and Sahoo. A</b>	2015	circulation fluidized bed and used ANSYS	cylindrical column ID=12 cm with 70 cm high made from Perspex (acrylic),	The particle with density of 1300 kg/m <sup>3</sup>	The researcher gets his experimental results and theoretical results getting from CFD to validate
23	<b>Pakam Y. et al</b>	2016	Air at evaporator part and water at condenser part	13 heat pipes with 320 mm overall long also used MATLAB	temperature range (100-140) $^{\circ}$ C .with flow rate (180-230)L/min	maximum hot air inlet at 140 $^{\circ}$ C getting maximum effectiveness of about 91%.
24	<b>The present work</b>	2019	Three heat pipes with particles in evaporator part and fresh air in condenser part	Simulate cement factory chimney and used ANSYS FLUENT	superficial velocity from (0.8739 to 1.377) particles bed thickness increased from (0 to 10) cm	maximum Nusselt Number was (35.125) which was achieved at maximum particle bed height (10cm) at maximum superficial velocity (1.377m/s)

**CHAPTER THREE**

**MATHEMATICAL**

**MODEL AND**

**NUMERICAL ANALYSIS**

## **CHAPTER THREE**

### **Mathematical Model and numerical analysis**

The current chapter deals with the project from three views:

The first view is concerned with the main heat pipes manufacturing principles, heat pipes limitation with a described meaning for all limited and equation to calculate it. The second view is devoted with fluidize bed description and the main properties that benefit to calculate it and main equation govern their behavior. The third view is a package computer program to create numerical study by using (ANSYS-18- FLUENT Workbench) which studies the particle flow effect on heat pipes performance.

#### **3.1 Basic design of heat pipe**

Many thermodynamic properties aspect heat pipe was discussed by Vasiliev. L. L. [6], Kobayashi. Y. [35], Akbarzadeh. A. [36],. Tien. C. L [37].

The description of heat pipes working and mechanism of movement for working fluid could be found in D. Reay and P. Kew [2].

Figure (3-1) describes the schematic draw heat pipe with a kind of capillary –driven, clearly the thermodynamics and fluid transfer way and fluid mechanics are clarified. All heat pipe calculation and equations concerned are listed in appendix A.

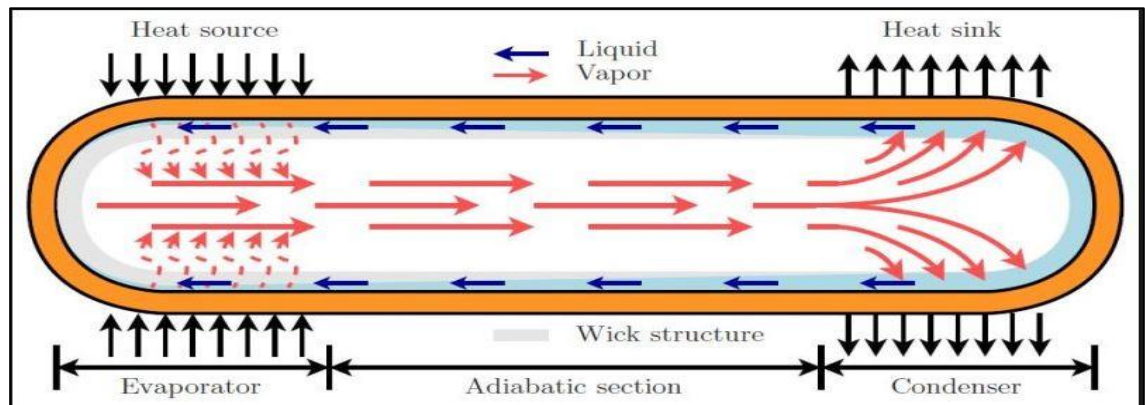


Figure (3.1): Heat pipe construction with a porous wick[38]

### 3.2 Particle motion model

In the fast bed regime, the circulating fluidized bed (CFB) normally operates, the CFB system contains strand or cluster while gas source pushes and separates the soiled particles.

The first phenomenon about heat transfer mechanism is that the particles move at cluster form. When that group becomes close to surface then heat transferred; after that this group moved away from surface and replaced by another particles group.

The second phenomenon CFB system studies told that the particle impact the surface immersed in it as groups but not as continuous stream of particles and each group travels for a short distance and then replaced with new one.

The particle porosity  $\varepsilon$  could be calculated from equation(3.2) [39]

$$\varepsilon = 1 - \frac{\Delta P}{gH(\rho_s - \rho_g)} \quad \dots (3.1)$$

So when calculating the properties, the mixture properties must be calculated [40],[41].

The mixture density was different for density of particle and gas, or liquid that flows. And that could be calculated from the flowing equation . [43]

$$\rho_f = (1-\varepsilon)\rho_p + \varepsilon\rho_g \quad \dots (3.2)$$

### 3.3 Effective thermal conductivity

Many studies deal with the suitable amount and good correlation that represent the correct value of effective thermal conductivity to mixture gas and particles. Approximately, all that correlation depends on the gas and solid thermal conductivities, particle diameter, porosity (void age), and gas speed.

But most equations that represent the present case are Colakyan and Levenspiel (1986) correlation [65]

$$K_{eff} = K_{es} + K_{ef} \quad \dots (3.3)$$

$$K_{es} = k_g \left( \frac{K_p}{K_g} \right)^{0.28 - 0.757 \log_{10} \varepsilon - 0.057 \log_{10} \left( \frac{K_p}{K_g} \right)} \quad \dots (3.4)$$

$$K_{ef} = 0.1 \rho_g C_{pg} d_p U_{mf} \quad \dots (3.5)$$

### 3.4 Model and correlation

The most important things in studying heat transfer in fluidized bed were choosing the correct relation that are suitable the case, because there was a large number of studies that deal with fluidized bed and surface immersed in it. As a result, there are many mathematical correlations to calculate heat transfer coefficient, so it is difficult to make a comparison between them. Most of them take the time that particles spend on the surface in consideration.

There were two models to forecast heat transfer convective between suspension and a tube in cross-flow.[40]

(1) The Deflecting Model: It results under the statement that solid particles bounced after striking the tube bottom and joining the gas-solid flow. Summation of heat transfer coefficient results from two components; heat

transfer via convection by gas and convection heat transfer via solid particles. The input of the flowing gas was expected to be constant. The input of the solid particles was expected to strike only under the tube. The lower part of the tube was covered by the solid particles.

(2) The Sliding Model: it is assumed that the solid particles hitting the underside of the probe are forced to slide along the probe, as shown in figure (3.2). present work depends on this model.

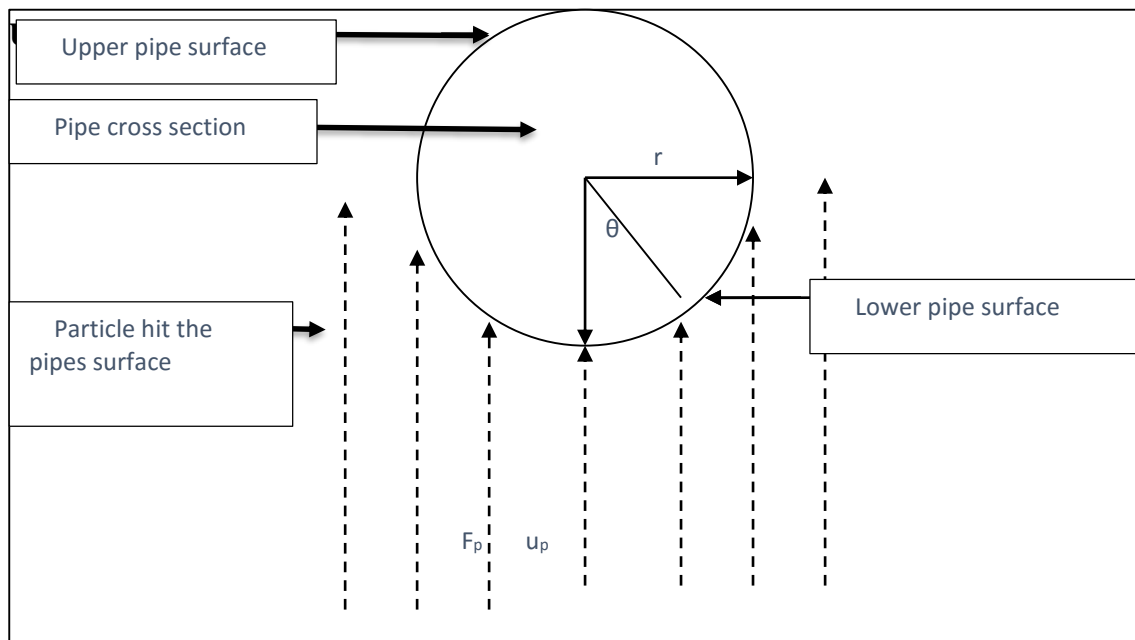


Figure (3.2): Cross Flow Diagram[45]

### 3.5 Gas-Solid Separator

In cyclic fluidized bed, cyclone was widely used to separate the particles from gas, the cyclone performs that matter by radial centrifugal force applied on particles, the particles driven to cyclone at the same time were going down to the outlet part.

Its shap is easy to design and has low cost and maintenance, since it has no movable parts.

Cyclone has an important part called vortex tube, this tube improved cyclone efficiency since it is fixed at the top exit and center of cyclone. This part descends flow down the cyclone while reverses in the down part of the cyclone into an up flow in the vortex. The vortex tube services the up flowing holdup around the tube and down to the opening.

The efficiency of cyclone decreased with degreasing cyclone size, similarly when decreasing the pressure drop inside it. Thus, the main test of the cyclone project is to control a cyclone dimension that will bounce satisfying separation efficiencies and at the similar period will make a sensible pressure drop[41].

Martin Fler[42] deal with Stairmand established two regular strategies for gas-solid cyclones:

High-efficiency cyclone: This kind of cyclones has a considerable big body, small inlet and gasses outlet are relatively small orifices and high recoveries. The big rate designs take as medium recoveries, but they also give us low resistance to stream, so that a unit of a given size will give much amount of air capacity. In present work depend on this cyclone type.

High rate cyclones: This type has a big inlet, gases outlet, but typically shorter. These two types and their dimensions were listed in table (3-1) below, as a relative of cylindrical diameter (Da).



Table (3.1): Cyclone dimensions according to stairmand theory

Cyclone type	The cyclone dimensions relative to ( $D_a$ )						
	H	$h_z$	$h_t$	$b_e$	$h_e$	$D_v$	$D_x$
(a) High efficiency	4	1.5	0.5	0.2	0.5	0.5	0.375
(b) High gas rate	4	1.5	0.875	0.375	0.75	0.75	0.375

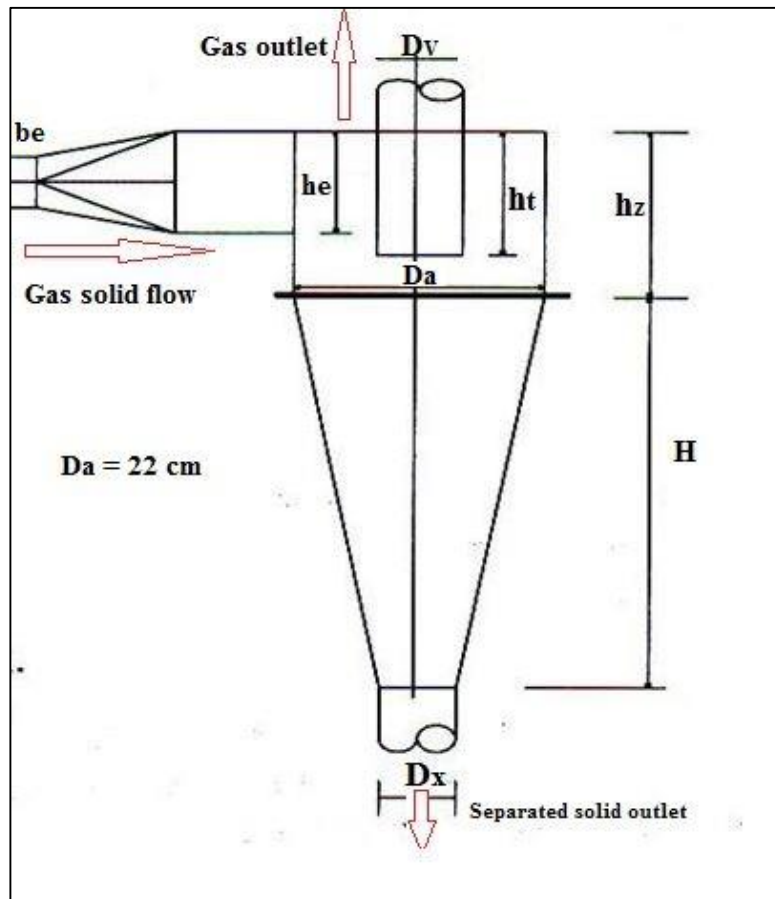


Figure (3.3): Details of High-Efficiency Cyclone[42]

### 3.6 Basic calculations

Sample of design calculation listed below.

#### 3.6.1. Rate of heat transfer

The amount of the heat transferred from the air- particle mixture to heat pipe surface (heat absorbed) is given by[48]

$$Q = \dot{m}_{air} \times C_f \times (T_b - T_s) \quad \dots (3.6)$$

Where  $T_b$  was bed temp. and  $T_s$  heat pipe surface temp.

Surface temperature is measured by calculating average values of thermocouples reading, that fixed on heat pipe surface which is five thermocouples.

$$T_s = \frac{T_1+T_2+T_3+T_4+T_5}{5} \quad \dots (3.7)$$

The bed temperature measured by calculating average heat measured values via thermocouples fixed in bed around heat pipe which is two or three thermocouples.

$$T_b = \frac{T_{after}+T_{befor}}{2} \quad \dots (3.8)$$

$$\dot{m}_{air\ eva} = \rho \times U_s \times A_{eva} \quad \dots (3.9)$$

#### 3.6.2 Mixture specific heat

The specific heat for air-particle mixture calculated from previous equation[44]

$$C_f = (1 - \varepsilon)C_s + \varepsilon * C_g \quad \dots (3.10)$$

#### 3.6.3 Heat transfer coefficient

Heat transfer coefficient was calculated in the present work by applying Newton's law. Amount of heat transfer coefficient depends on air

and particle physical properties which are calculated experimentally. The flowing equation was applied.[48]

$$Q = h_{out} A_s (T_b - T_s) \quad \dots (3.11)$$

$$h_{out} = \frac{Q}{A_s (T_b - T_s)} \quad \dots (3.12)$$

The outer surface area for heat pipe in evaporator part

$$A_s = \pi \times d_o \times L_{ev} \quad \dots (3.13)$$

### 3.6.4 Nusselt Number

The Nusselt number can be calculated from the heat transfer coefficient outside the tube according to the following equation:[50]

$$Nu_o = \frac{h_o d_o}{K_{eff}} \quad \dots (3.14)$$

### 3.6.5 Reynolds Number

Reynolds number could be calculate [46]

The outer heat pipe diameter was (2.25 cm):

$$Re = \frac{\rho_f \times U_s \times d_o}{\mu} \quad \dots (3.15)$$

$$U_s = \frac{\dot{m}}{\rho \times A_{eva.}} \quad \dots (3.16)$$

## Numerical Method

The Ansys works by dividing the work domain to small cells and applying governing equation, Ansys fluent 18.0 was the software that used in present work to simulate fluidized bed behavior due to the high quality in animation and visualizations that coming from Ansys CFD processing. To model the multiphase flow, there were two approaches.

Euler –Euler approach (granular flow model), in this approach the particle dealt with a magnified molecule. The other was Euler- Lagrange approach which is used when there was low volume fraction to the second phase typically less than (10-12) %.[47]

In the present work fluidized bed with the two-phase flow was modeled using the Euler model for air and particle flow with different parameters that depends on variable tested parameters which depending on the experimental result to validate CFD results.

### **3.7 Problem Assumptions**

The following assumptions, was made to simulate the flow in a test section. Where air used as phase one, and cement fly ash as the second phase.

1-Steady state flow for 3D model and transient for 2D model.

2-Turbulent flow.

3-Temperature based solver.

4-The gravity in the Y direction ( $-9.81 \text{ m/s}^2$ ).

Figure (3.4) represents numerical analysis flow chart.

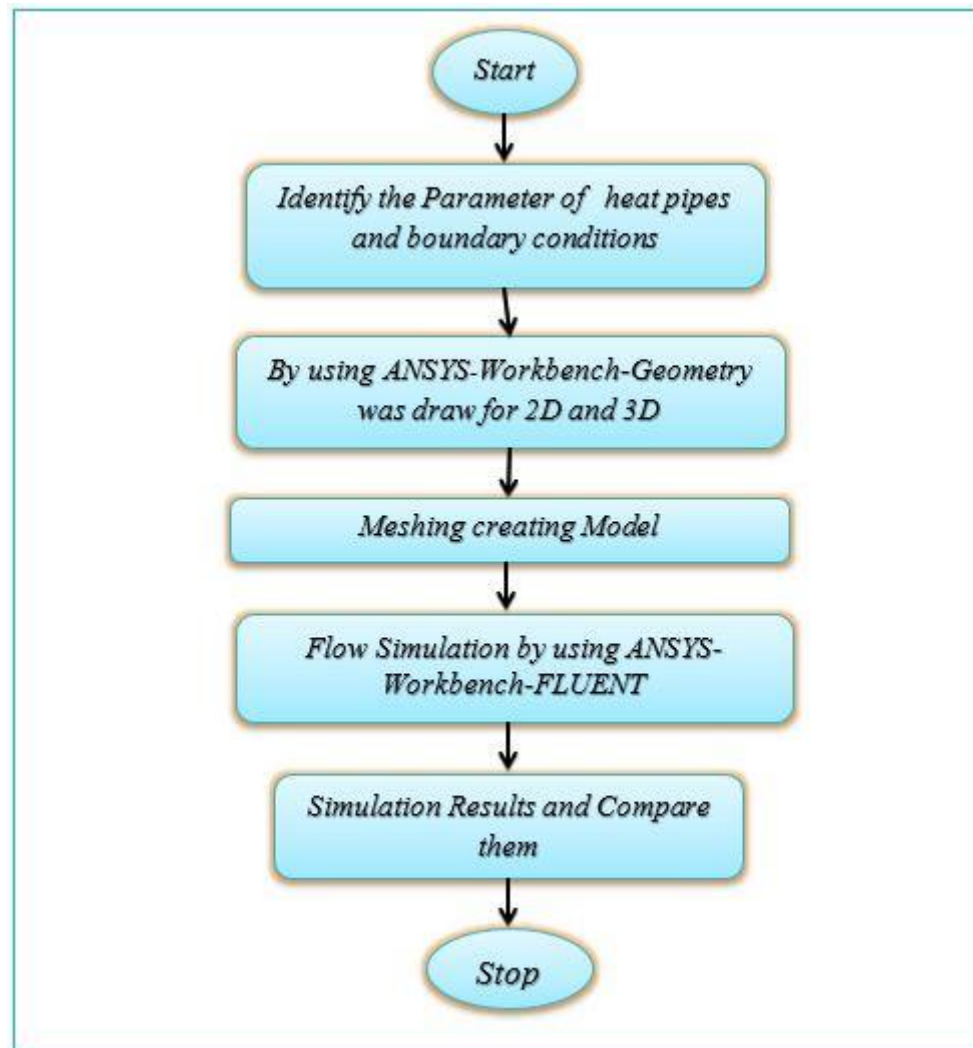


Figure (3.4): Numerical Analysis flowchart

### 3.8 Simulation Models

Eulerian-Eulerian model was the suitable model for the present work (fluidized bed with two-phase flow). We have a continual phase which was air while the other phase was a cement fly ash setting as a granular.[53]

Enable the energy equation and RNG option.

#### 3.8.1 Governing Equation

Choosing Euler model leads to a solved continuity, momentum, conservation, and energy equations for each phase whether the phase was granular or not; the result was different .So, CFD takes coupling manner [54] [55].

General equation that applied in Ansys fluent 18.0 were [56]

### 1-Continuity equation

The mass flow inside every control volume equals to the mass entering to that control volume minus that out from it, that statement could be written mathematically as

$$\frac{\partial \rho}{\partial t} + \frac{\partial u}{\partial x} + \frac{\partial v}{\partial y} + \frac{\partial w}{\partial z} = 0 \quad \dots (3.17)$$

In fluidized bed, continuity equation is used to calculate volume fraction. volume fraction is calculated for mixture from equation

$$\frac{1}{\rho_{rq}} \left( \frac{\partial}{\partial t} (\alpha_q \rho_q) + \nabla \cdot (\alpha_q \rho_q \vec{v}_q) \right) = \sum_{p=1}^n (\dot{m}_{pq} - \dot{m}_{qp}) \quad \dots (3.18)$$

### 2-Momentum equation

The equation in the general form is as below:

$$\begin{aligned} \frac{\partial}{\partial t} (\alpha_q \rho_q \vec{v}_q) + \nabla \cdot (\alpha_q \rho_q \vec{v}_q \vec{v}_q) = & -\alpha_q \nabla p + \nabla \cdot \bar{\tau} + \alpha_q \rho_q \vec{g} + \\ & \sum_{p=1}^n (\vec{R}_{pq} + \dot{m}_{pq} \vec{v}_{pq} - \dot{m}_{qp} \vec{v}_{qp}) + \\ & (\vec{F}_q + \vec{F}_{\text{lift-q}} + \vec{F}_{\text{vm,q}}) \end{aligned} \quad \dots (3.19)$$

The stress-strain tensor ( $\bar{\tau}_q$ ) is represented as:

$$\bar{\tau}_q = \alpha_q \mu_q (\nabla \vec{v}_q + \nabla \vec{v}_q^T) + \alpha_q \left( \lambda_q - \frac{2}{3} \mu_q \right) \nabla \cdot \vec{v}_q \bar{I} \quad \dots (3.20)$$

Where is  $\mu$  the viscosity and  $\lambda$  is the bulk viscosity.

For granular gas-solid flow. momentum conservation equation becomes:

$$\begin{aligned}
\frac{\partial}{\partial t}(\alpha_s \rho_s \vec{v}_s) + \nabla \cdot (\alpha_s \rho_s \vec{v}_s \vec{v}_s) = & -\alpha_s \nabla p - \nabla p_s + \nabla \cdot \vec{\tau}_s + \alpha_s \rho_s \vec{g} \\
& + \sum_{l=1}^N (K_{ls} (\vec{v}_l - \vec{v}_s) + \dot{m}_{ls} \vec{v}_{ls} - \dot{m}_{sl} \vec{v}_{sl}) \\
& + (\vec{F}_s + \vec{F}_{\text{lift},s} + \vec{F}_{\text{vm},s}) \quad \dots (3.21)
\end{aligned}$$

### 3- Energy Equation

In Euler multiphase the conservation of energy could be described as in equation (3.22) which is written for each phase:

$$\begin{aligned}
\frac{\partial Q}{\partial t}(\alpha_q \rho_q h_q) + \nabla \cdot (\alpha_q \rho_q h_q \vec{u}) = & \alpha_q \frac{\partial p_q}{\partial t} + \tau_q : \\
\nabla \vec{u}_q - \nabla \cdot \vec{q} + S_q + \sum_{p=1}^n (Q_{pq} + \dot{m}_{pq} h_{pq} - \dot{m}_{pq} h_{pq}) & \quad \dots (3.22)
\end{aligned}$$

### 4-Turbulence Model

Ansys Fluent 18.0 offers many approaches for the (k-ε) turbulence model in the multiphase flow:

A-Turbulence mixture

B-Turbulence dispersed

C-Turbulence model for all phase separately

Turbulence RNG model was set for fluidized bed model that can be expressed through these equations (Fluent User's Guide).

$$\frac{\partial}{\partial t}(\rho_m k) + \nabla \cdot (\rho_m \vec{v}_m k) = \nabla \cdot \left( \frac{\mu_{t,m}}{\sigma k} \nabla k \right) + G_{k,m} - \rho_m \epsilon \quad \dots (3.23)$$

$$\frac{\partial}{\partial t}(\rho_m \epsilon) + \nabla \cdot (\rho_m \vec{v}_m \epsilon) = \nabla \cdot \left( \frac{\mu_{t,m}}{\sigma_\epsilon} \nabla \epsilon \right) + \frac{\epsilon}{k} (C_{1\epsilon} G_{k,m} - C_{2\epsilon} \rho_m \epsilon) \quad \dots (3.24)$$

The density and the velocity of the mixture can be found by using previous equations.

$$\rho_m = \sum_{i=1}^N \alpha_i \rho_i \quad \dots (3.25)$$

$$\vec{v}_m = \frac{\sum_{i=1}^N \alpha_i \rho_i \vec{v}_i}{\sum_{i=1}^N \alpha_i \rho_i} \quad \dots (3.26)$$

The turbulent viscosity and kinetic energy of the mixture could found by using the following equations.

$$\mu_{t,m} = \rho_m C_m \frac{k^2}{\epsilon} \quad \dots (3.27)$$

$$G_{k,m} = \mu_{t,m} \left( \nabla \vec{v}_m + (\nabla \vec{v}_m)^T \right) : \nabla \vec{v}_m \quad \dots (3.28)$$

The present work constant was listed at the table (3.2)

Table (3.2) Model Constants

The constant	Value
<b>C<sub>mu</sub></b>	0.0845
<b>C<sub>1</sub> – Epsilon</b>	1.42
<b>C<sub>2</sub> – Epsilon</b>	1.68
<b>Dispersion Prandtl number</b>	0.75

### 3.9 Geometry Model

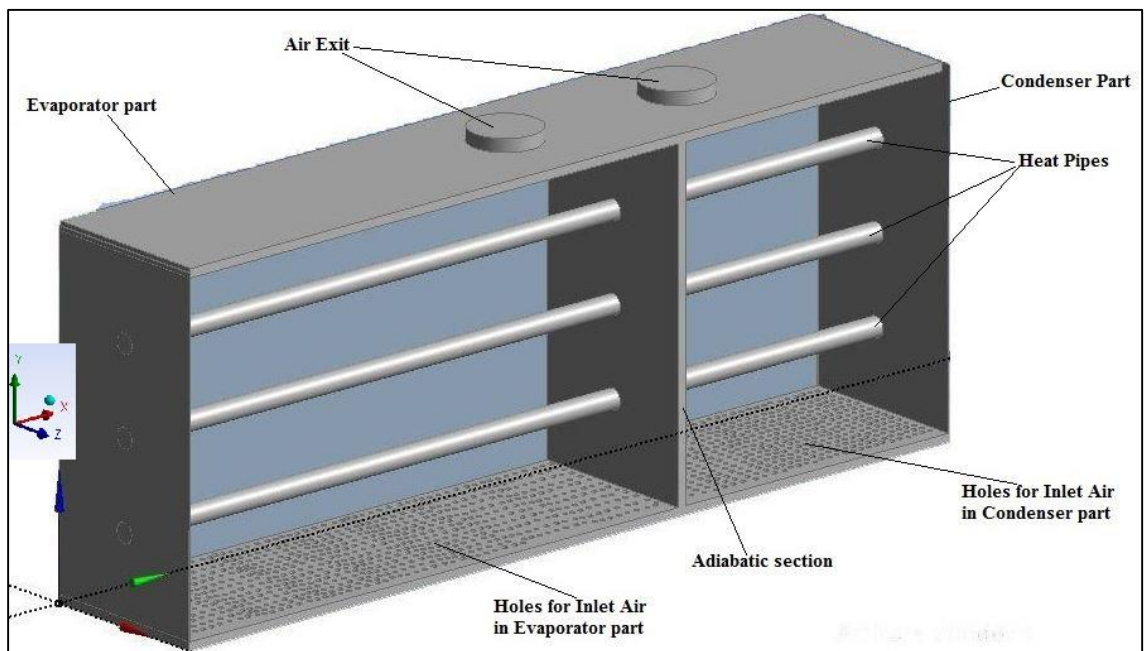
Figure (3.5 a-b) represent the test section description which consists of three heat pipes fixed horizontally with an isolated box. In the evaporator part, four different heights of particle were taken (2.5,5,7.5, 10) cm., and



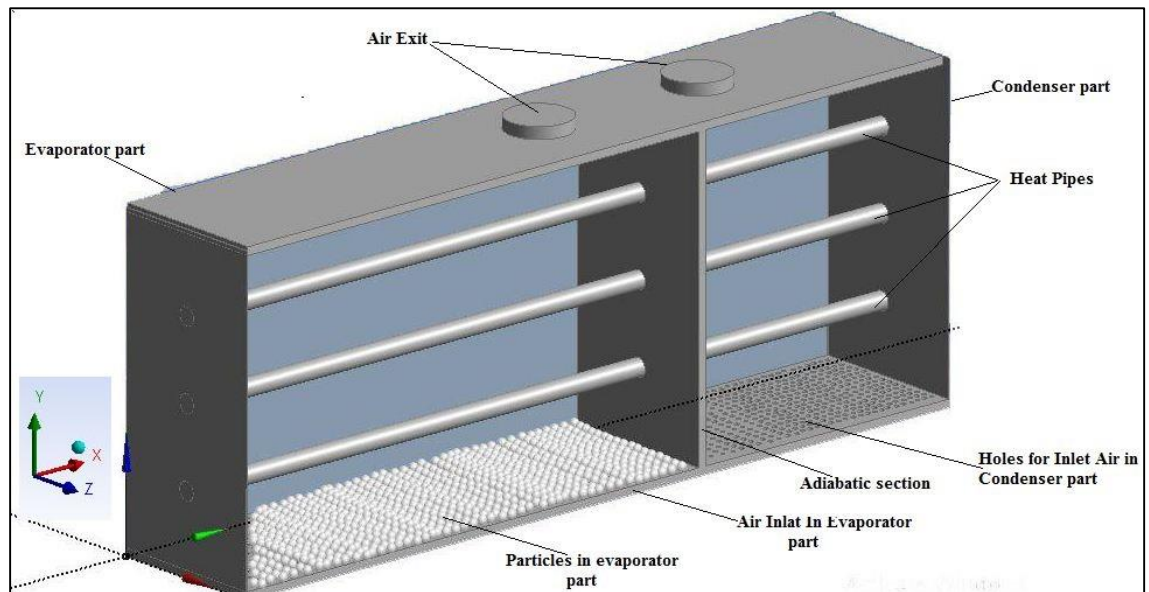
three air flow rates (0.133, 0.171, 0.209) kg/s. while the air flow rate at the condenser part was constant for each case at (0.0285) kg/s.

At evaporator part, it represents the box wall which set to be with zero particle velocity while the bottom side set to be the hot air inlet and at the top side there was a hole with (10.16) cm. as an outlet and its set to be an absolute pressure and set as (Reflect). It is taken heat pipe surface temperature as boundary conditions. At condenser part, the heat pipe surface temperature was taken from the experimental part as a boundary condition.

To simplify the solution, the evaporator and condenser part are separated to reduce number of mesh and time to converge. More simplification is by taking symmetric shape for both condenser and evaporator parts.



a-without particle



b-with particle

Figure (3.5): Test section geometry with and without particle bed

### 3.9.1 The Geometry

In the present work, to understand the heat temperature distribution, the geometry model was designed in 3D for each evaporator and condenser part as shown in figure (3.6). 2D is used in evaporator part to describe the velocity vector and particles behavior that it takes a clear vision. Design modeler engaged in Ansys workbench 18.0 is used to draw a rectangular shape in X-Z plan with 100 cm. length and width 19.5 cm. and draw line at 64.5 cm from start X axis. All that surface was generated and extruded normally with height 40 cm. New axis was created at the top box to sketch two circles that represent air outlet for evaporator and condenser part with a diameter of 10.16 cm. At Y-Z plain sketch, three circles with diameter 2.22 cm at half width and at height of (10,20,30) cm. were drawn from the base and chosen them as a cut material and generate it and extrude it for 100 cm. name selection for all parts will be the last step.

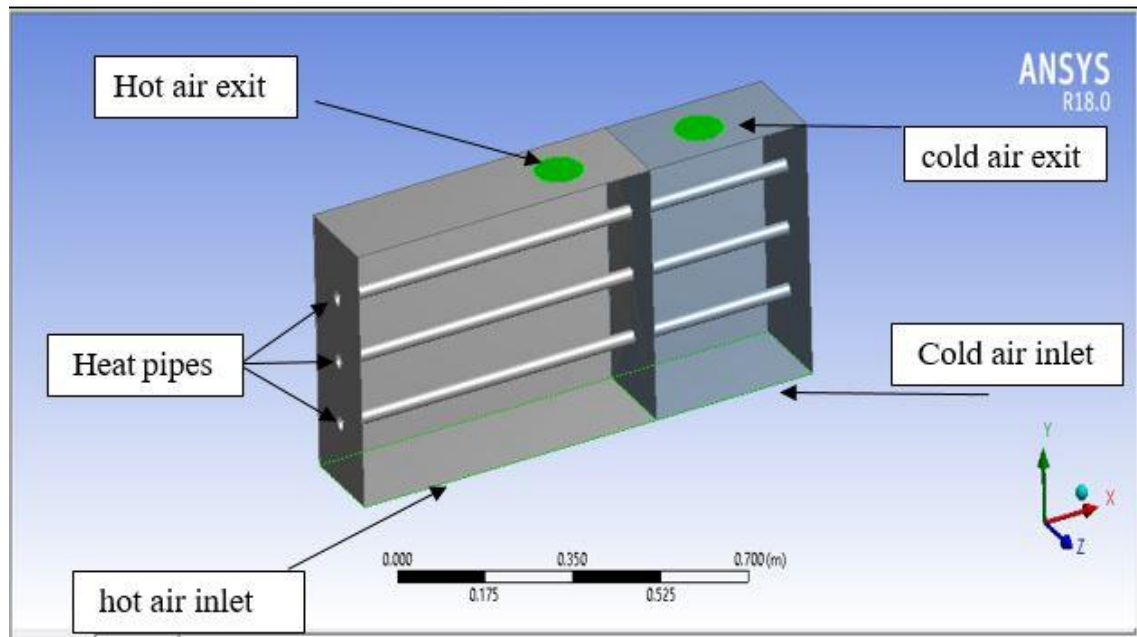


Figure (3.6): Test section geometry by Ansys

### 3.10 The mesh

There are more than one methods to meshing inside working area, choosing the typical method depends on many parameters such as geometry, flow field, and complexity, for the type and size of the mesh have severe effect on the accuracy of solution and time to reach convergent[57].

CFD has a suitable method to solve the problem in three dimensions since its solution depends on solving conservation, energy, momentum and continuity equation [57].

In case of two dimensions used a small element with a square shape (hexahedral) using meshing engaged with ANSYS FLUENT18.0. maximum size will be  $(4.5702 \cdot 10^{-3})$  and minimum size will be  $(4.570 \cdot 10^{-5})$  through smooth relevance. Under that condition, it produced (74608) node and (73705) element. Figure (3.7) shows the final mesh in two dimensions.

In three-dimension shape used (tetrahedral) mesh with a maximum and minimum size of  $(7.7997 \cdot 10^{-3})$  and  $(7.7997 \cdot 10^{-5})$  respectively that produced (1464078) element and (265908) nodes. Figure (3.8) shows final

mesh at three dimensions. The governing equation model was solved for each element at model geometry

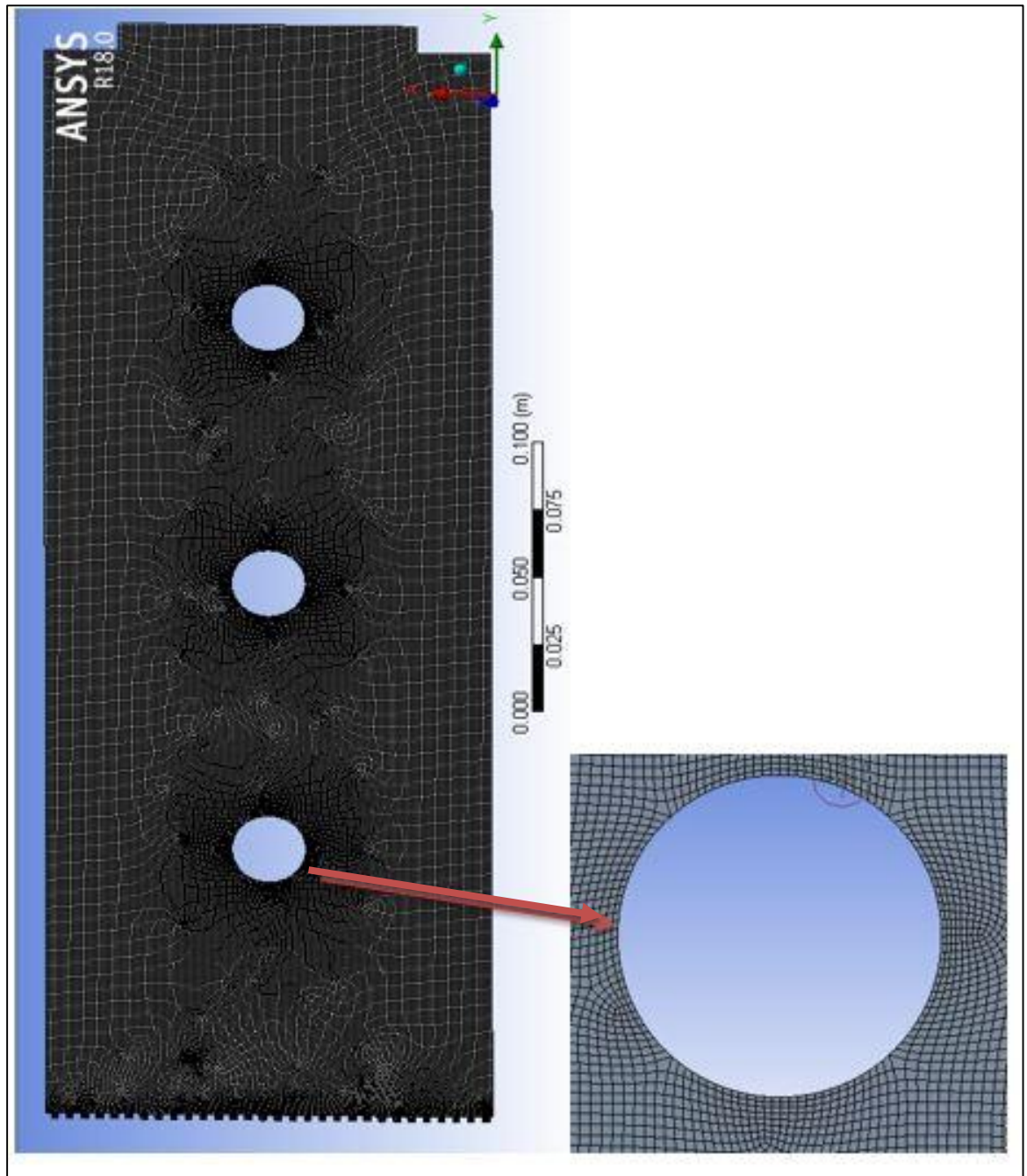


Figure (3.7): Two Dimensional Model Z-Y plane

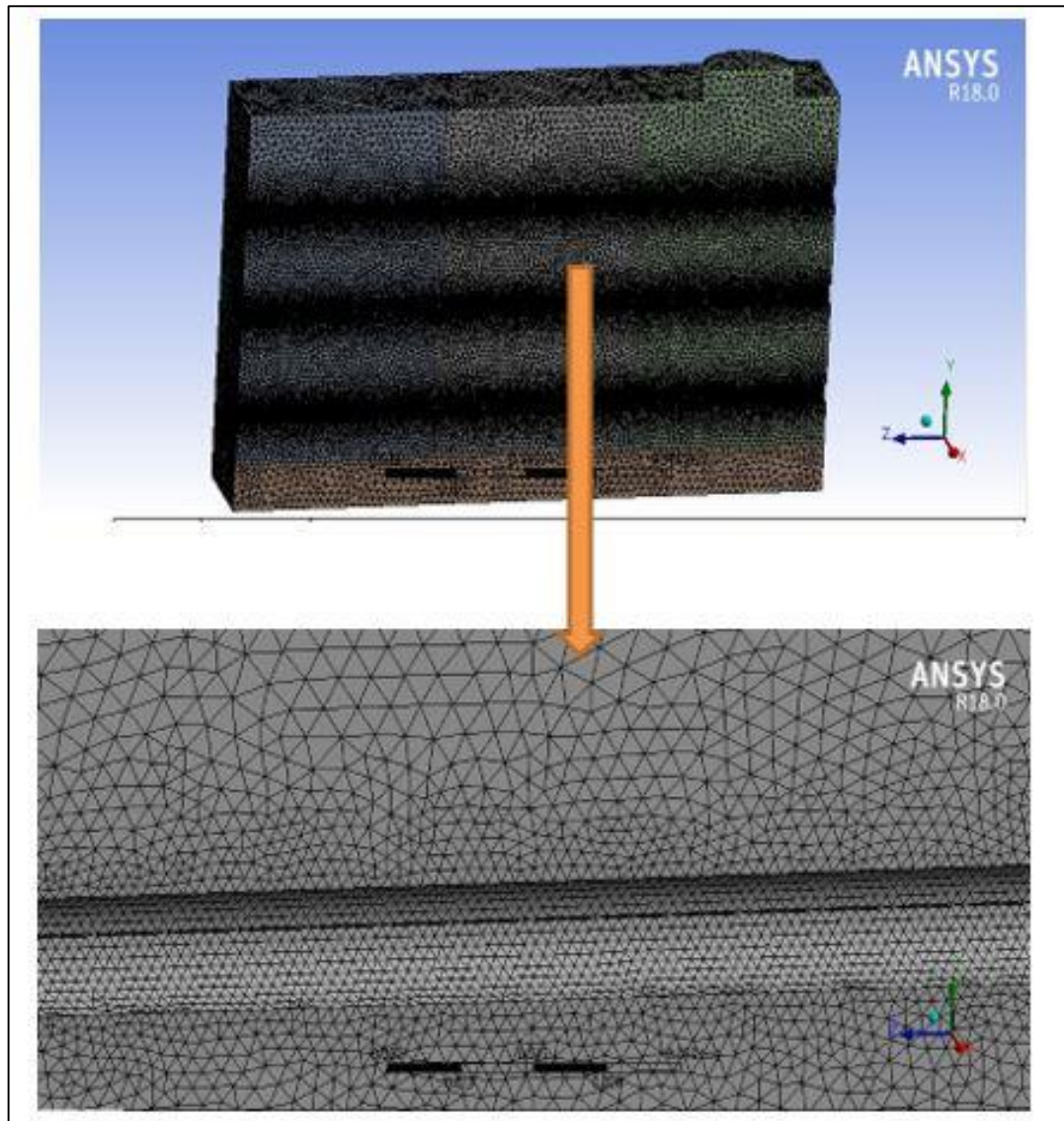


Figure (3.8): Three Dimensional Meshed Model

### 3.11 Boundary Conditions

Pressure, velocity and the temperature were defined for two and three dimensional model for the fluidized bed.

All walls were considered as isolated and there was no heat flow through. Also, there was no motion closed to the wall and roughness constant was 0.5.[56].

At air inlet from the bottom part of the box in the evaporator part the mass flow rate and the temperature of the air inlet to the box after heated were the important parameters. The air flow rate range is (0.133 to 0.209) kg/s and

the air velocity depends on the amount of air inlet. Set the lower part as (wall jet) is to prevent return particles inside the pipe. The outlet part which was the upper part of geometry set as (reflect) to prevent run particle out of box. The pressure outlet at evaporator and condenser part was specified as the outlet domain atmospheric pressure ( $P_o= 0$ ). Table (3.3) represents air flow rates at evaporator part for each velocity amount at evaporator line. At the pipe surface,( trap) option was activated since some of the particles were residual on the pipe surface. Table (3.4) summarizes the boundary conditions. At condenser part, the air flow rate (0.0285) kg/s was the boundary condition at inlet which is the lower part in the condenser; and at the exit the atmospheric pressure was ( $P_o= 0$ ), and the heat pipe surface temperature.

Table (3.3) flow rate at evaporator part

<b>Velocity (m/s)</b>	<b>3.5</b>	<b>4.5</b>	<b>5.5</b>
<b>Discharge(kg/s)</b>	<b>0.133</b>	<b>0.171</b>	<b>0.209</b>

Table (3.4): Boundary conditions summery

EVAPORATOR PART				
B.C.NO.	HEAT PIPE SURFACE	INLET	OUTLET	WALL
1	(Trap)	$v= 0.8739-1.1236-1.377$ m/s	Reflect surface	Roughness friction = 0.5
2	Surface temp. from experimental	$m' =0.133-0.171-0.209$ kg/s	$P_{out} = 0.0$	
3		(wall jet )		
CONDENSER PART				
	HEAT PIPE SURFACE	INLET	OUTLET	WALL
1	Surface temp. from experimental	Air flow rate =0.028 kg/s	$P_{out}= 0.0$	Roughness friction = 0.5

### 3.12 Under Relaxation Factor

To prevent divergence solution. the under-relaxation was applied as follows [58]

$$\phi_{new} = (1 - \alpha)\phi_{prevoius} + \alpha\phi_{calculated} \quad \dots (3.29)$$

Where;

$\alpha$  : is under- relaxation factor.  $\phi_{-new,prevoius,calculate}$  : scalar dependent variable for new, previous, and calculated value at simple method.

The value for the under-relaxation factor should be in the range ( $0 < \alpha \leq 1$ ). The relaxation for the present work for momentum, pressure and volume friction were shown in table (3.5)

Table (3.5) Under relaxation factors

Variable	Relaxation factors
Pressure	0.3
Momentum	0.7
Volume fraction	0.55
Turbulent kinetic energy	0.8
Turbulent dissipation rate	0.8
Density, body force Energy ,turbulant viscosity	1

### 3.13 Steps To Simulation model

The previous steps were taken to simulate the test section in computational fluid dynamics.

1-Geometry modeled by ANSYS design modular workbench 18.0.

2-The mesh at ANSYS workbench 18.0 was generated, the mesh type depends on whether 2D or 3D model.

3-Chosen mathematical model.

4-Defined material of each phase.

4-Set each phase and determine the boundary condition.

5-Solution initialized.

6-The calculation took place at 2D with a time step of (0.005) sec. and with a number of time steps of (400), and maximum iteration for each time step is (30), and for 3D. The present work deals with it as a steady state; and number of iteration was (100). The residual of solution for 2D and 3D are shown in figures (3.9) and (3.10) respectively.

The result of the temperature distribution and particle move direction were extracted.

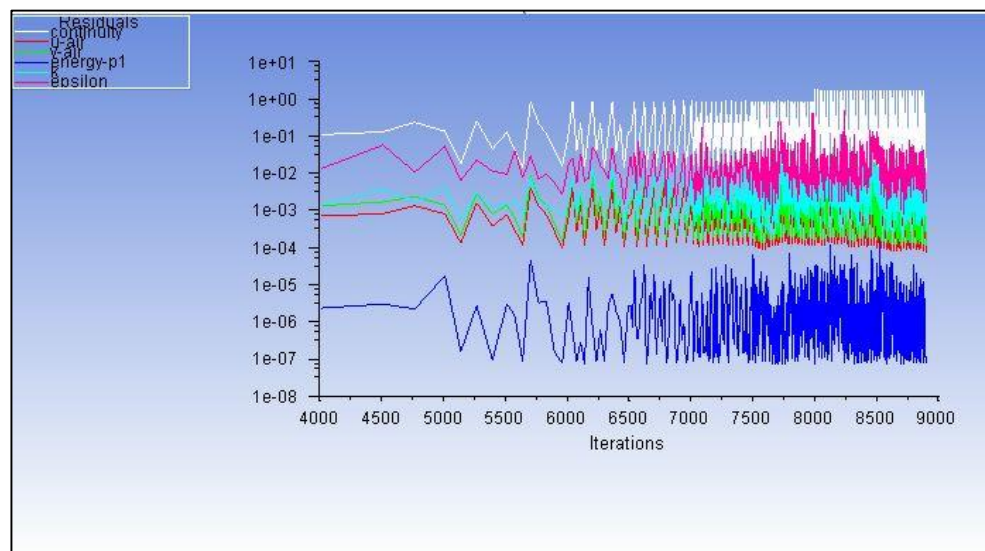


Figure (3.9): The Residuals error monitor 2D



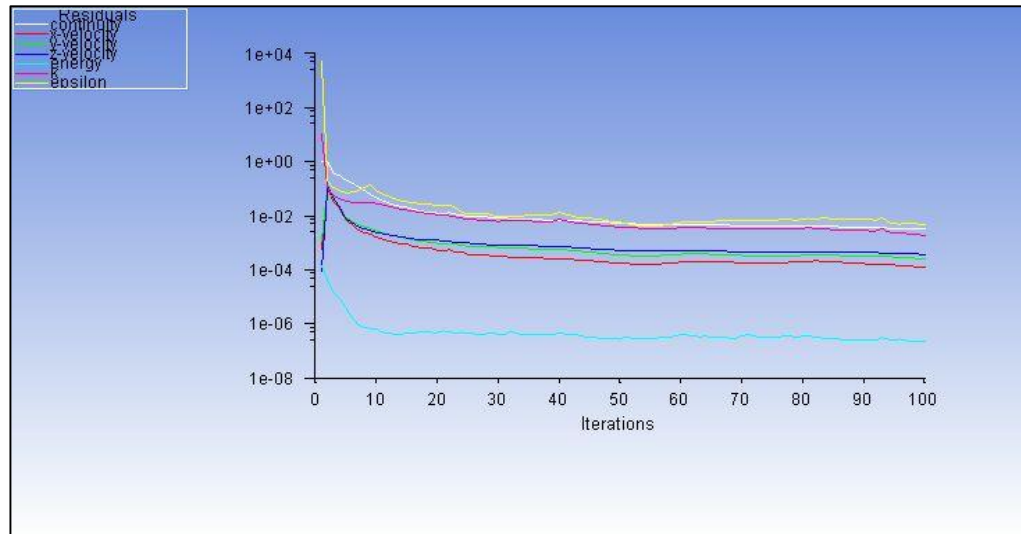


Figure (3.10): The Residuals error monitor 3D

### 3.14 Demonstrating the Results

In order to find heat distributions in fluidizing bed model. And to compare the result of Nusselt number, exerted from numerical with the experimental value. In numerical study, measuring the temperature at the same position depends on an experimental part; and studying the effect of fluidization on heat transfer performance to heat pipe. For more comprehension to particle motion, 2D model shows how the second phase behaves under mixture flow.

**CHAPTER FOUR**

**EXPERMANTIL**

**METHOD**

## CHAPTER FOUR

### Experimental method

In this chapter suitable heat pipe component was chosen in order to get the maximum amount of power transfer through it.

The experimental rig was designed, to get the effect of fluidization on heat transfer coefficient value. And also fluidization effect on heat pipe transmission power value. The study deals also with pressure drop during fluidized bed and its relation with porosity, and to describe the practical part. it can be classified into:

- 1- Fabricated the test rig body and the main components.
- 2- Heat pipe manufacturer.
- 3- Heat pipe tested.
- 4- Choosing particles and their properties.
- 5- Measuring devices that used and calibration.
- 6- Experiment procedure.

#### 4.1 Fabricated rig body and the main component

The operational part was carried out in heat transfer laboratory, in the college of engineering, University of Kufa. Plate (4-1) and figure (4-1) represent a photo and schematic diagram for the experimental test rig, respectively.

The rig consists of a wooden box with three heat pipes that were put inside horizontally. Wooden plate divided that box to create heat pipes evaporator and condenser parts; air passes through each part, in evaporator

part heater was used to heat air before entering the box and putting particle to enhance heat transfer to heat pipe with different velocities, approximately all parts were manufactured manually and tested before start running.

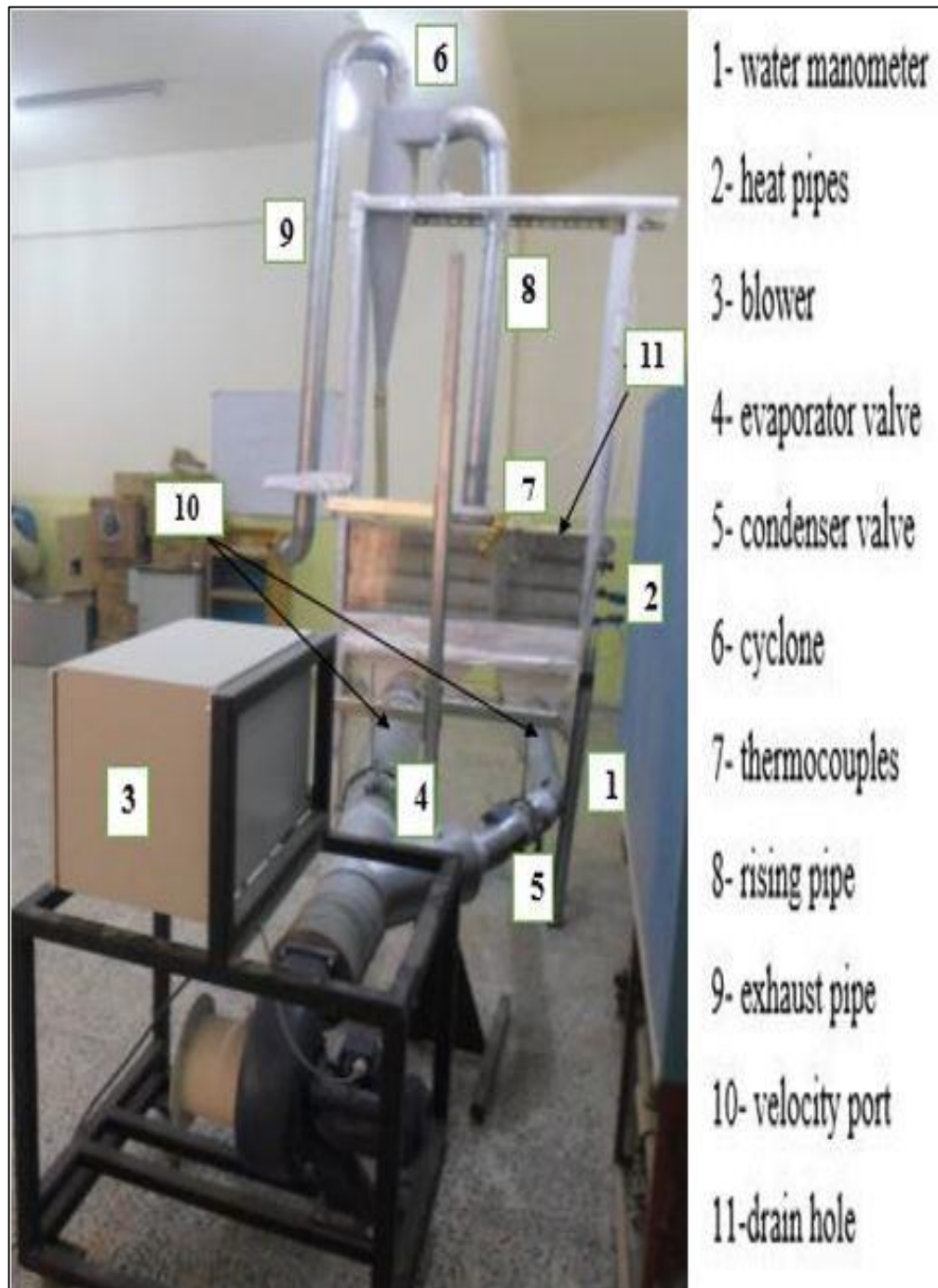


Plate (4.1): The experimental apparatus

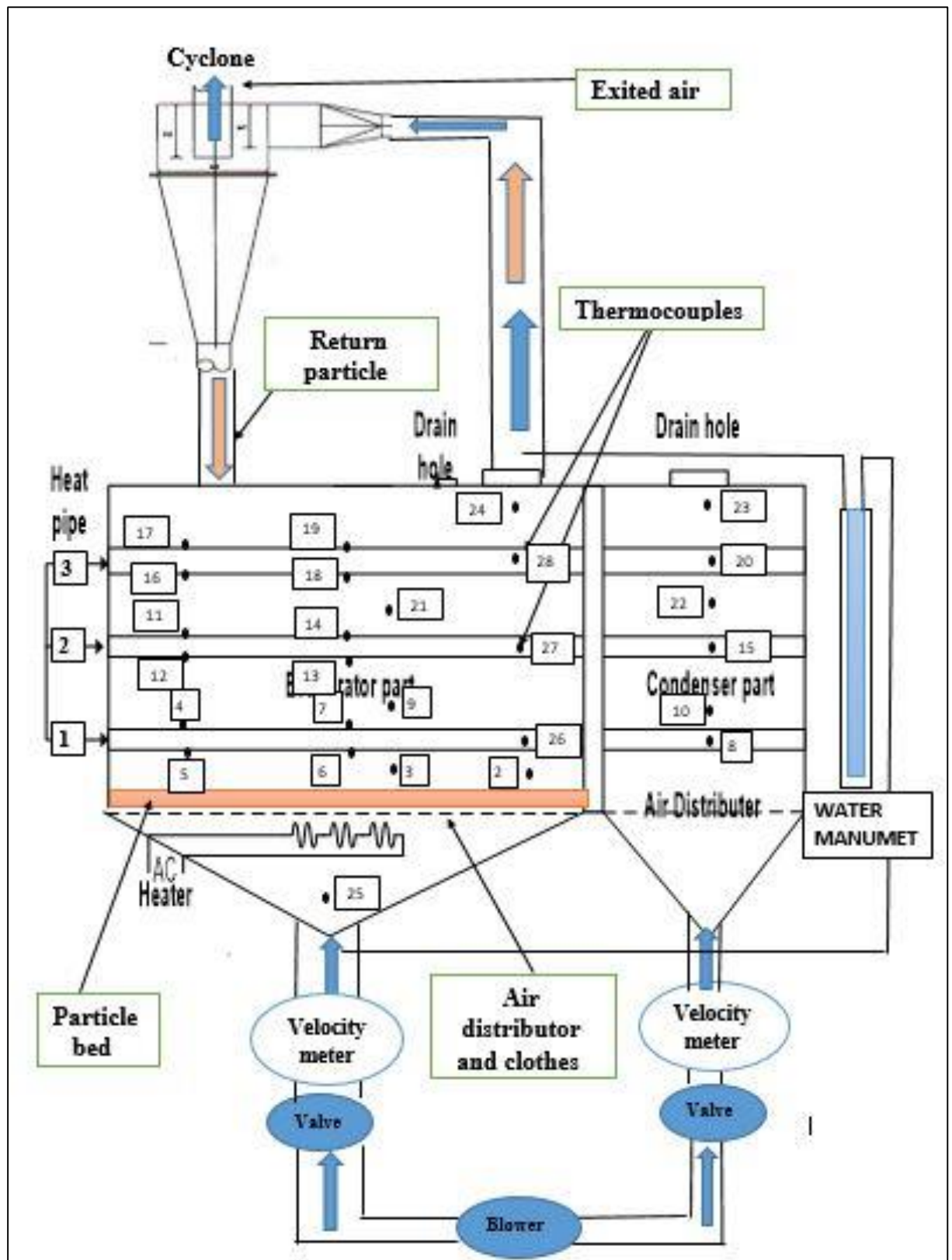


Figure (4.1): Schematic of the Experimental apparatus

### 4.1.1 Main box Body

The body of the rig was fabricated from plywood with thickness 1 cm. since the most important item in heat transfer calculation was heat loss. In that work, there was an attempt to reach to the hypothesis that the wall was isolated as much as possible.

The main body was divided into two parts evaporator and condenser, from previous studies that the evaporator part has a severe effect on amount of power that absorbs from heat pipe [59]. Therefore, evaporator part is made longer than condenser part, evaporator part is (64.5 cm) and condenser part is (34.5cm) and there is adiabatic section separated the two parts with (1 cm) thickness. The width of wooden box was (20 cm) and with height of (40 cm); the forward face of the box was made by slab of glass to easily observe particles behavior and also to watch the thermocouple sensor stability.

Each one of the used three heat pipes was fixed horizontally between evaporator and condenser part passing through a circular hole in adiabatic section and the distance between each one is (10cm) as shown in Plate (4.2).

The air is coming from the air supply, and to have uniform distributed inside evaporator and condenser parts there were two inverse conical shape that were fixed in lower condenser and evaporator parts to ensure a good air distributed when enter in to the box.



Plate (4.2): Main body box

#### 4.1.2 Distributed Plate

To have a good air distributed inside each part of box and also to create a base to carry particles, aluminium plate was used with (1mm) thickness fixed at the bottom of the box; and making holes in it with diameter (6mm) and fixed the aluminium rod under it to reinforce the base. That procedure repeated at each part separately, the plate properties at evaporator part fixed at table (4.1), Plate (4.3) shows distributed plate.

Table (4.1): Distributed plate properties

Hole diameter	Hole number	Open area mm <sup>2</sup>	Dead area mm <sup>2</sup>	Open area ratio	Type
6 mm	435	12299	116701	8.92 %	Hole type



Plate (4.3): Air distributed plate

### 4.1.3 Heating Source

To heat the air that enters the main box; to the desire temperature Electrical heater with consumable current (16.3 AMP) under (220 V) voltage and (3586) Watt was used, Plate (4.4) shows the electrical heater

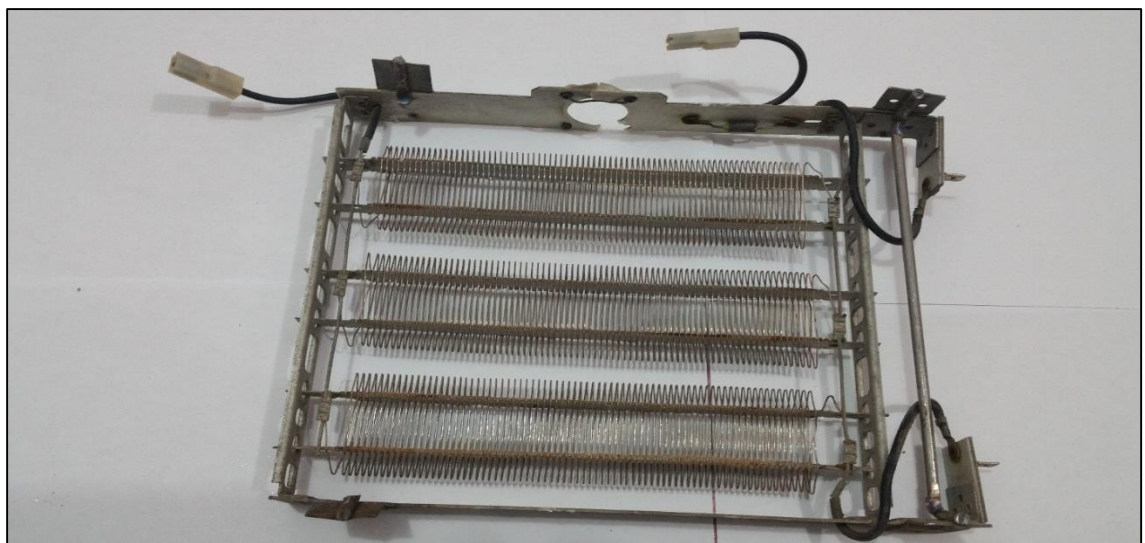


Plate (4.4): Electrical heater

### 4.1.4 Connected lines

From air source to the box used two diameters connected pipes. One of them is with (20 cm) diameter that transfers the air to the evaporator part, and the other was (10cm) diameter to transfer the air to the condenser part. Each one from that lines have butterfly valve to control the air amount and



also each one has a small hole near the box to insert the hot wire sensor to measure the air velocity, as shown in Plate (4.5).



Plate (4.5): Connected line

#### 4.1.5 Air supply source

To measure the effect of fluidized bed on heat transfer to the heat pipe, the air supply amount should be a constant flow rate during the process. It is also looking for air supply accouter enough air to move the particle to the box roof. That's why it cannot use air compressor but it can choose air blower. Blower with GUNT HL710 type, 1.0KW was choosing, Plate (4.6) represents air blower.



Plate (4.6): Air Blower.

### 4.1.6 Particle Separator Device (Cyclone)

The most important part in cyclic fluidized bed was cyclone. That device is in charge of returning particles to the main box. So, in the present work, the dimensions that listed in table (3.1) were adopted, where the pipe rising to cyclone 4" and return particle pipe was 2", as shown in Plate (4.7).



Plate (4.7): Cyclone

## 4.2 Heat pipe design and manufacture

### 4.2.1 Heat pipe structure

The main purpose of heat pipe container was to provide a seal space for working fluid and to prevent leakage and also to prevent out pressure that comes inside heat pipe due to the heat pipe initially evacuated before charging with working fluid; Figure (4.2) showed the main parts of a standard heat pipe. Choosing the correct heat pipe material was very important to get as large as possible from heat transfer. So many items should be taken in account such as, the ratio of strength to weight, thermal

conductivity, machinability. In the present work, copper pipe was chosen where the container consists of: -

**A-** shell: it is made of copper with length (100cm) and out diameter (2.22cm) and inside diameter was (1.98cm) as shown in figure (4.8)

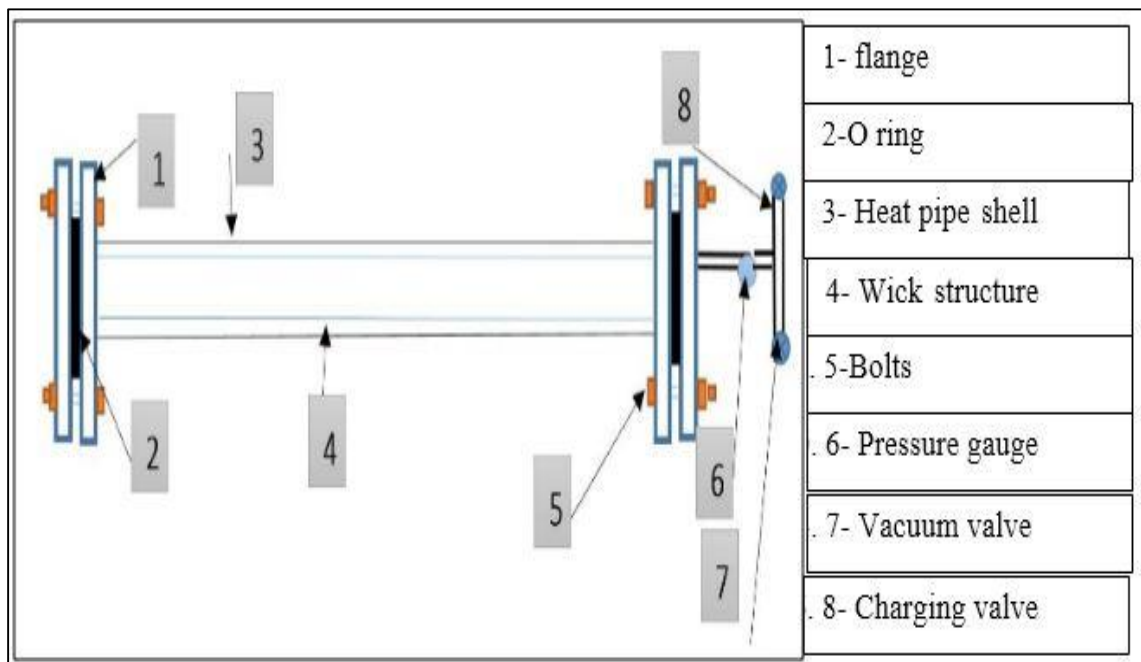


Figure (4.2): Heat pipe and charging parts



Plate (4.8): Copper pipe

**B-Flanges:** There are two flanges welded to the ends of each pipe, by brass welding which is suitable to weld brass with copper. Each one of that flange has the central hole equal to the outer pipe diameter. Also has four holes with (10mm) diameter. To connect the flange with a plate that covers it at two ends O ring was put between them to prevent leakage as shown in figure (4.9). At one end, small hole was made with (6mm) diameter to weld the pressure gauge, vacuum and charging valve as shown in Plate (4.10).



Plate (4.9): Flange and plate



Plate (4.10): The heat pipe flange and plate and charging unit

### 4.2.2 The wick

The wick was a very significant part in heat pipe construction. It lies inside pipe touching to its inner diameter. The wick was in charge of returning working fluid from condenser to evaporator by capillary force. If the wick holes are so tiny, it means high capillary force that leading to increase pumping force; that also increasing flow resistance during the wick.

The heat transferred to heat pipe from the pipe surface to wick until reaching to working fluid radially. So, porosity has severe effect on the amount of heat transfer since it affects temperature drop.

Thermal conductivity and porosity of wick were related to each other; low porosity leads to high thermal conductivity.

Insuring of wick saturated with working fluid and low fabricating cost were very important points in the choice of wick.

In the present work, a leaf of wire screen mesh with (100) cm length and (31.1) cm width was turned around 0.5 inch a copper tube with (150) cm length to make wick assembly as five layers of screen mesh. The copper pipe with the mesh coatings is inserted into the container and removed to line the inside wall of the container, while the copper tube removed sensibly to ensure that there is not any wick perms for that perm has counter productivity on heat pipe performance. The wick has (7086) hole/ meter and with wick thickness (0.11) mm.

The wick fitting inside heat pipe is shown in Plate (4.11).



Plate (4.10): Wick inside the heat pipe

### 4.2.3 Working Fluid

The main important part of heat pipe design was the working fluid due to its responsibility on heat transfer from evaporator to condenser part. So, there were many properties that should be found in the working fluid such as: high latent heat to transfer large amount of heat under low pressure, high surface tension to work against gravity if needed and to saturate wick structure, also its stability under high rang of operation temperature, and low cost. That's why in present work, distilled water was used as a working fluid [60]

The working fluid calculation are listed in appendix A, table (4.4) listed all heat pipe specification

Table (4.2): Heat pipe specification

NAME	SYMBLE	VALUE
Container outer diameter	(Do)	22.225mm
Container inner diameter	(Di)	19.8 mm
Overall length	L	1000 mm
Evaporator length	Le	645 mm
Condenser length	Lc	345 mm
Adiabatic length	La	10 mm
Working fluid	Distilled water	65.56 cc
Porosity	$\epsilon$	0.773
Number of the screen layer	NO	5
Vapor radius	rv	9.35 mm
Wick zone thickness	t	0.55mm

#### 4.2.4 Cleaning heat pipe before charging

If there were impurities inside the heat pipes during the manufacturing process, they must be removed before charging with working fluid. The procedures below were done for cleaning [61].

A-Cleaning the container after welding flanges on the two sides by using (trichloro ethane) which is a solid material that was removed by clothes.

B- Washing the container with cold water.

C- The container was immersed in chloric acid (HCL) for three minutes at room temperature.

D- Washing the container by distilled water to remove the acid.

E- Drying the pipe by using nitrogen to prevent oxidize creation.

Then, turning the wick inside heat pipe container is started and fixed the flange in two ends after putting the “O” ring between flanges to prevent leakage.

#### 4.2.5 Heat pipe Evacuated and Charging With Working Fluid

Figure (4.3) shows the fulling system of buret with calculated amount of working fluid. Fulling procedure are listed below:

- 1- Closing Valve A and opening each C & B valves.
- 2- Running the evacuated pump for half an hour and immersed the heat pipe in boiling water at that procedure all the air exited from the heat pipe resulting the pressure inside heat pipe reaching to (-30 psi).
- 3- Closing the valve B and opening gradually the valve A and putting the heat pipe in ice water, hence the working fluid enter the heat pipe and closing valve A when working fluid finished inside buret and valve C also closed.

The valve C will remain in heat pipe, in the same way, each one of the three heat pipes was charged.

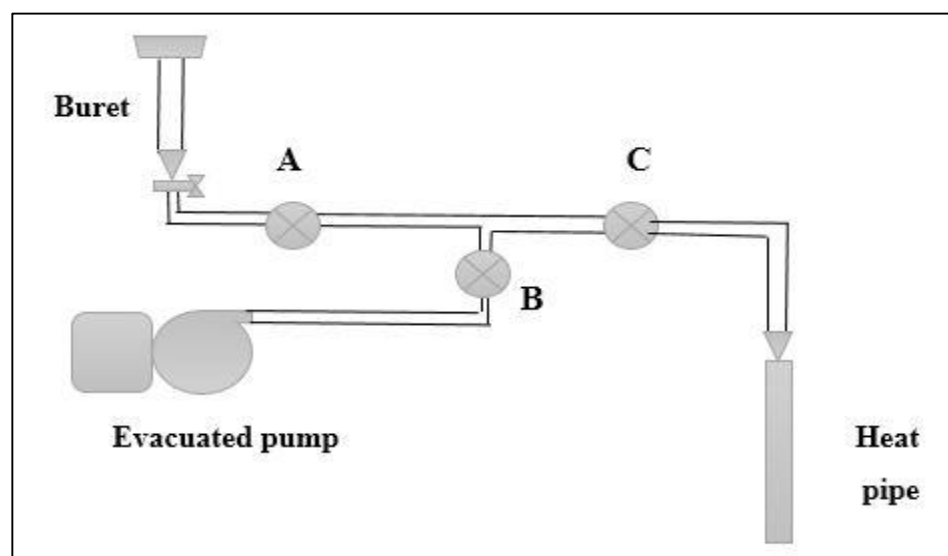


Figure (4.3): Charging system



### 4.2.6 Heat pipe limitation

Heat pipes experience showed that heat transfer limitations depend on the working fluid, the wick structure, heat pipe dimensions, and the heat pipe operational temperature. These limitations included vapor-pressure, sonic, entrainment, capillary, and boiling limits[62]. There is a compound curve that gives the maximum heat transfer rate of the heat pipe as a function of the operational temperature. The concept of these limitations and equations that represent them by showing their results were all mentioned in appendix A, results of the above mentioned limitations were calculated are listed in table (4.3).

Table (4.3): Present work heat pipe limitation

Capillary limit (W)	Viscous limit(W)	Sonic limit (W)	Entrainment limit(W)
$3.1813 * 10^4$	$23.08 * 10^5$	$15.637 * 10^3$	$17.013 * 10^3$

### 4.3 Heat Pipe Tests

There were many simple tests that might be done on heat pipe After manufacturing, cleaning and charging. [63]

1-Shaking the heat pipe hard, in case that there were any water impinging inside the heat pipe which means the wick was not saturated with working fluid whether heat pipe was a good design.

2- Heat pipe exposed to a high amount of heat that may encounter during the experiment and observing its behavior.

3- Putting one end of heat pipe at hot water and checking the response speed to reach the heat to another end by touching it. Figure (4.4) represents the

flow chart of manufacturing and testing steps of the heat pipe to be ready to use in experimental work.

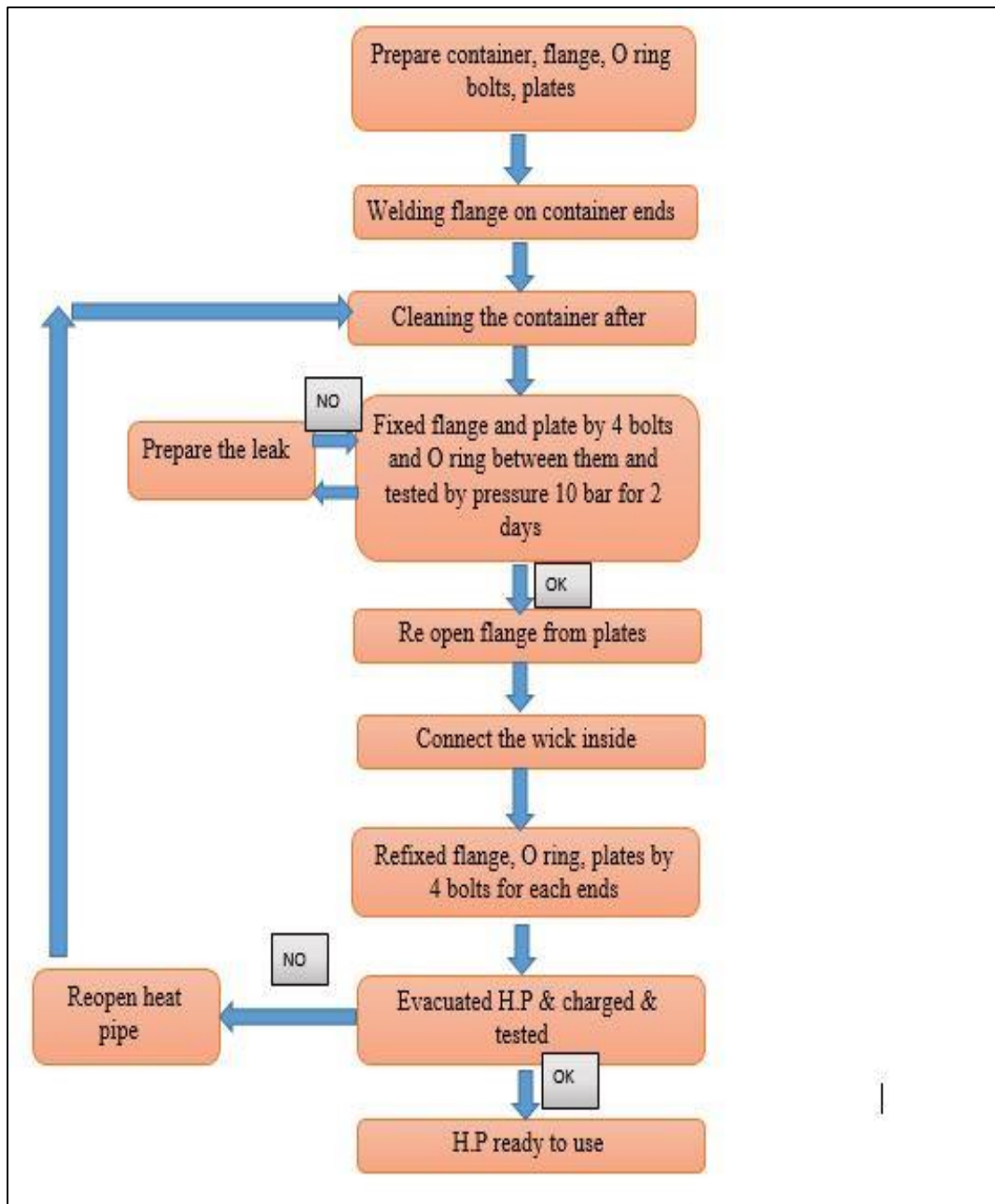


Figure (4.4): Flow chart for heat pipe manufacture and testing

#### 4.4 Choosing Particle And Its Properties

The cement fly ash of Al-Kufa cement factory was chosen to simulate its chimney and try to find the amount of energy recovery that could be achieved when used heat pipe. Variable charge from ash will be used by supplying the ash in different heights in evaporator part (2.5, 5, 7.5 and 10) cm. to simulate different amounts of fly ash in cement chimney.

##### 4.4.1 Particle density

Through employing known dimensions' cylinder with the help of an accurate electronic scale, it was found that the density was equal to (1117 kg / m<sup>3</sup>) as shown in Plate (4.11).



Plate (4.11): Cylinder shape and sensitive scales

##### 4.4.2 Thermal conductivity

To measure the thermal conductivity of cement fly ash and according to the thermal conductivity device shown in Plate (4.11) a rigid model must be created from cement fly ash. So, fly ash and water were mixed together and put inside rectangular mould and press it and leave for four days to dry.

Then, the rectangular mould was cut by using a special tool into two cylindrical shapes with diameter (2.5 cm), the first and the second shapes have lengths (4.45 cm) and (5.73 cm) respectively. Each one of those shapes was deeply holed at both ends with (3 mm) diameter reaching the center of the shape, as shown in Plate (4.11).

Thermal conductivity for cement fly ash was measured (1.25 KW/m.c)



Plate (4.11): Thermal conductivity device and samples

#### 4.4.3 Particle Diameter

As shown in plate (4.12) sieving method was used to determine the particle diameter. Five sieves with holes (0.417, 0.289, 0.147, 0.074, and 0.053) mm were used, and by measuring the amount of remained particles over each sieve and the sphericity amount for each sieve hole and by using equation  $d_p = 1 / \sum(x_i / (d_{pi} * \Phi_i))$  ... (4.1)

the particle diameter is calculated as shown in table (4.4) which is equal to (105  $\mu\text{m}$ ) [51].

Then, the overall calculated particles properties were listed in the table (4.5).

Table (4.4): Sieve diameter and sphericity to calculate particle diameter

$d_{pi}(\text{mm})$	Weight (gram)	$x_i$	$x_i \%$	sphericity
0.417	4	0.004	0.4	0.9616
0.289	28	0.028	2.8	0.9718
0.147	588	0.588	58.8	0.9853
0.074	343.5	0.343	34.3	0.9924
0.053	30.5	0.0305	3.05	1
less	6	0.006	0.6	

$$d_p = 1 / \sum(x_i / (d_{pi} * \Phi_i))$$

$$d_p = \frac{1}{\left(\frac{0.004}{417 \cdot 0.9616} + \frac{0.028}{289 \cdot 0.9718} + \frac{0.588}{147 \cdot 0.9853} + \frac{0.343}{74 \cdot 0.9924} + \frac{0.0305}{53 \cdot 1}\right)} = 105 \mu\text{m}$$



Plate (4.12): Set of the sieve and digital balance

Table (4.5): Cement fly ash particles properties

$\rho$ kg/m <sup>3</sup>	$C_p$ J/kg k	K W/ m .k	dp $\mu$ m
1117	860	1.25	105

## 4.5 Instrument devices And Calibration

### 4.5.1 Air Flow Measurement

To measure the amount of air that flow through evaporator part and condenser part, hot wire anemometer (TES 1340) was used to measured velocity. Plate (4.13) shows the hot wire that used in the experiment and its certificate. Hot wire properties listed at appendix B.



Plate (4.13): Hot wire thermos- anemometer sensor model (TES 1340)

### 4.5.2 Pressure drop measurement

To measure the pressure drop during the evaporator part, water manometer was used and pressure drop was measured for each velocity under each particle height as shown in Plate (4.14).



Plate (4.14): Water manometer

### 4.5.3 Temperature recorder

To measure the temperatures in the test section. Temperature recorder of type BTM with 12 channels was used, and stored the data on SD RAM. Many kinds of thermocouples could be connected with it just to choose the thermocouple type. In data recorder before start reading. It will be set at 2 minutes, as a time steps to record the data and with an overall time of 30 minutes for each run. Data recorder and its certificate were shown in Plate (4.15).

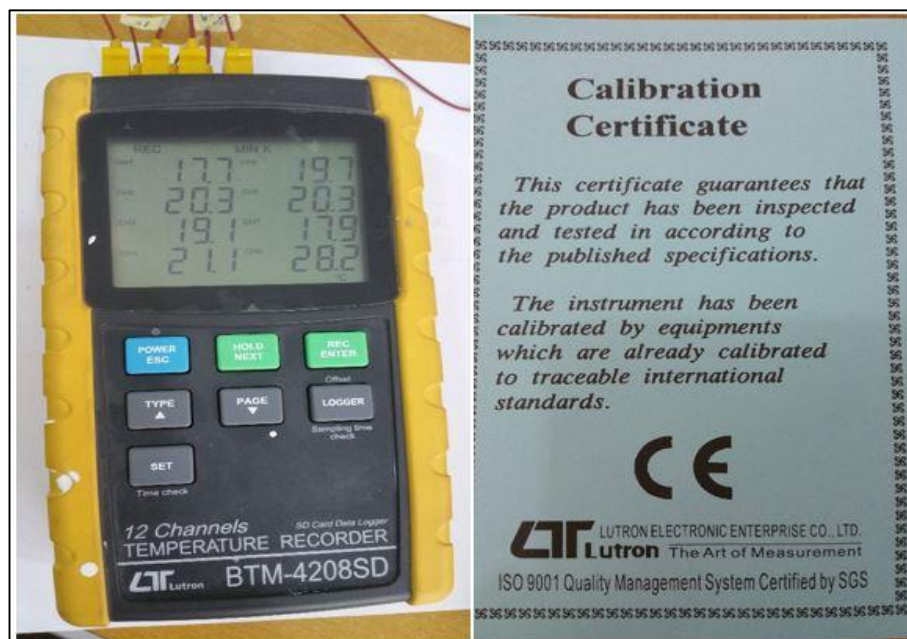


Plate (4.15): Data recorder

#### 4.5.4 Thermocouples

Twenty-eight thermocouples type K were used in the present work, five of them were on the surface of each one of the three heat pipes at evaporator part; and one at the condenser part surface, one is before the heater and another one is after it in evaporator part, two are above of the distributed plate and one is after each pipe in evaporator part and three are after each pipe in condensers part, see Figure (4.1). Each one of thermocouples was calibrated as shown in appendix (B). Plate (4.16) represents K type thermocouple.



Plate (4.16): K type thermocouple

#### 4.6 The error analysis

The percentage error was calculated for all used thermocouples in the present work as listed in appendix (C) [64]

#### 4.7 Experimental procedure

1- Firstly, the test starts with no particle on the evaporator part. Run the blower, the hot wire was used to measure the air velocity in evaporator as 3.5m/s and at condenser parts as 3m/s.



- 2- Run the electrical heater (3586) Watt to heat the air inlet to the box, at the same time run the data recorder to start recording the temperatures to memory card for (28) thermocouples, that is after setting the data recorder to record data each 2 minutes and take the final data within 30 minutes.
- 3- Record the water manometer reading for this speed.
- 4- Turn off the heater and leave the blower running for some time to cool the heat pipe until reaching to starting temperature.
- 5- Increase the evaporator air velocity to (4.5) m/s and leave the condenser velocity at (3) m/s and that happened by butterfly air control valve.
- 6- Run the electrical heater and record the thermocouples readings for half an hour by 2 minutes time step.
- 7- Record the water manometer reading for this speed.
- 8- Repeat steps 4, 5, 6,7 with another velocity at evaporator part (5.5) m/s and record the new temperatures and manometer readings.
- 9- Add cement fly ash particles to the evaporator part in the box by removing the upper box cover, starting with (2.5) cm height.
- 10- Repeat the steps from one to eight to take the set of reading at 2.5 cm particles height and recording three reading sets, one for each velocity (3.5, 4.5, 5.5) m/s
- 11- Repeat the step 9 with cement fly ash thickness 5 , 7.5 and 10cm. and for each thickness take three sets of reading, one set for each velocity.

### 4.7.1 Calculation procedure

time-min.	1	2	3	4	5	6	7	8	9	10	11	12
2	90.4	55.7	52.6	35.8	36	45.8	42.6	25.4	51.3	21.2	33.6	33.5
4	91.8	58	54.9	40.5	40.7	50.2	45.8	26.7	52.3	21.4	36.9	36.8
6	91.2	59.5	56.3	43.4	43.5	52.4	48.1	27.9	53.9	21.6	39.4	39.4
8	91.2	60	57	45.3	45.4	53.8	49.7	28.9	54.5	21.7	41.5	41.5
10	91.2	60.2	57.3	46.6	46.6	54.3	50.8	29.7	54.2	21.8	43.1	43.2
12	93.6	60.4	57.6	47.5	47.4	54.6	51.3	30.1	55.3	21.8	44.4	44.5
14	91.8	60.3	56.8	48	47.9	54.8	52.5	30.6	54.5	21.9	45.5	45.6
16	91.5	60	57	48.4	48.3	54.7	52.5	30.9	54.5	21.8	46.3	46.4
18	87.9	60.4	57	48.9	48.8	54.8	52.4	31	54.7	21.9	47	47.1
20	85.7	60.4	57.2	49	48.8	55.1	53.9	31	58.8	21.9	47.6	47.9
22	91.9	61.2	57.8	48.8	48.7	55.2	55	31.1	55.5	22	47.9	48.4
24	90.6	61.3	58.4	49.4	49.3	55.9	55.2	29.6	55.8	22.3	47.5	49
26	89.7	61.8	58.8	50.2	50.1	56.3	54.2	28.9	56.3	23	47.6	48.8
28	87.4	61.6	58.7	50.6	50.6	56.4	54	29.2	55.6	24.5	47.8	48.5
30	91.2	61.7	58.7	50.9	51.3	56.7	54.6	29.8	55.7	24.9	47.1	47.6

time-min.	13	14	15	16	17	18	19	20	21	22	23	24	25	26	27	28
2	38.3	33.4	26.6	32.7	31.9	34	32.6	28.2	47.2	25.1	25.4	44.8	18.3	44.4	34.4	34.6
4	42.7	37.2	28	35.4	34.6	38.4	36	30.7	48.1	25.4	25.6	46.2	18.3	51	42.9	39.3
6	46	40	29.3	37.8	37	41.8	38.9	32.2	49.2	25.7	25.4	46.9	18.9	55.5	46.2	43.3
8	48.4	42.2	30.5	39.7	39	44.5	41.1	33.3	51.5	26.1	26.6	49.1	19	57.2	49.4	46.4
10	49.9	43.6	31.5	41.4	40.7	46.1	43	35.2	51.4	26.3	27.5	47.9	19.2	58.2	51.4	48.3
12	50.9	44.6	32.3	42.6	41.9	47.7	44.1	36.5	51.3	26.8	28.1	49.5	19	58.5	52.3	49.3
14	51.5	45.2	33.1	43.8	43.1	48	45.3	38.2	51.2	27.1	29.5	49.3	18.9	59.1	53.2	50.3
16	52	45.8	33.4	44.6	43.9	49.6	45.8	39.3	51.3	27.5	30.5	49.2	19	59	53.8	50.5
18	52.4	46.2	34.5	45.2	44.6	50.2	46.4	40.2	50.5	27.6	31.4	48.9	19.3	58.8	54.5	51.6
20	52.7	46.8	36.4	45.9	45.2	50.7	46.8	41.5	54.4	27.9	32.4	51.8	19.4	59.2	54.6	51.7
22	53	47.2	38.8	46.6	45.9	51	47.3	42.2	51.5	28.1	33.1	49.6	19	59.9	54.7	52.9
24	53.5	47.9	40.5	47.4	46.6	50.9	47.9	43.1	51.8	28.3	33.5	49.8	18.9	59.6	54.6	52.8
26	52.4	47.6	41.2	47.8	47	51.9	47.9	44.5	50.2	29.1	34.9	48.2	19	60.6	55.7	52.3
28	51.9	48.1	42.7	48.3	47.6	52	48.3	45.2	51.3	30.3	35.8	48.1	18.9	60.5	55.7	52.3
30	51.1	47.1	41.7	44.5	43.5	46.5	44.6	46.4	51.6	31.1	36.5	47.9	18.3	60.8	52.6	47.5

Figure (4.5): Sample of Thermocouples experimental reading

In present calculation, we take in the consideration took place in the heat pipe NO.1 at superficial velocity 0.8739 m/s in evaporator and particle bed height 5cm. where X axis represents the thermocouple number and Y axis represents the time step increased which is 2 minutes.

**1-heat pipe surface area**

in evaporator part

$$A_{hps} = A_{hpev} = 2\pi r_o L = 2\pi \times 0.011 \times 0.645 = 0.045 \text{ (m}^2\text{)}.$$

In condenser part

$$A_{hps} = A_{hpco} = 2\pi r_o L = 2\pi \times 0.011 \times 0.345 = 0.024 \text{ (m}^2\text{)}.$$

**2-Air flow rate**

In evaporator part

$$A_{ev} = \frac{\pi d^2}{4} = \frac{\pi \times (0.2)^2}{4} = 0.031 \text{ (m}^2\text{)}.$$

$$\dot{m}_{air\ eva} = \rho VA = 1.21 \times 3.5 \times 0.031 = 0.133 \text{ (Kg/sec)}.$$

In condenser part

$$A_{con} = \frac{\pi d^2}{4} = \frac{\pi \times (0.1)^2}{4} = 7.85398 \times 10^{-3} \text{ (m}^2\text{)}.$$

$$\dot{m}_{air\ con} = \rho VA = 1.21 \times 3 \times 7.85398 \times 10^{-3} = 0.028 \text{ (Kg/sec)}.$$

**3- Particle porosity  $\varepsilon$** 

$$\varepsilon = 1 - \frac{\rho_w * g * h}{g H(\rho_s - \rho_g)} = 1 - \frac{1000 * 9.81 * 0.048}{9.81 * 0.4(1117 - 1.21)} = 0.892$$

**4- Equivalent density of (gas- particle) mixture**

$$\rho_f = (1 - \varepsilon)\rho_s + \varepsilon * \rho_g = (1 - 0.892)1117 + 0.892 * 1.21 = 121 \text{ (Kg/m}^3\text{)}.$$

**5- Specific Heat of (gas- particle) mixture**

$$\begin{aligned} C_f &= (1 - \varepsilon)C_s + \varepsilon * C_g \\ &= (1 - 0.89) \times 860 + 0.89 \times 1011 = 994.76 \text{ (J/Kg.k)} \end{aligned}$$

## 6- Superficial velocity $U_s$

$$\dot{m}_{air\ eva} = \rho \times U_s \times A_{c\ box}$$

$$0.133 = 1.21 \times (0.645 \times 0.2) \times U_s$$

$$U_s = 0.873 \text{ m/s}$$

## 7- Effective Thermal Conductivity

$$K_{es} = K_g \times \left(\frac{K_p}{K_g}\right)^{0.28 - 0.757 \log_{10} \epsilon - 0.057 \log_{10} \left(\frac{K_p}{K_g}\right)}$$

$$K_{ef} = 0.1 \times \rho_g \times C_g \times d_p \times U_s$$

$$K_{eff} = K_{es} + K_{ef} = 3.52 + 0.11 = 3.63 \text{ (W/m.k.)}$$

## 8- heat gain

$$T_{Mean} = \frac{T_2 + T_3}{2} = \frac{61.5142 + 58.8341}{2} = 60.17 \text{ (}^\circ\text{C)}$$

$$Q_{gain} = \dot{m}_{air\ eva} \times C_f \times (T_{mean} - T_9)$$

$$= 0.133 \times 994.76 \times (60.17 - 55.4) = 620.6 \text{ (Watt)}$$

## 9- Heat Transfer Coefficient

$$T_{surf} = \frac{T_4 + T_5 + T_6 + T_7 + T_{26}}{5}$$

$$= \frac{50.8 + 50.9 + 56.1 + 54.7 + 60.8}{5} = 54.6 \text{ (}^\circ\text{C)}$$

$$T_{bed} = \frac{T_2 + T_3 + T_9}{3}$$

$$= \frac{61.51 + 58.83 + 55.48}{3} = 58.6 \text{ (}^\circ\text{C)}$$

$$Q_{gain} = h A_s (T_{bed} - T_{surf})$$

$$h = \frac{Q_{gain}}{A_s (T_{bed} - T_{surf})} = \frac{620.6}{0.045 (58.61 - 54.66)} = 3496.5 \left(\frac{W}{m^2.K}\right)$$

**10- Nusselt Number**

$$\text{Nu} = \frac{h d_o}{K_{\text{eff}}} = \frac{3496.5 \times 0.022}{3.63}$$

$$\text{Nu} = 21.4$$

**11-Reynolds Number**

$$\text{Re} = \frac{\rho_f U_s d_o}{\mu} = \frac{121 \times 0.87 \times 0.022}{19.8 \times 10^{-6}} = 118692$$

**12- heat transfer to condenser part**

$$\Delta T = (T_{10} - T_{25}) = 24.9391 - 18.3 = 6.6 (^{\circ}\text{C})$$

$$\begin{aligned} Q_{\text{gain}} &= \dot{m}_{\text{air con}} \times C_g \times \Delta T \\ &= 0.0285 \times 1011 \times 6.6 = 119.295(\text{Watt}). \end{aligned}$$

**CHAPTER FIVE**

**RESULTS AND**

**DISCUSSIONS**

## CHAPTER FIVE

### RESULTS AND DISCUSSION

In the current chapter, the experimental and numerical results were listed and discussed. The results include test fluidized bed behavior inside the wooden box under different circumstances and studies that changes upon heat pipe performance. The particle bed thickness inside evaporator part has a range (2.5-10) cm. And with air superficial velocity (0.879-1.377) m/s. All tests were performed under Reynold Number ( $Re=2400,99279,118898,143421,192468,3085,137106,162330,200167,253768,3781,175283,206113,260766$  and  $318728$ ); In this chapter, the effect on physical properties of mixture on Nusselt number, and relation between Nusselt and Reynold Numbers were shown.

The 2D and 3D numerical model of heat pipe test rig was carried out to study the fluidization behavior with different inlet air mass flow rate and under empirical conditions to get a set of results from numerical models.

The experimental data was comprehending with the numerical result that obtained from [(ANSYS- FLUENT- bundle (18.0)].

#### 5.1 Experimental Conditions

In experimental tests the amount of heat transferred to the heat pipe with applying only hot air and then by using cement fly ash with air are done with the next conditions.

- 1- Air mass flow rate in evaporator part (0.133,0.171,0.209) kg /s.
- 2- Cement fly ash layer thickness (0, 2.5, 5, 7.5 ,10) cm.
- 3- The result was conducted under Reynolds numbers range (2400-318728).

## 5.2 Experimental Results

### 5.2.1 Evaporator temperature distribution

At start of experimental part, it was done by test up to reaching to a steady state with the time for all heat pipes, Figure (5.1) represents increasing heat pipes surface temperature with time at superficial velocity 0.8739m/s and bed thickness 2.5 cm, which is shown reaching to steady state after 30 minutes.

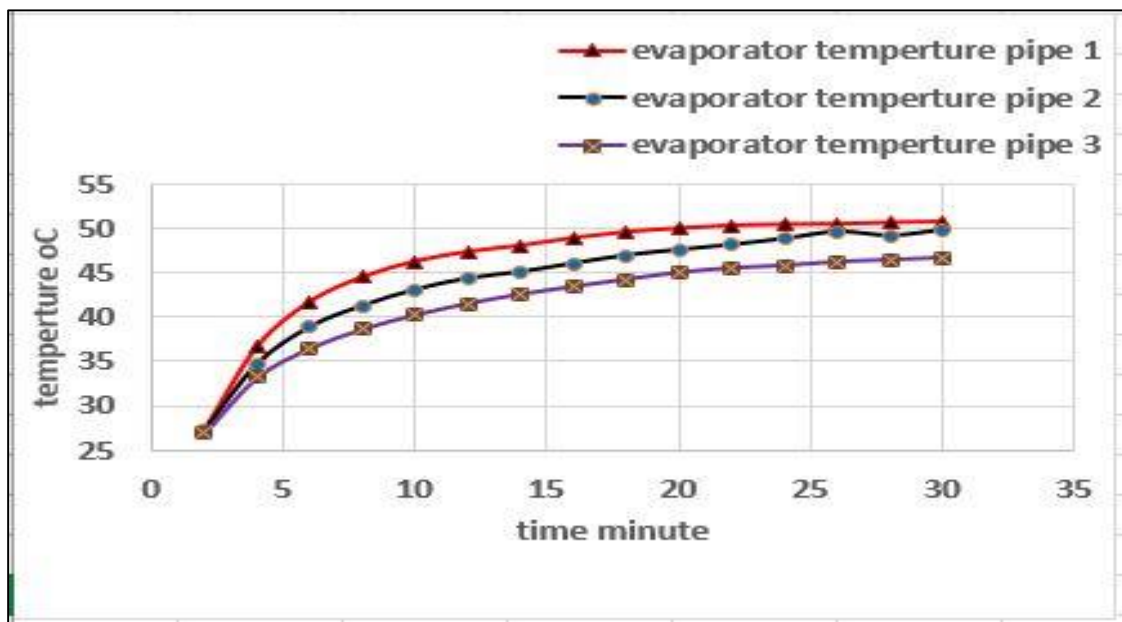


Figure (5.1): Steady state test at  $v=0.8739\text{m/s}$  and bed 2.5cm

### 5.2.2 The Influence of heat pipes locations

Figure (5.2) shows the amount of heat gained for each heat pipe for a different range of air flow superficial velocity (0.8739, 1.1236 and 1.377) m/s and also different particle layer thickness (2.5, 5, 7.5, 10) cm. It can show that the heat pipe number (1) has maximum amount of heat gained due to its location which is closed to heat source, also a big amount of particles impacts it. Maximum amount of heat gain in evaporator part was achieved at high superficial velocity 1.337 m/s and at high particle bed 10 cm for such conditions more turbulent take place and more particle hit the heat pipes for unit time.



Maximum heat gain will be occurred in heat pipe number (1) with (57) % if compared with heat pipe number (3), that achieved at superficial velocity 1.377 m/s and (5) cm of bed thickness.

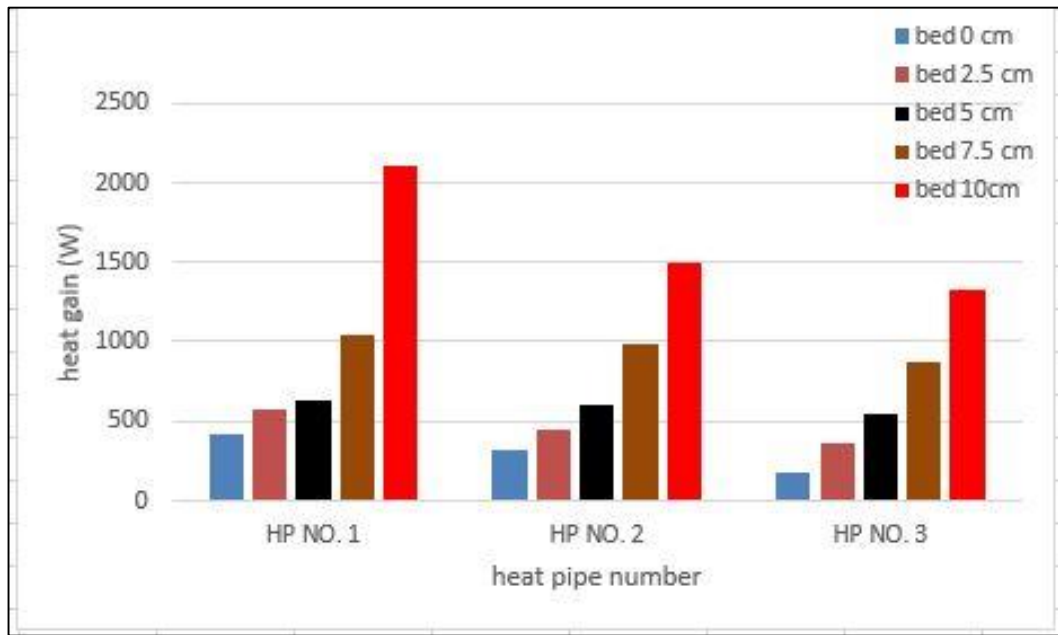


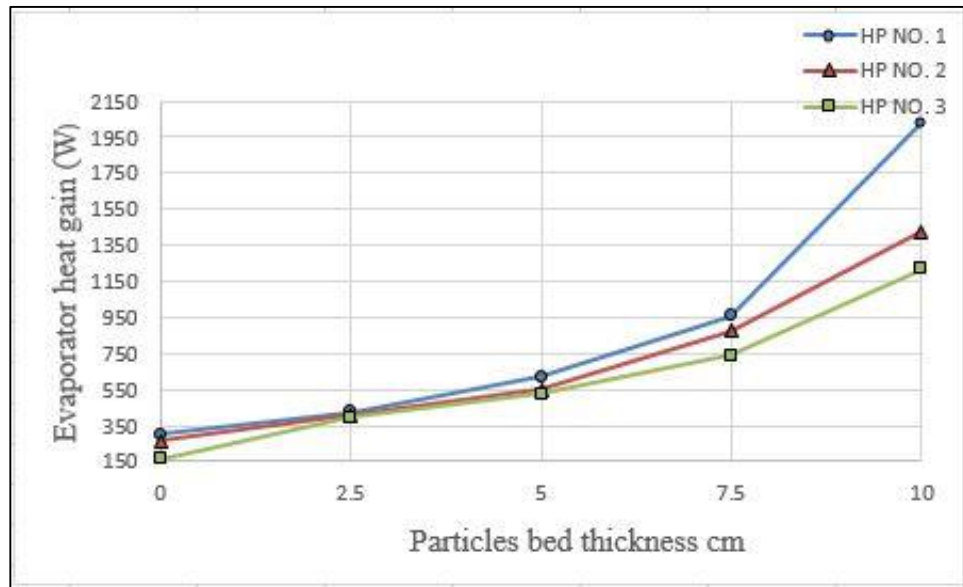
Figure (5.2): Heat gain in evaporator part for superficial velocity 1.1236 m/s

### 5.2.3 Influence of particle bed thickness

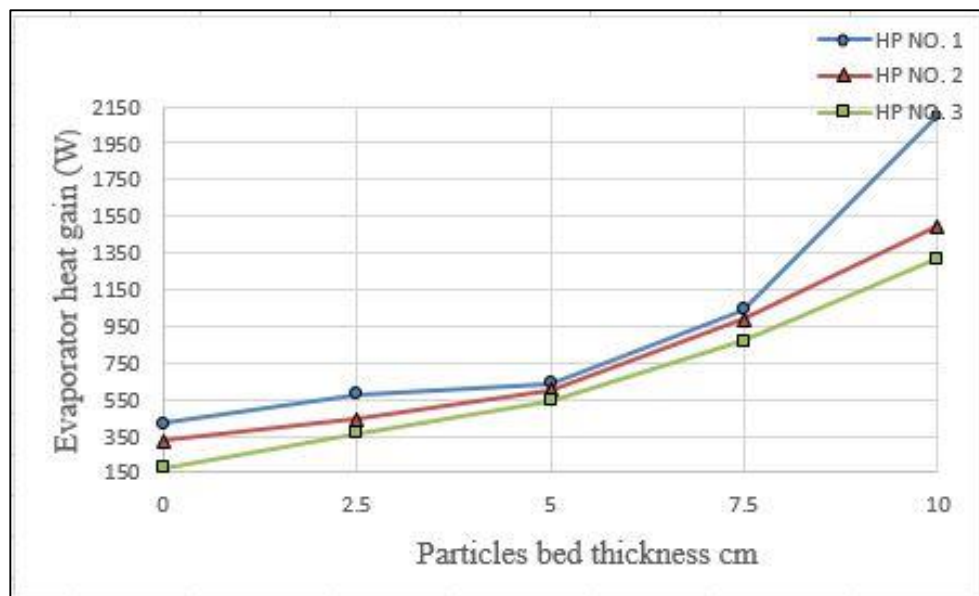
Influence of particle layer thickness on heat pipe performance was shown in figures (5.3 a-c) with different values of air superficial velocity (0.8739, 1.1236 and 1.377). When particle height increase, the elevation of particles rises and the spaces among the solid particles decrease since the volume that contains the particle was constant,

So when air superficial velocity increased, the air pushed the particles into high elevation that takes a good air- particle mixture (complete fluidization). The maximum effect of particle bed height appears at heat pipe number (1) and at superficial velocity 1.377. m/s, the increase in heat gained by 85% from initial value without particle. that because at high air velocity and high particle height most of them reach to first heat pipe and airlift force

is enough to transfer particle to higher pipes. For most the heat transfers to particle of lower heat pipe. In general, with increasing particle height heat pipe gained increased for all pipes as shown in figure (5.3 a-c)

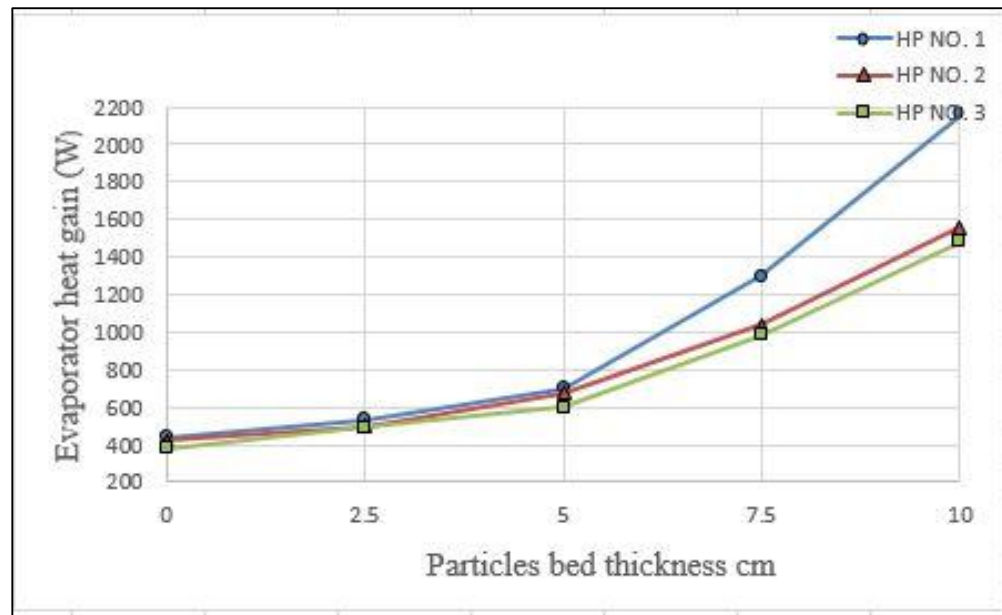


a- Air superficial velocity 0.8739 m/s



b- Air superficial velocity 1.1236 m/s

Figure (5.3 a-c): Particle bed thickness effect on heat gained in evaporator part for all heat pipes at different air velocities



c- Air superficial velocity 1.377 m/s

Figure (5.3) continued

#### 5.2.4 porosity variation

Figure (5.4) represents porosity at different air superficial velocities and particle bed height and clearly can be shown that porosity increased when decreasing particle bed high and that because of decreased amount of practical in region. It's also noted that at increasing velocity, the porosity decreased because at high velocity, there was more amount of pressure drop, when the particle bed increased from (2.5 to 10) cm the porosity decreased by approximately (9%) for all superficial velocities; for increasing superficial velocity from (0.8739 to 1.377) m/s the porosity decreased by 2%.

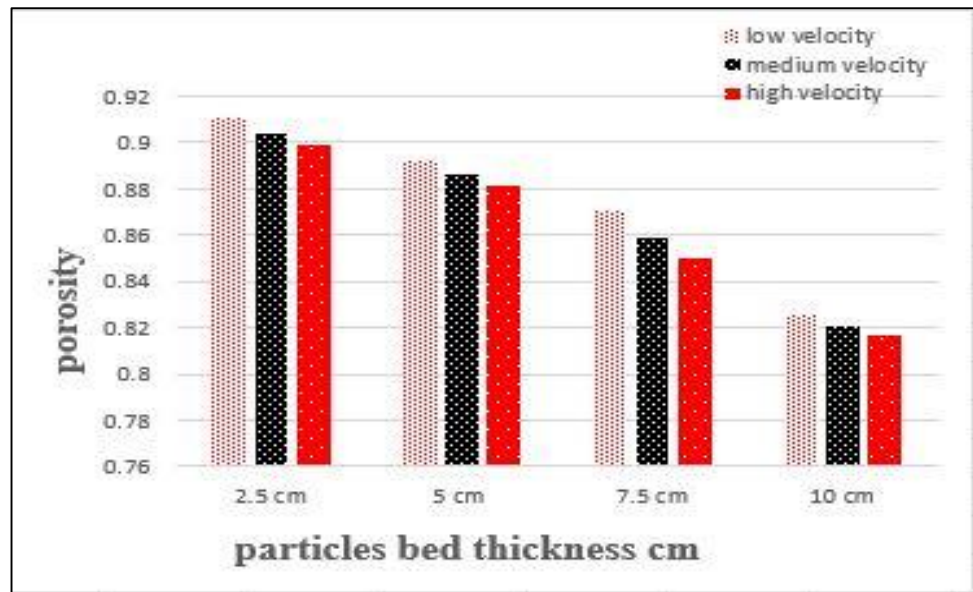
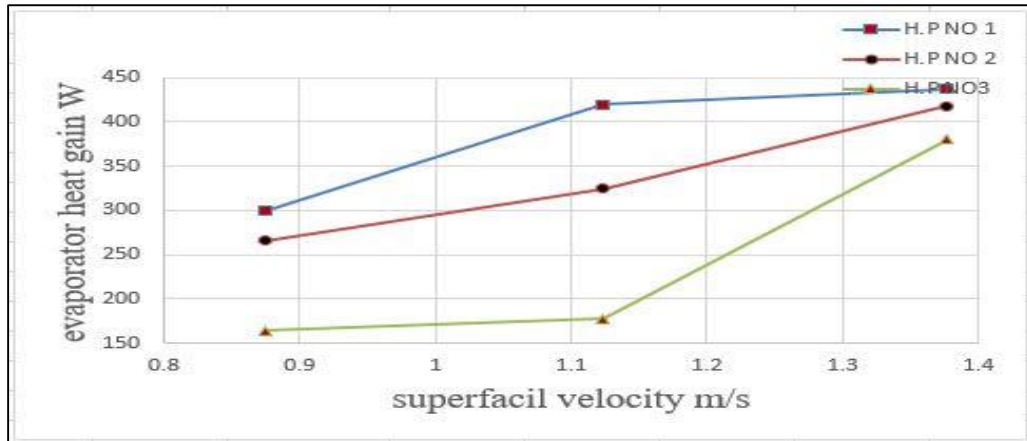


Figure (5.4): The effect of particle bed thickness on the porosity for different velocities

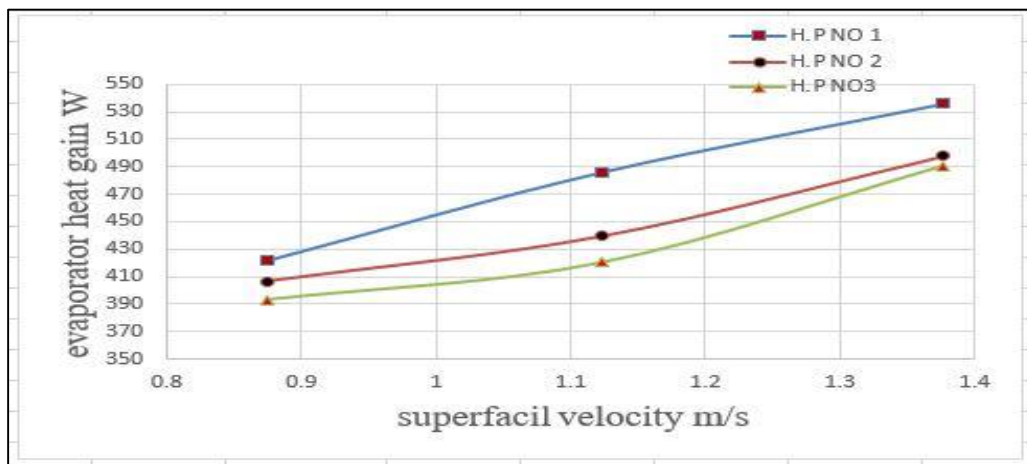
### 5.2.5 Influence of Air velocity

Figure (5.5 a- e) shows the air velocity effect on heat gained of the heat pipes at different particle bed thickness and obviously. It shows that increasing air superficial velocity raises the elevation of the solid particle inside wooden box. Also, spaces between particle increased the matter that led to perfect air-particle mixture guiding to more heat gained.

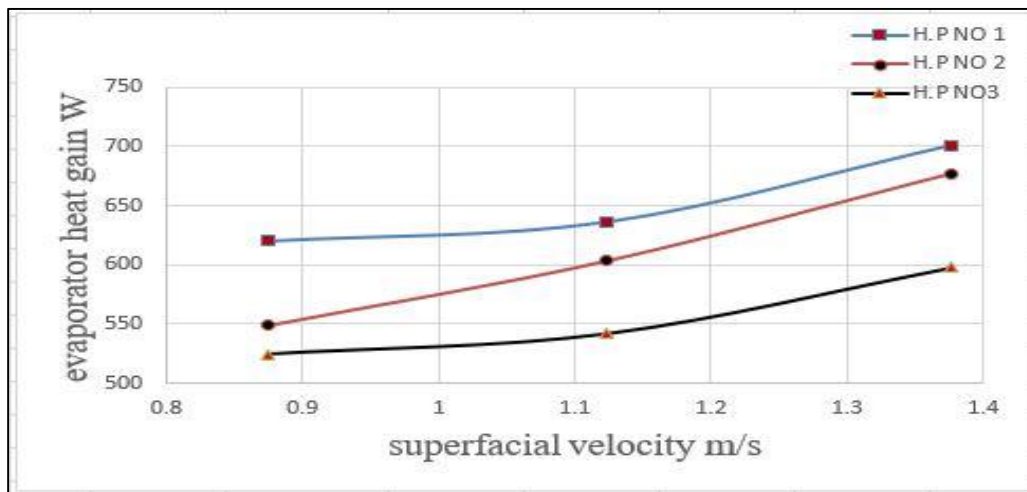
Increasing the air superficial velocity from (0.8739 to 1.377) m/s increased heat gained at evaporator part for maximum and minimum value (21 and 8) % at heat pipe (1) and (3) respectively.



a-particles layer thickness (0) cm

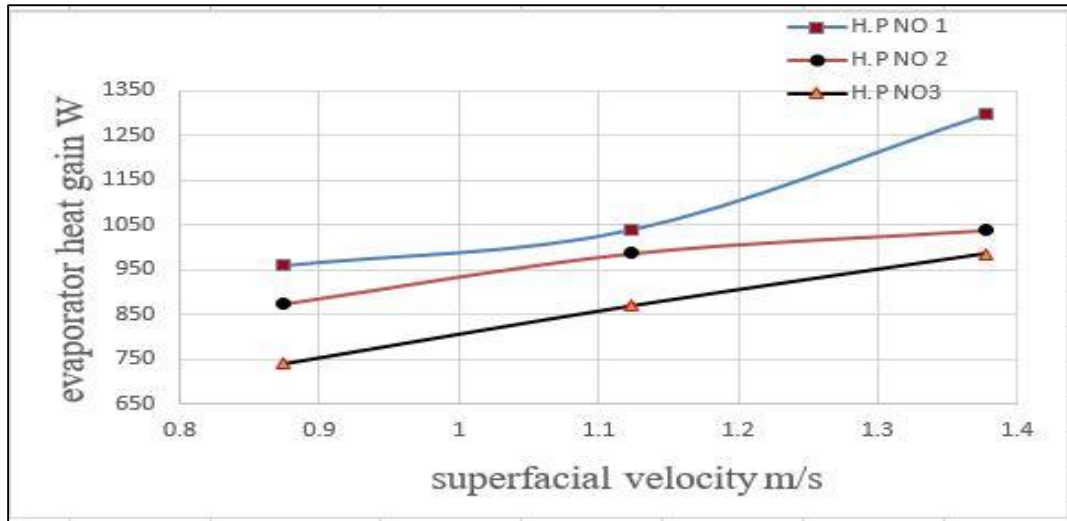


b-particles layer thickness (2.5) cm

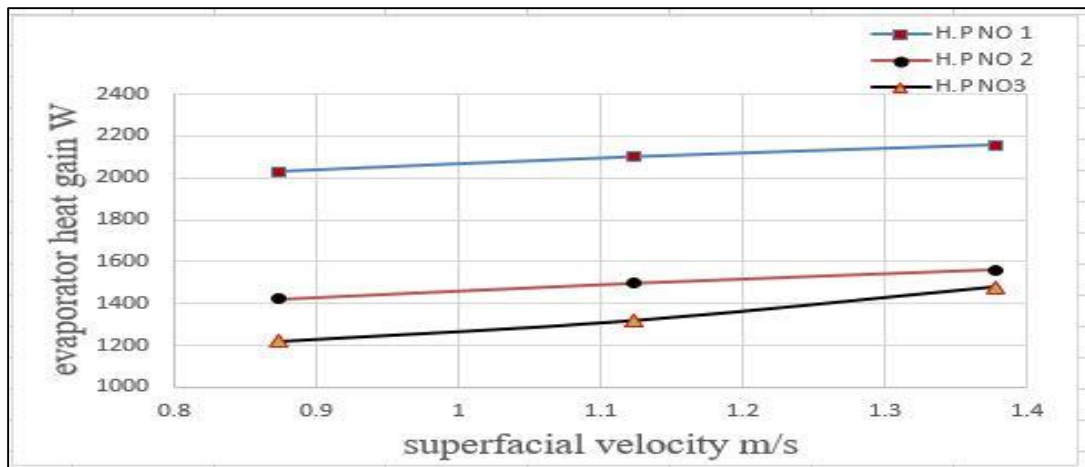


c-particles layer thickness (5) cm

Figure (5.5): Variation of evaporator heat gain with air superficial velocity for different particle bed thickness



d-particles layer thickness (5) cm



e-particles layer thickness (10) cm

Figure (5.5) continued

### 5.2.6 pressure drop

Figure (5.6) represents the pressure drop variation at the evaporator section for different particle beds and air velocities. Clearly it can be noted that pressure drop increased with increasing particle bed thickness due to increasing flow resistance. Increasing particle bed thickness from (0 to 10) cm increased the pressure drop by 65%, while with changing air superficial velocity from (0.8739 to 1.377) pressure drop does not exceed (13%).

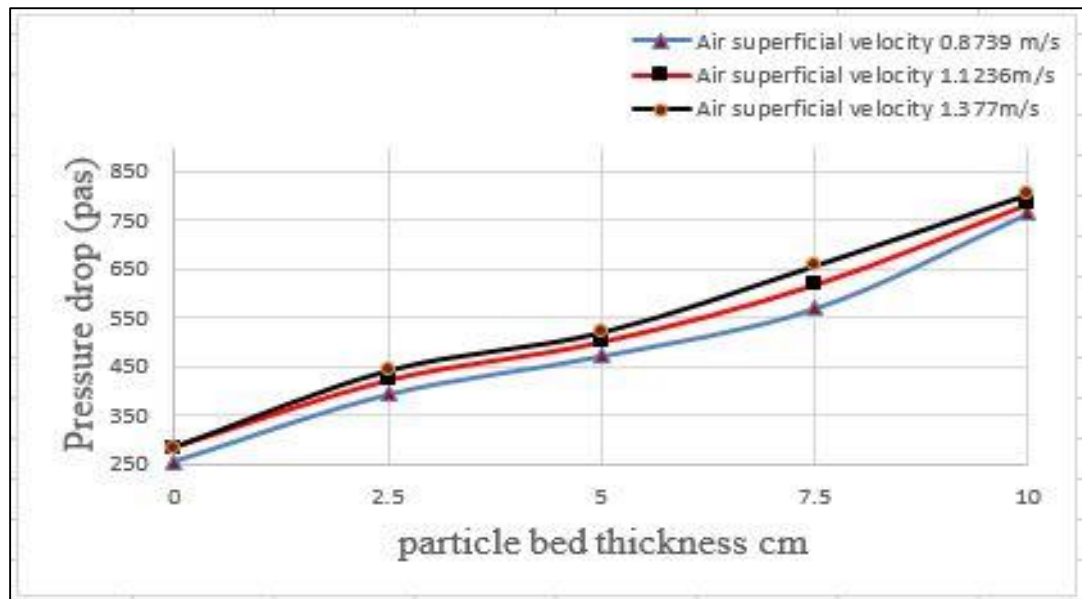
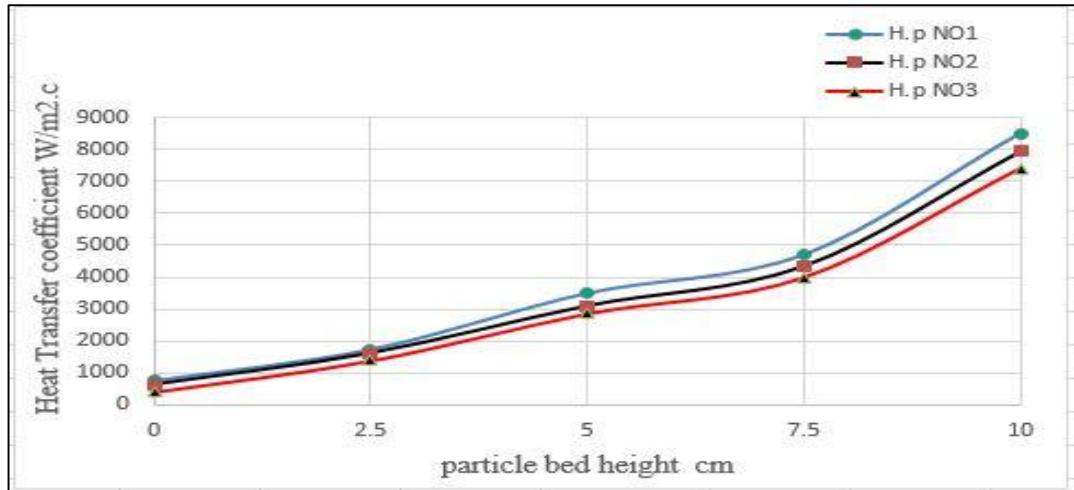


Figure (5.6): Influence of pressure drop with particle bed thickness at different air velocity

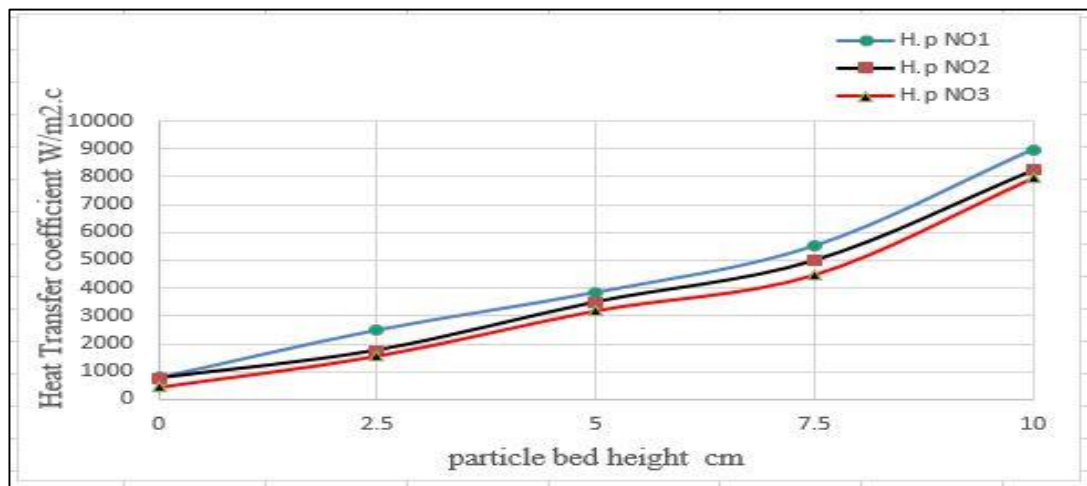
### 5.2.7 influence of particle bed on heat transfer coefficient

Figure (5.7 a-c) represents bed thickness effect on heat transfer coefficient at different air velocities for all heat pipes. It can be obviously shown that increasing particle bed height increased heat transfer coefficient for all velocities and that occurs because of increasing of the specific heat for mixture with increasing particle bed height.

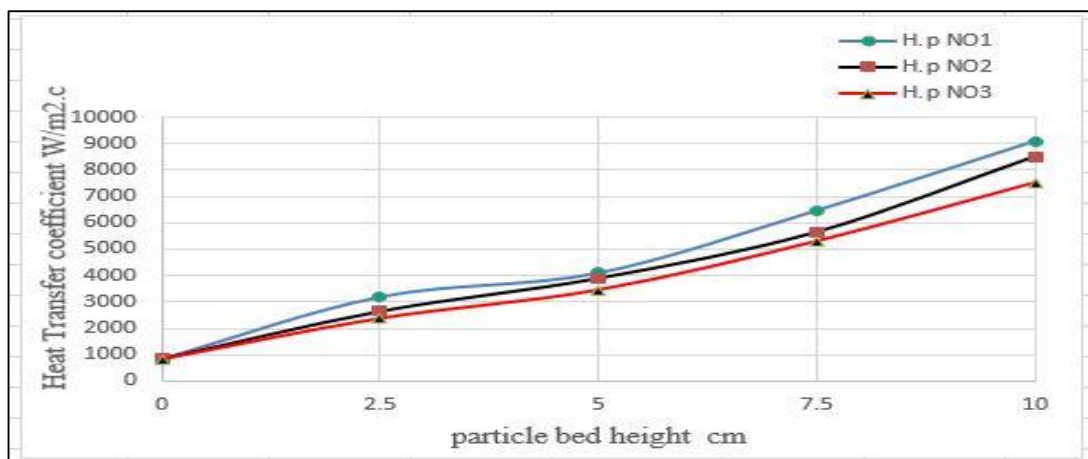
The heat transfer coefficient at particle bed height (10) cm increased by (90%) than no particle bed found at the same superficial velocity.



a-Air superficial velocity 0.8739 m/s



b-Air superficial velocity 1.1236 m/s



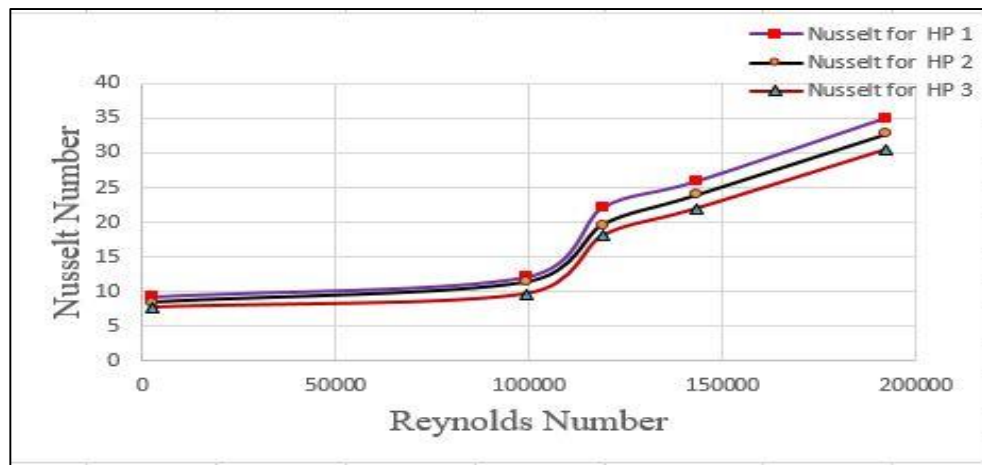
c-Air superficial velocity 1.377 m/s

Figure (5.7): Influence of particle bed thickness on heat transfer coefficient  
At different air velocity

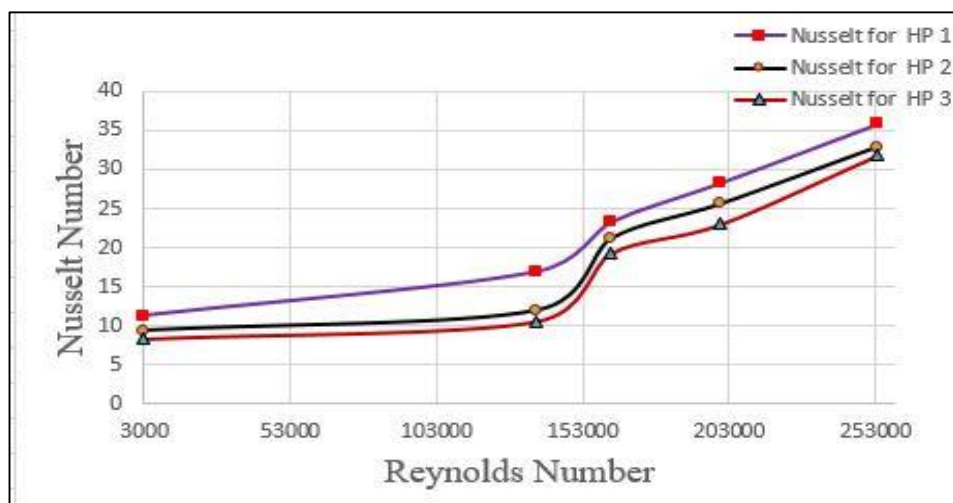


### 5.2.8 Nusselt Number. variation with Reynolds Numbers

The variation of Nusselt number with Reynolds number at different particle bed heights and superficial velocities were shown in figure (5.8 a-c). Clearly, it can be noted that increasing Reynolds number leads to increasing Nusselt number for all bed height and superficial velocities. The maximum Nusselt number (35.125) has been achieved at maximum particle bed height (10cm) and maximum superficial velocity (1.377m/s). The maximum enhancement in Nusselt number was (75.7%) due to increasing heat transfer coefficient with increasing particle bed thickness.

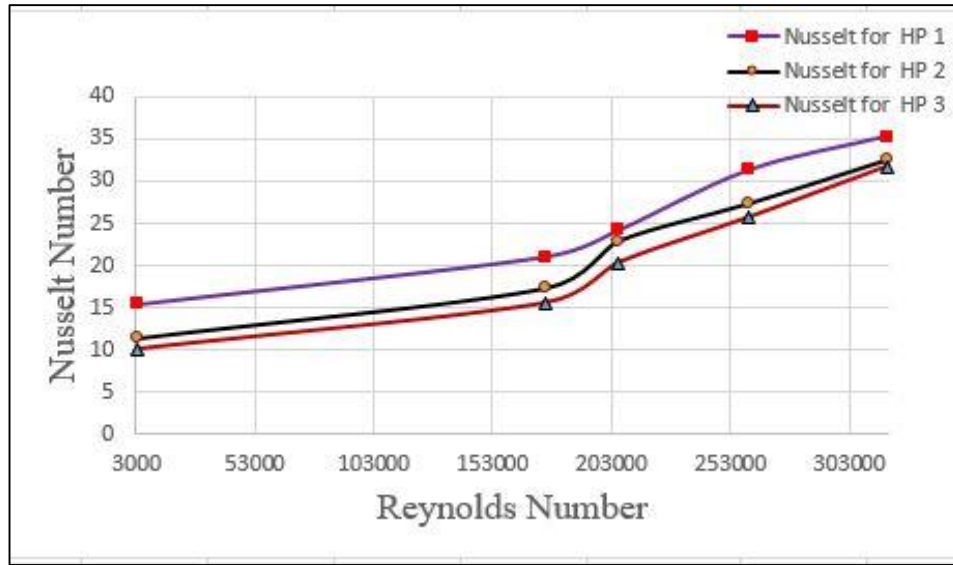


a-Superficial velocity 0.8739 m/s



b-Superficial velocity 1.1236 m/s

Figure (5.8): Relationship between Nusselt and Reynolds numbers for all heat pipes at different bed thickness and superficial velocities



c-Superficial velocity 1.377 m/s

Figure (5.8) continued

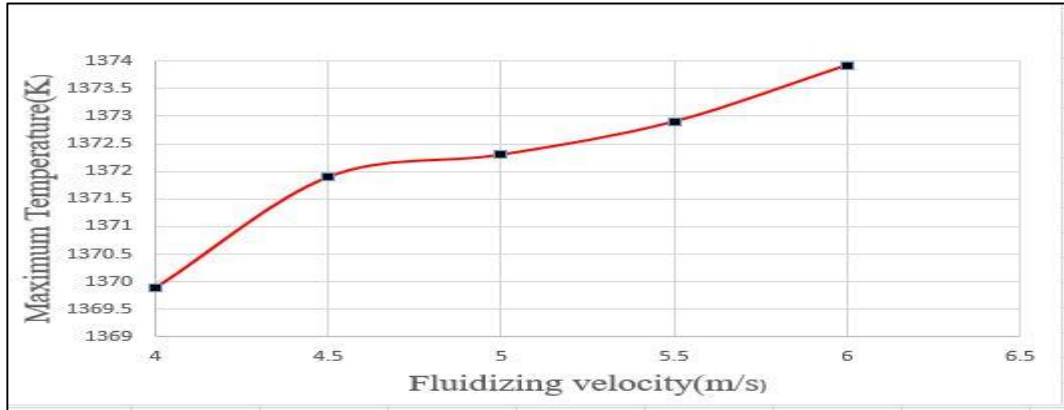
### 5.3 Numerical conditions

In numerical procedure after modelling and meshing the rig, it was taken in consideration boundary conditions such as air flow rate, heat pipe surface temperature, and exit pressure; the flowing results were obtained

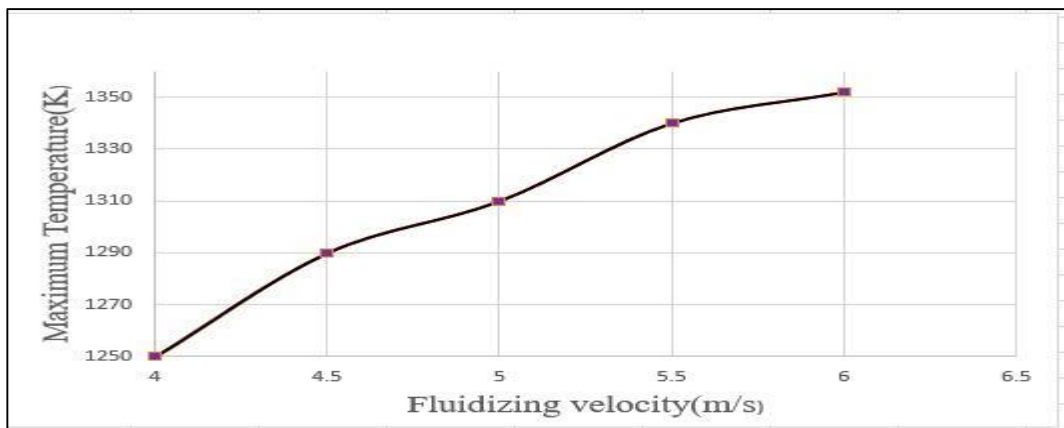
#### 5.3.1 Program Validation

To verify the numerical code, the calculated two-dimension profile of the temperature is compared with the numerical results of the previous study made by Ravindra Kumar [15] about the fluidized bed (air and soiled) through divergent furnace, rectangular vertical channel. The parameters were. The particle size has taken 5 mm and fluidizing velocity (4-6) m/s, for a 2D CFB furnace, estimate the primary air is flowing at 503 k and 4m/s which is flowing through the nozzles. The secondary air is injected at the level of 2.3 m from the level of the bottom at 473 k and 2m/s and the fuel feed rate 0.5 kg/s is injected at the level of 1.5m from the level of the bottom furnace high was 15 m. used K-epsilon method and discrete phase model to simulate two phase flow. A acceptable agreement was detected between the numerical results of temperature study and the numerical results of Ravindra

Kumar [15] with an average maximum percentage error of (7.8) %. These results have validated the accuracy of the numerical code, as shown in figure (5.9)



Maximum temperature with fluidizing velocity at kumar work



Maximum temperature with fluidizing velocity at present work

Figure 5.9: The validation of the numerical code with the numerical results of Kumar [15]

### 5.3.2 The Influence of heat pipe location

Figure (5.10 a-e) represents the heat temperature contours at evaporator part for constant air superficial velocity (0.8739 m/s) at different particle bed thickness for heat pipes evaporator part. It could be noted for all cases that the first pipe has the biggest amount of heat gained due to its closeness to heat source: The temperature was not the same alongside with heat pipe evaporator part. That happened because of working fluid acting inside. On the left side, the working fluid was still in liquid cool case which

absorbed much amount of temperature from the surrounding area. As a result, this leaves the surrounding domain on the left side cooler than the right one. This in comparison with the right side is the reverse. In other words, the heat pipes on the right side become hot since the working fluid itself become hot enough that they can do without absorbing the heat from the external space.

Figure (5.11) shows amount of evaporator heat gained for three heat pipes obviously. It could be shown that heat pipe number (1) has the maximum amount of heat gained

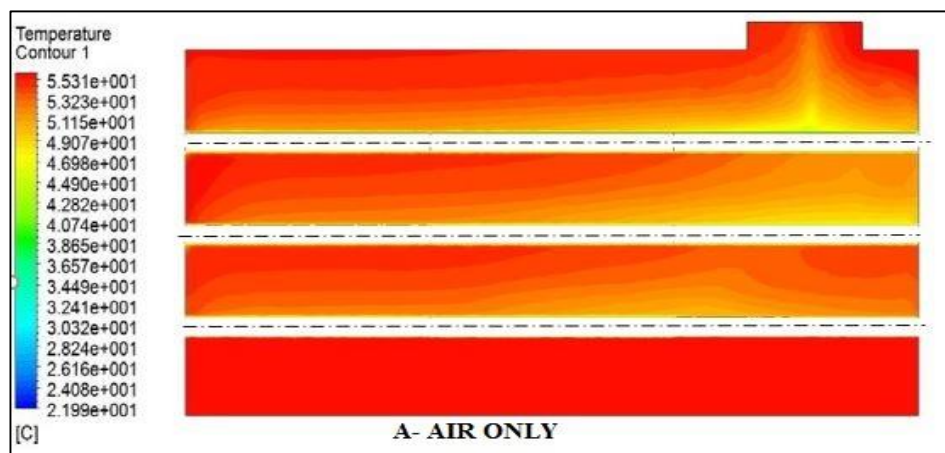


Figure (5.10 a-e): pipe location effect on heat gain at the same velocity

$$V = 0.8739$$

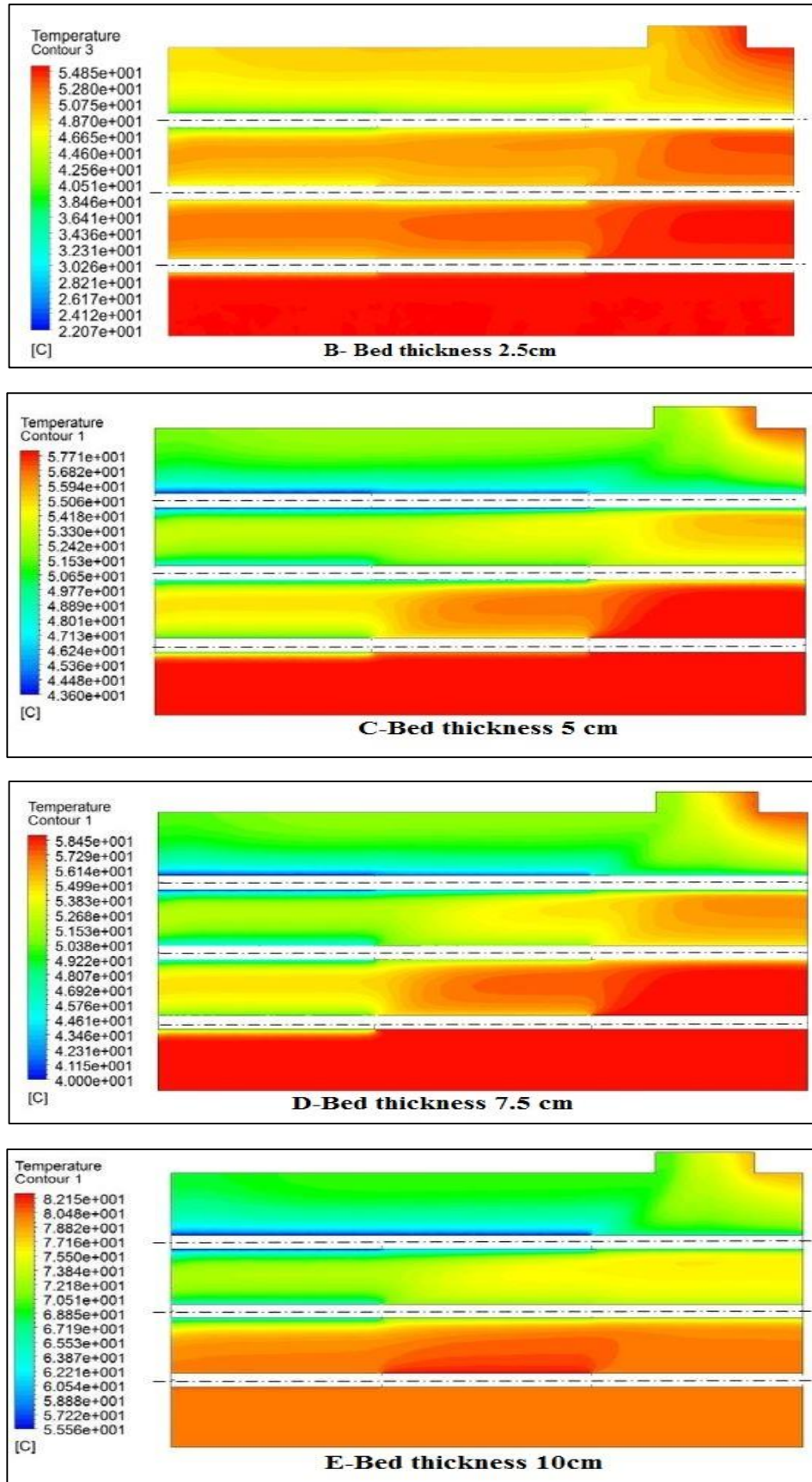


Figure (5.10) continued

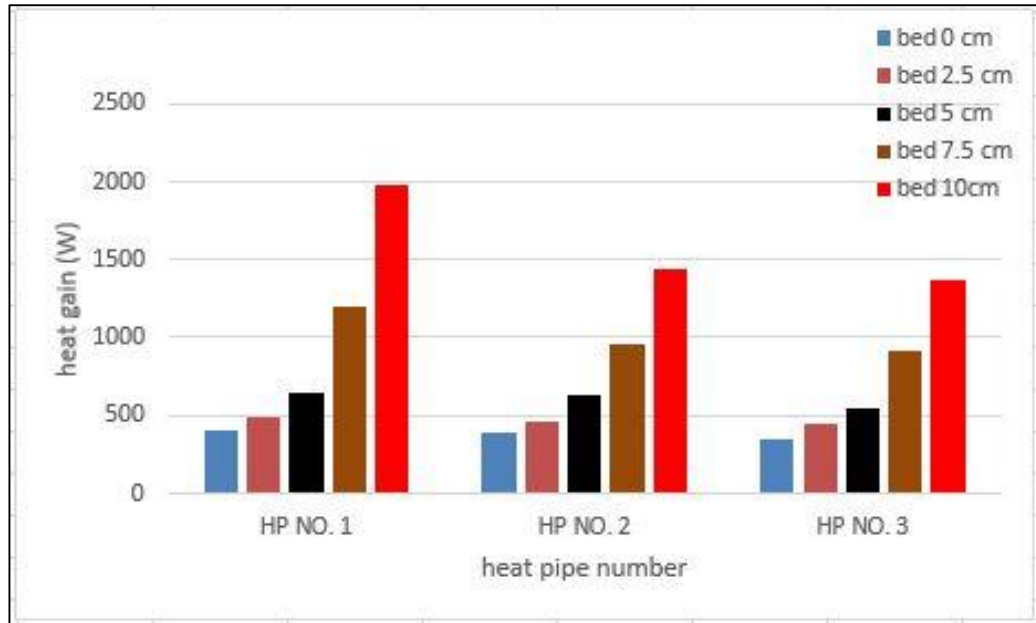
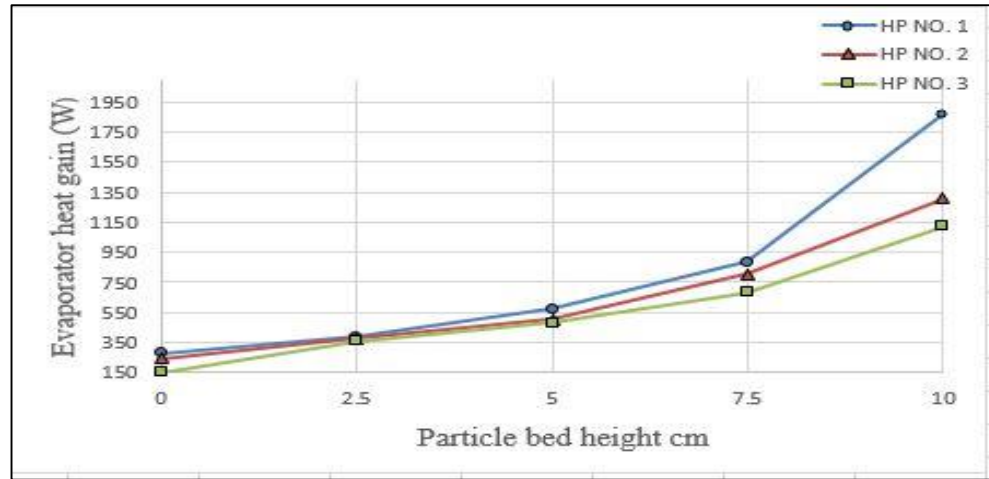


Figure (5.11): Pipe location effect on heat gain at a superficial velocity 1.377m/s

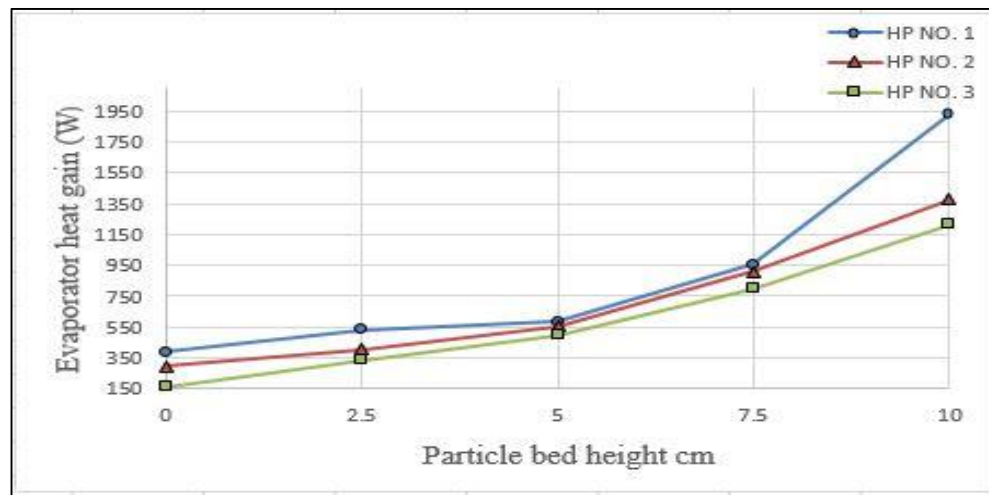
### 5.3.3 Influence of particle bed thickness

Figure (5.10 a-e) represents contours for different particle thicknesses inside evaporator part, that were particle amounts affected hardly on heat gained in heat pipes.

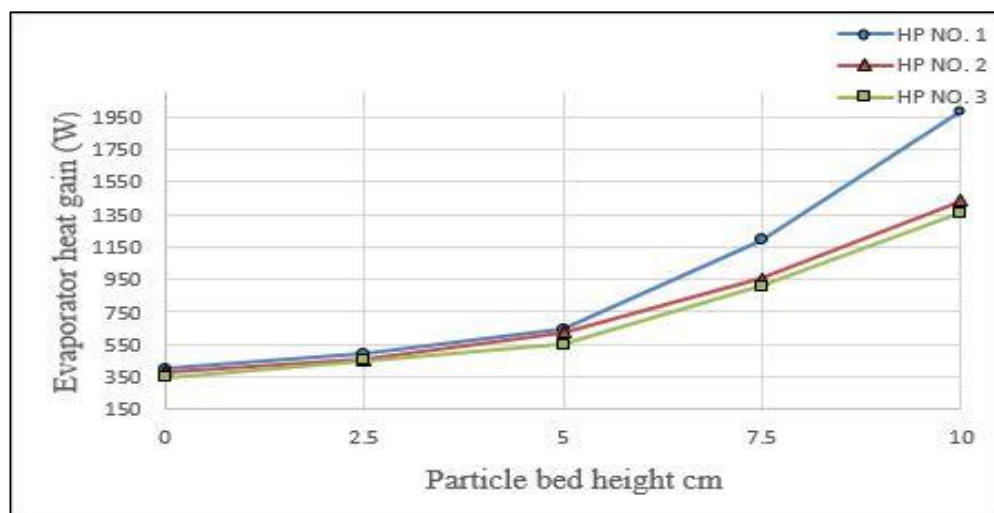
Figure (5.12 a-c) shows heat gained at different air superficial velocity and particle bed thickness, for all cases it can be shown that with increasing particle bed more power absorbed in heat pipe evaporator part. Heat pipe number (1) has 82% enhancement in heat gained if compared with no particles and that achieved at particle height 10cm. but the other two heat pipes enhancement is 80% for each one.



a-Superficial velocity= 0.8739m/s



b- Superficial velocity= 1.1236m/s



c-Superficial velocity= 1.377m/s

Figure (5.12): Variation of evaporator heat gained for the three heat pipes at different particle bed thickness for all superficial velocity cases

### 5.3.4 pressure drop

The numerical pressure drop values are charted at figure (5.13) and it can be noted that both effect of particle bed thickness and air superficial velocity have a direct proportion with pressure drop.

The maximum pressure drop increased because of particle bed effect was 66% occurs at a superficial velocity 1.377 m/s and bed thickness 10 cm. where bed thickness and superficial velocity increased the resistance which in turn, increases the pressure drop.

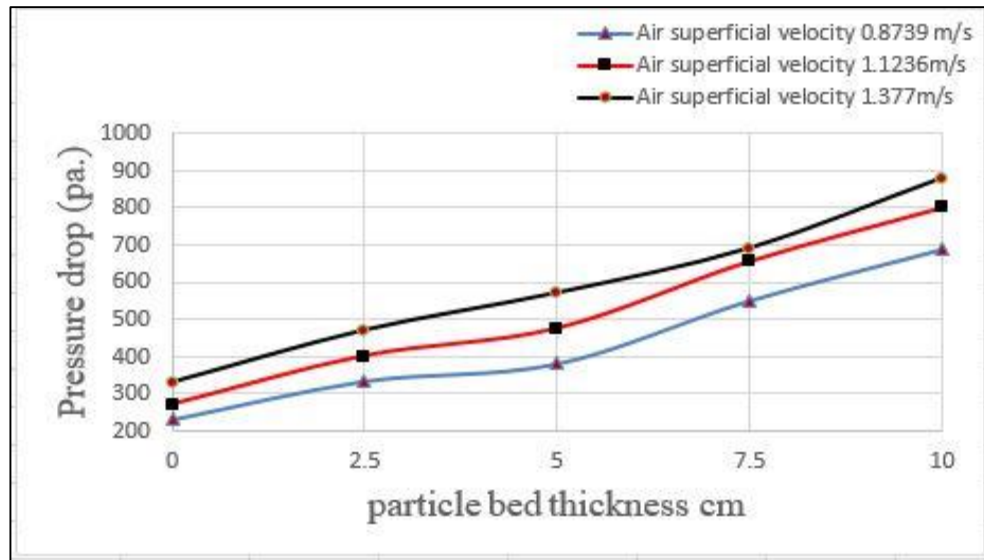


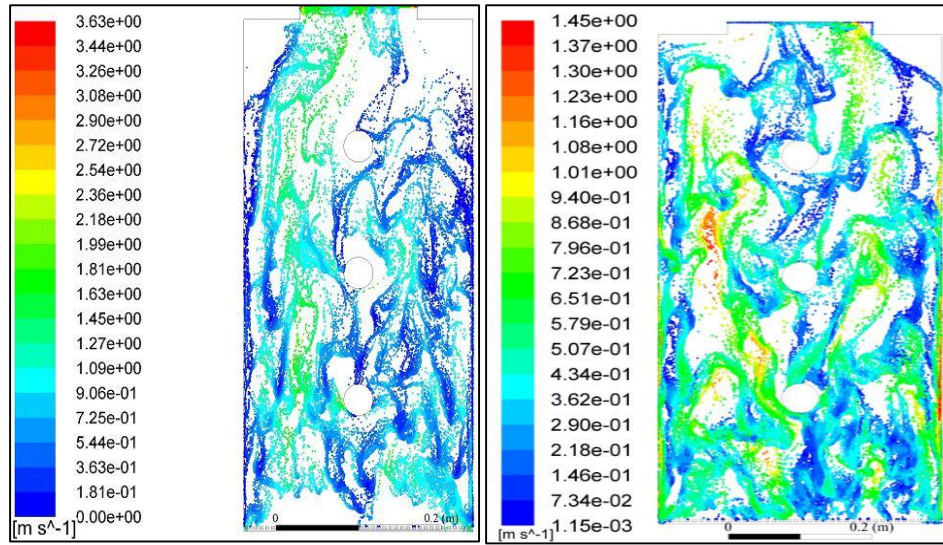
Figure (5.13): Pressure drop variation with particle bed thickness for different air velocities

### 5.3.5 porosity

Figure (5.14 a-c) represents particle velocity contours for superficial velocity (0.8739 to 1.377) m/s and for (2.5) cm. particle bed thickness. Explicitly, porosity decreased with increasing particle bed height for the same velocity for more particles bed height means less clearance between them at constant volume, while increasing velocity leads to more porosity value since it increased the distance between particles.

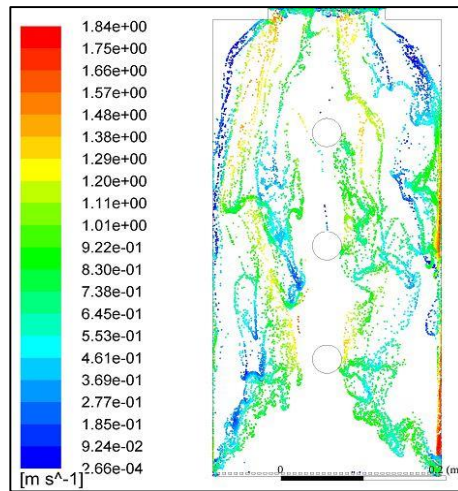


Figure (5.15) shows charting porosity values for all studied cases and the effects that were confirmed what ANSYS contour display.



a-  $v = 0.8739 \text{ m/s}$

b-  $v = 1.1236 \text{ m/s}$



c-  $v = 1.377 \text{ m/s}$

Figure (5.14 a-c): Represent particle distributed in (Y-Z) plane at bed 5cm and different superficial velocities

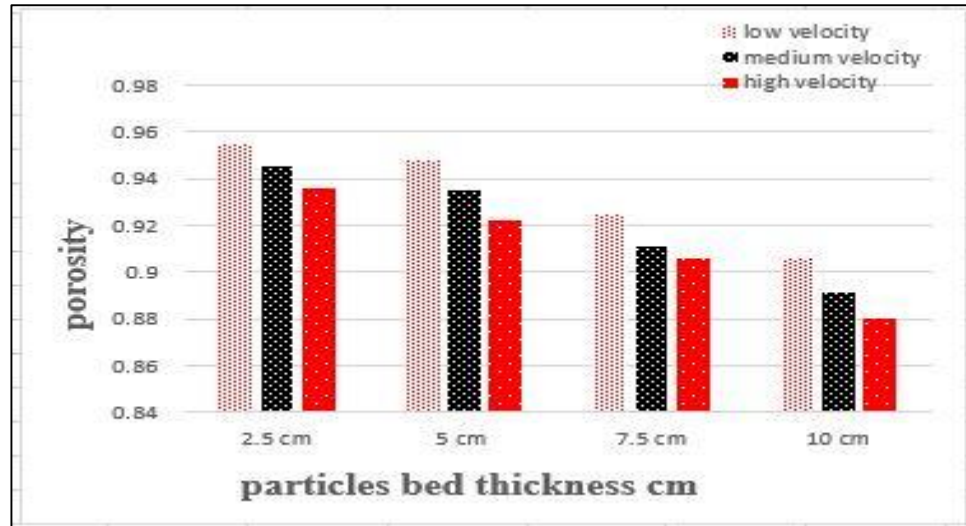


Figure (5.15): Porosity value for different particle bed height and different superficial velocities

### 5.3.6 Influence of Air velocity

Figure (5.16 a-b) represents air velocity contours. It seems that the figure shows that at low velocity less number of particles impact the pipe surface whereas at high velocity the particles impact the heat pipe surface for a unit time increased, that leads to increasing the heat gained with increasing velocity.

Also it could be noted that with increasing velocity, the path of the mixture will be banned to the heat pipe and be far away from test box wall, that decreased losses that may happen at wall and more mixture take the straight line passing over heat pipe surface.

Figure (5.17 a-e) represents the heat gained at superficial velocity (0.8739 to 1.377) m/s and for particle bed thickness (0 and 10) cm and it shows approximately converged values that appear in experimental results. More velocity leads to more heat gained at specific bed thickness.

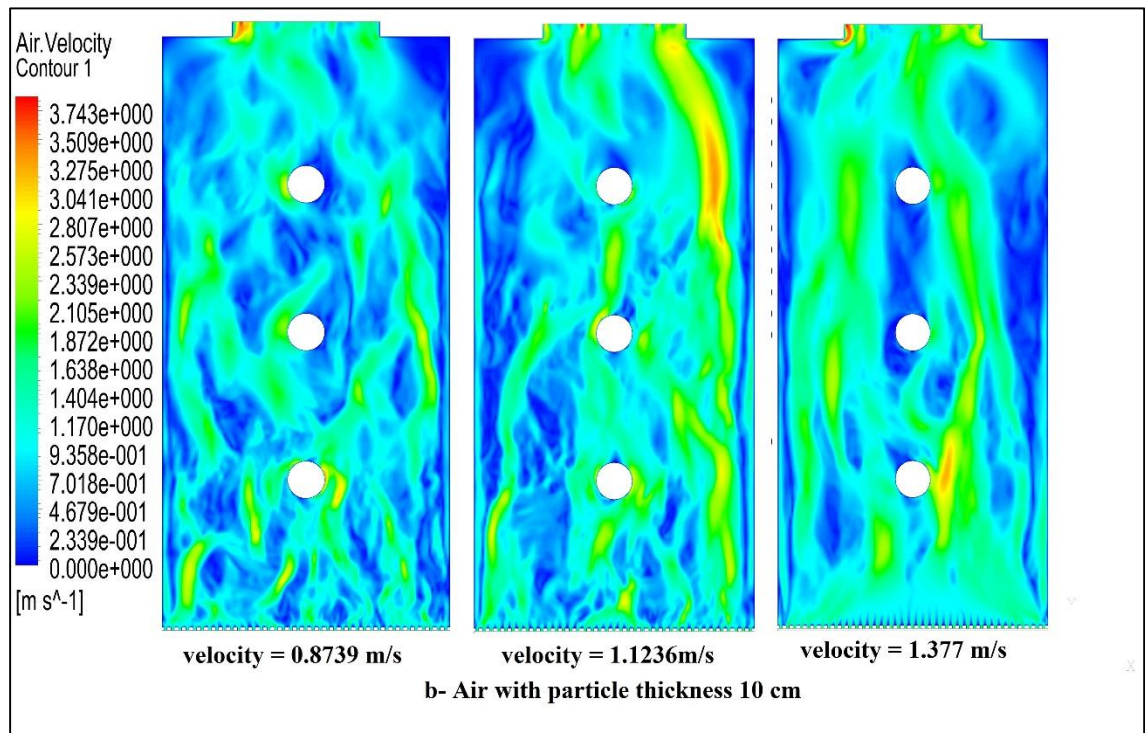
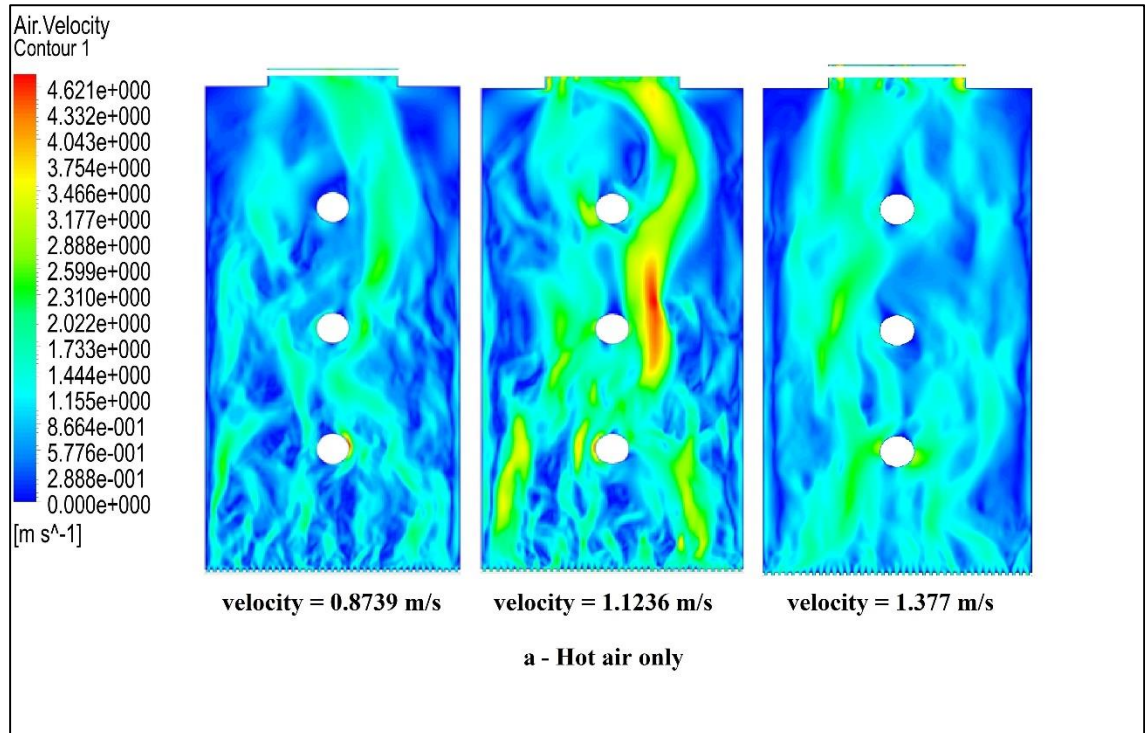
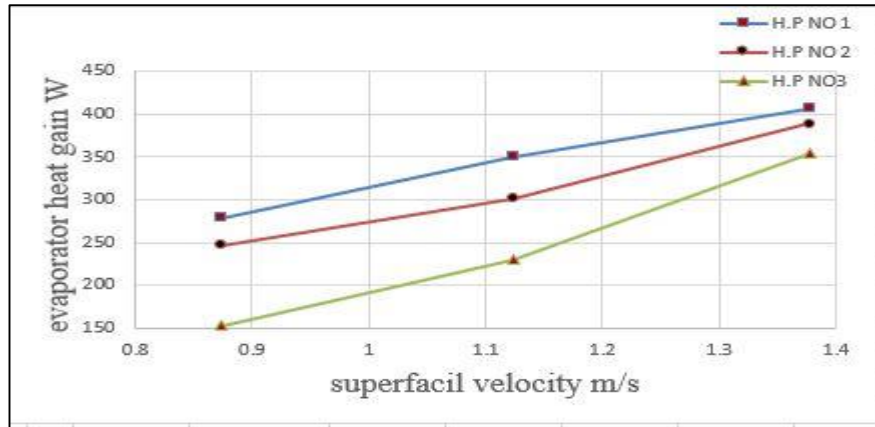
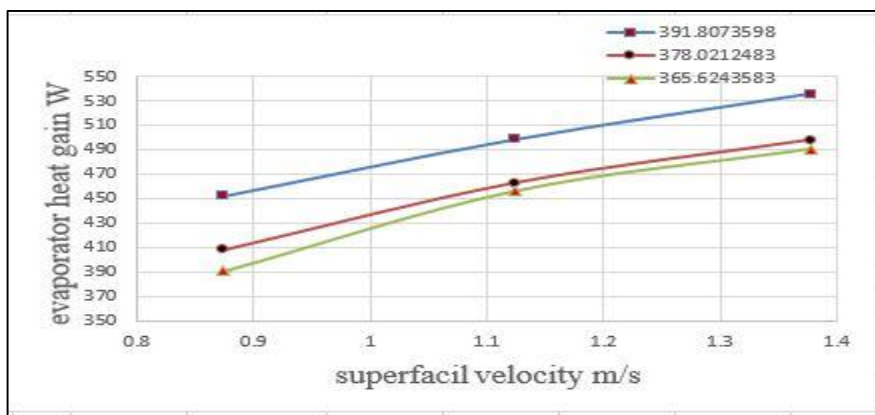


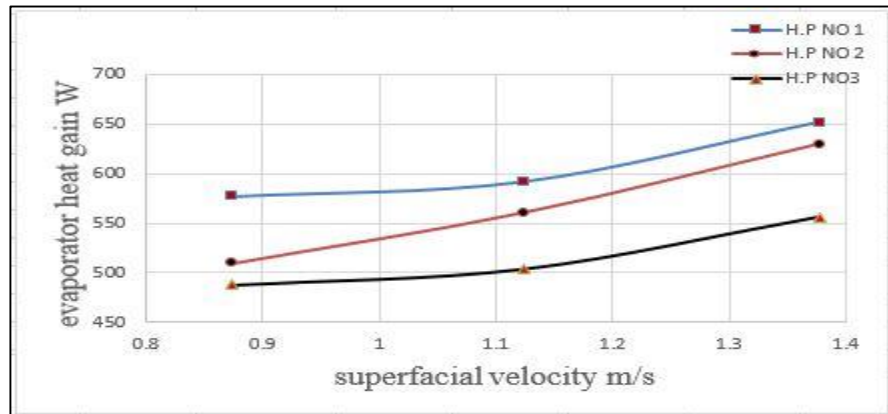
Figure (5.16 a-b): Represents air velocity contours for superficial velocity effect on heat pipe heat gain



a- No particle bed

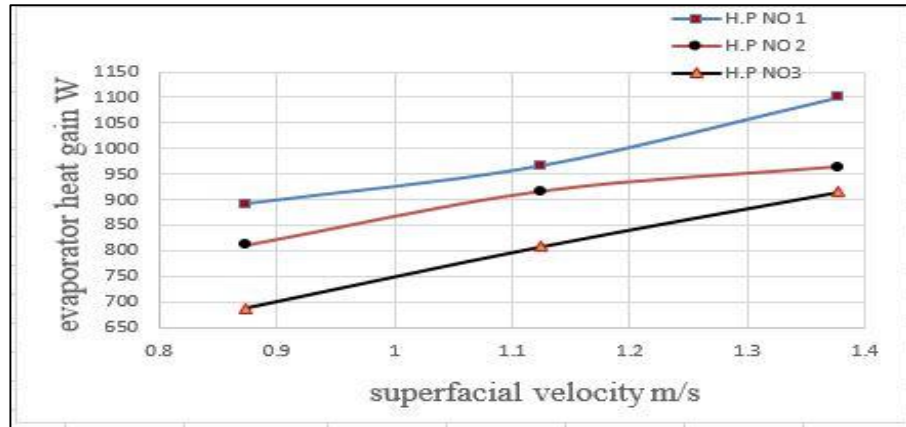


b-Air with particle bed thickness 2.5cm

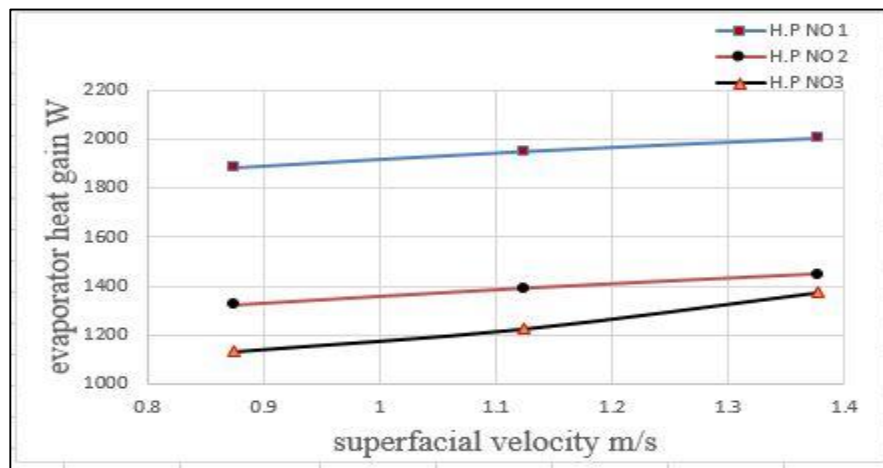


c-Air with particle bed thickness 5cm

Figure (5.17 a-e): The relationship between evaporator heat gained with superficial velocity for three heat pipes



d-Air with particle bed thickness 7.5cm



e-Air with particle bed thickness 2.5cm

Figure (5.17) continued

### 5.3.7 heat pipe surface temperature

Figure (5.18) represents velocity vector contours for test rig evaporator part at a superficial velocity 0.8739 m/s and particle bed thickness 2.5cm. From the below figure it could be noted that number of air streamline impact the lower surface directly and slipping to the heat pipe side that makes the lower heat pipe surface more than the upper surface. Moreover, from numerical temperatures contours, it could be stated that the increasing lower to upper surface is about (2 – 4) %.

The same figure could realize that when velocity increased more particle impact the lower surface while air stream separation increased in the

upper surface. That makes the difference in temperature will be more at high velocity. But more particles inside domain could make the distributed heat lead to more influence at constant superficial velocity. As a result, this will reduce the temperature differences between lower and upper surfaces

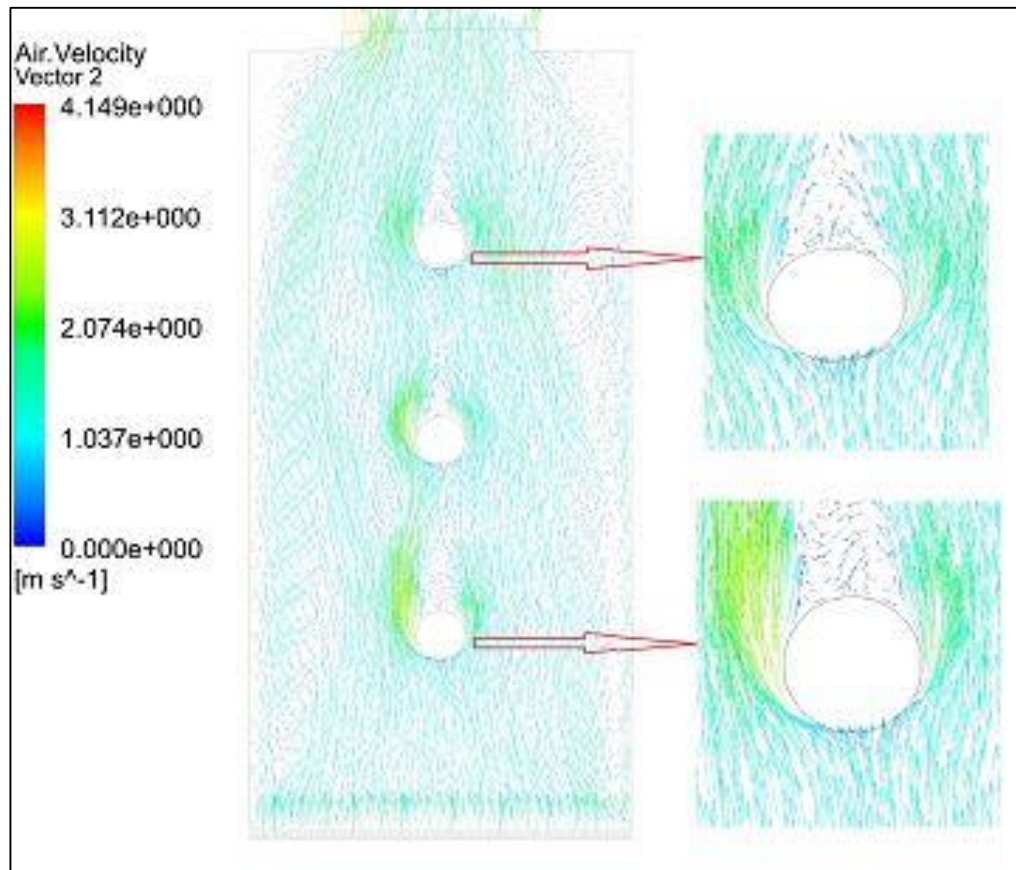


Figure (5.18): Velocity vector at bed height 2.5cm and superficial velocity 0.8739m/s

### 5.3.8 heat distributed inside condensers part

Figure (5.19) that represents temperature contour at condenser part, showed three heat pipes temperature surface, also the figure shows increasing in air velocity at exit hole where area become smaller.

Figure (5.20 a-c) represent heat distribution contours at condenser part at many superficial velocities and particle bed thickness. It seems that

the air enters with a low temperature and hits the heat pipe surface. Therefore, the pipe surface temperature decreases while the surrounding area temperature increases, when this process happens to the second upward pipe, the impact will be less. So, the absorbed temperature by the pipe is less than the previous one. When this occurs to the third upward pipe, the absorbed impact will be least where the surrounding are needless to get more temperature from the pipe surface. In sum, the third pipe is the hottest one if compared with the previous downward pipes.

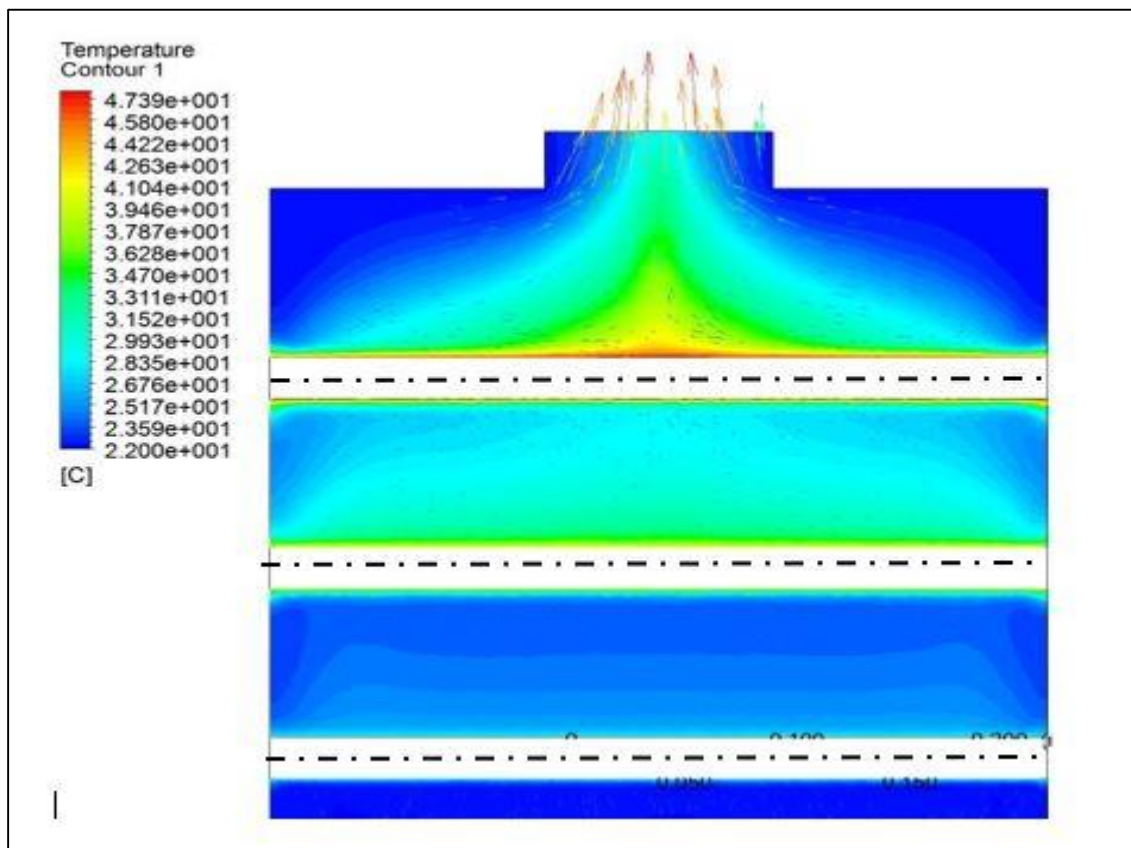


Figure (5.19): Air velocity vector and heat contour at condenser part

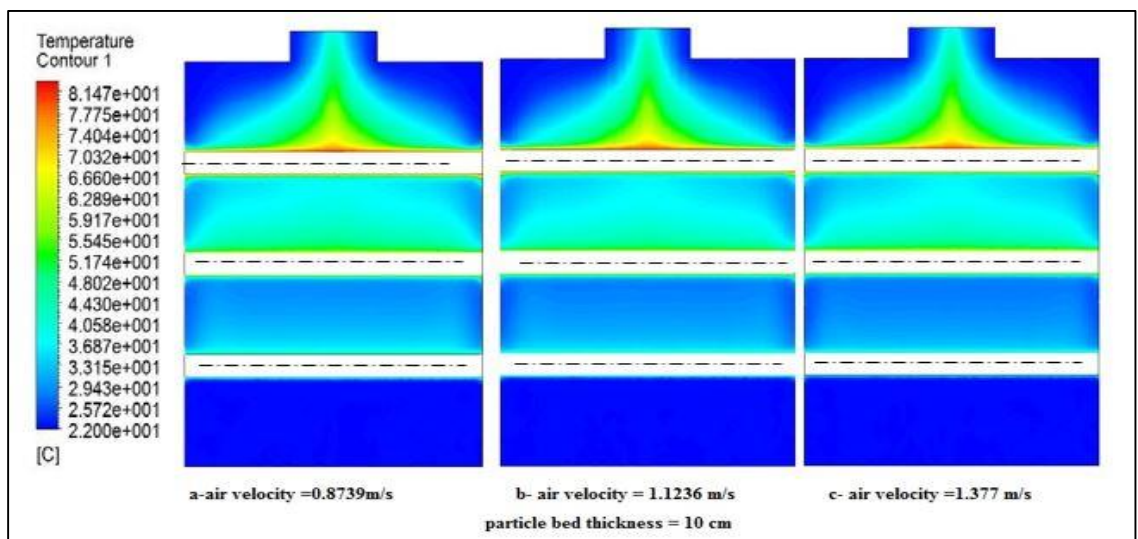
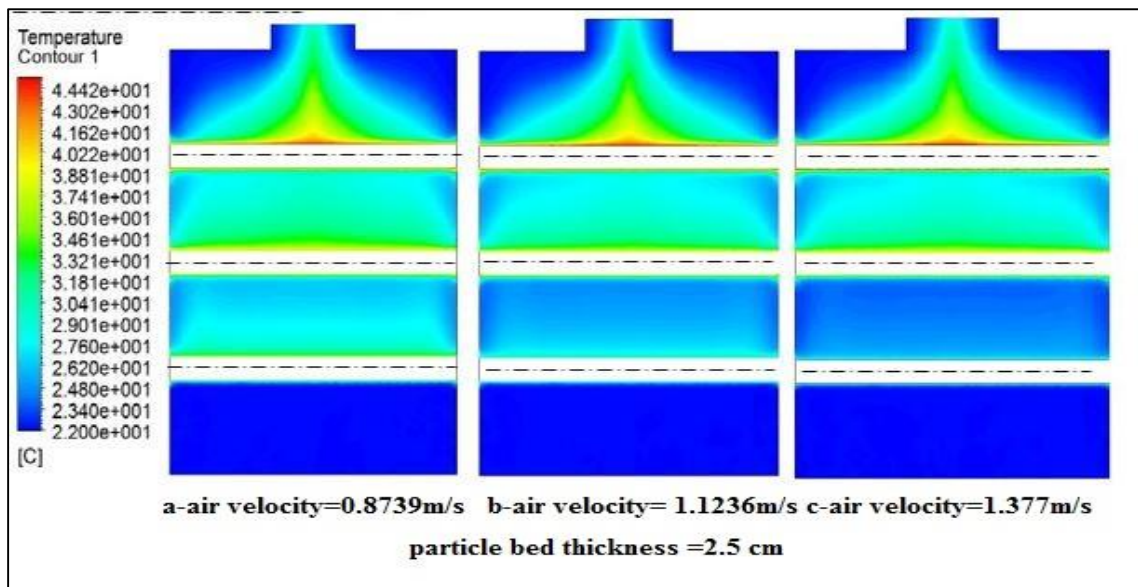
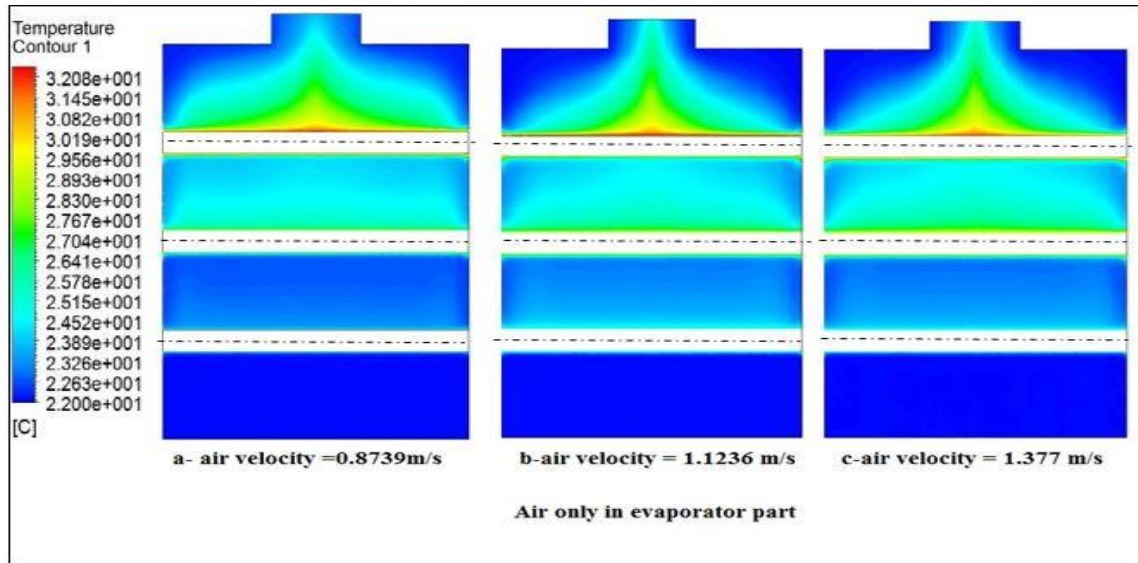
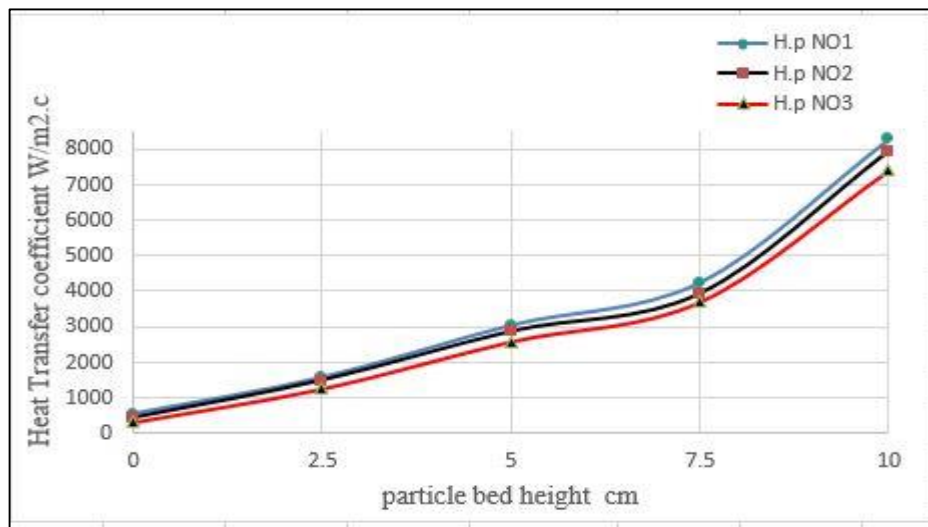


Figure (5.20): Condensers heat distribution at a different superficial velocity and different particle bed height

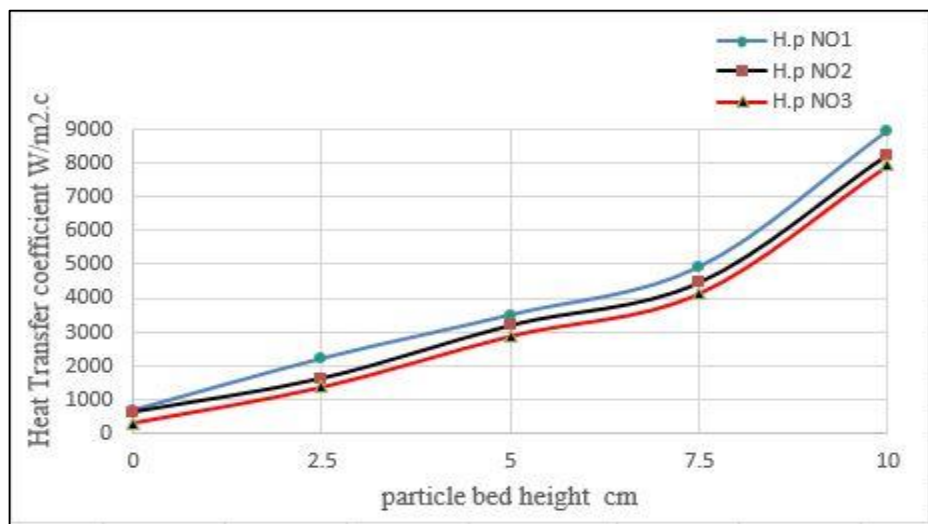


### 5.3.9 Influence of particle bed on heat transfer coefficient

Figure (5.21 a-c) clarifies heat transfer coefficient values under all operation conditions. The charts show increasing heat transfer coefficient with increasing particle bed thickness, and maximum enhancement about (95%) which occurs at particles bed 10 cm and superficial velocity (1.377) m/s at heat pipe number (1), while minimum enhancement was (90%) at bed 2.5 cm and superficial velocity (0.8739) m/s at heat pipe number (3).

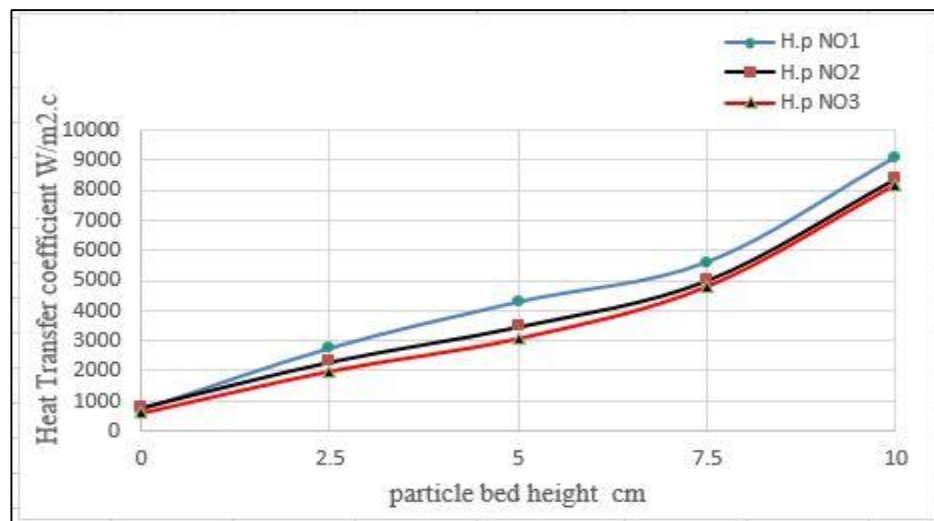


a-Air superficial velocity 0.8739 m/s



b-Air superficial velocity 1.1236 m/s

Figure (5.21): Influence of particle bed thickness on heat transfer coefficient at different air velocity

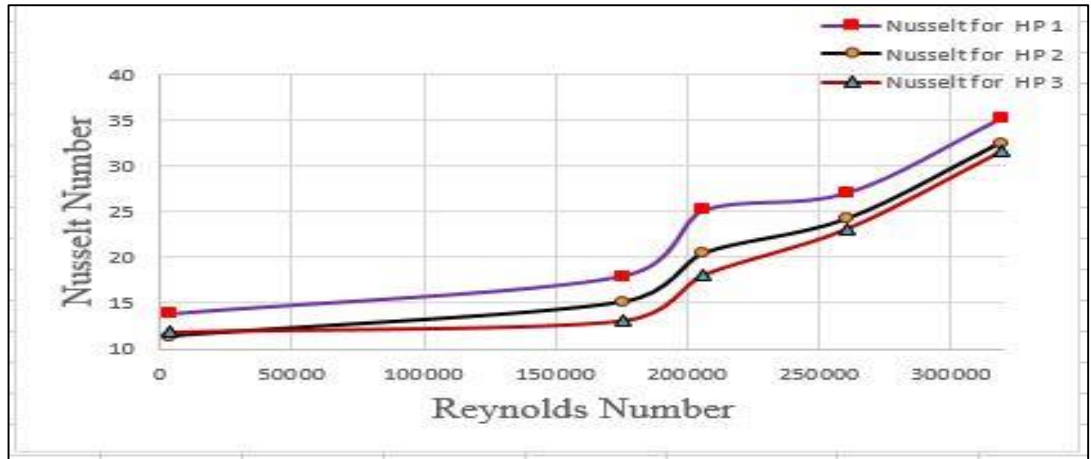


c-Air superficial velocity 1.377 m/s

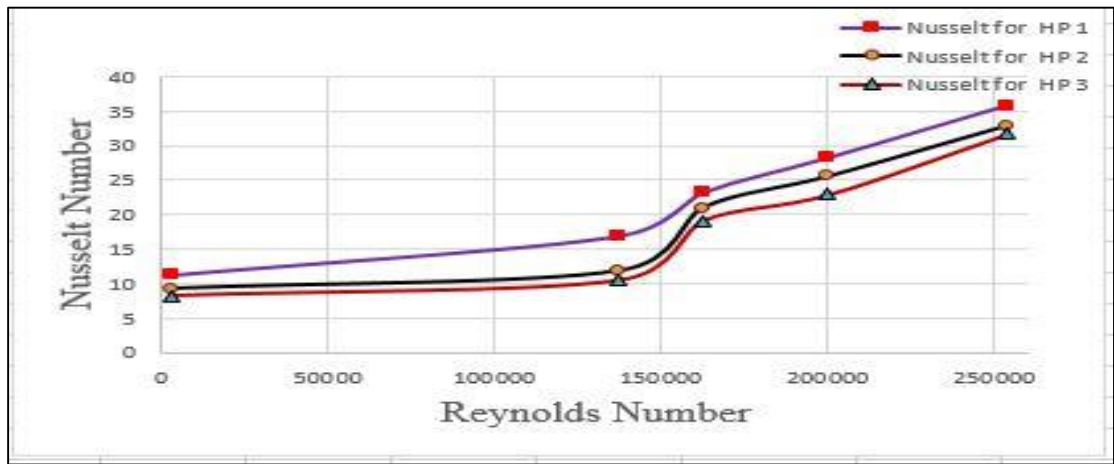
Figure (5.20) continued

### 5.3.10 Nusselt number variation with Reynolds Numbers

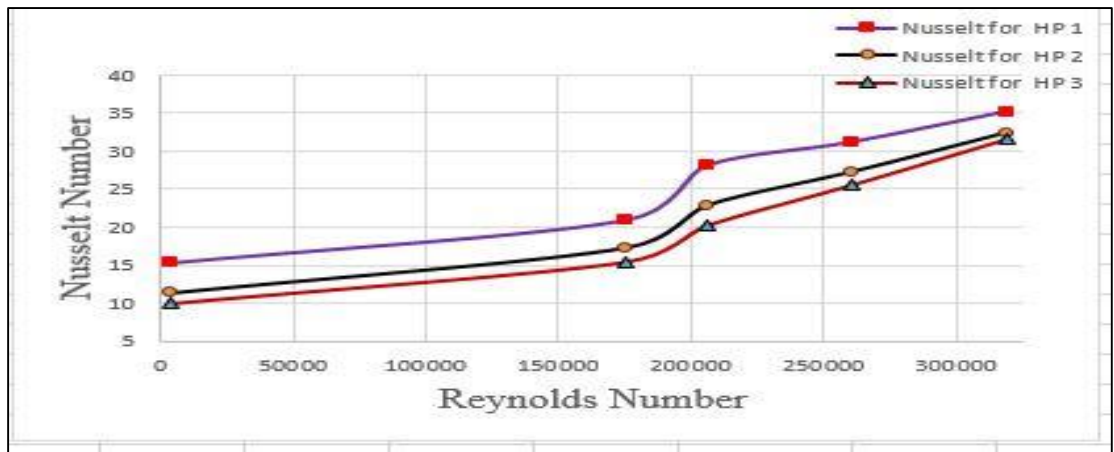
Figure (5.22 a-c) states numerical values for Nusselt and Reynolds numbers for superficial velocity (0.8739 to 1.377) m/s. Charts obviously show Nusselt number increase with increasing Reynolds number for all particle bed height and also increased with increasing velocity. Maximum increase in Nusselt number is about (76%) and that occurs at superficial velocity 1.377 m/s at heat pipe number (1) and at particle bed height 10 cm comparing with no particle was used; while minimum value (60.5%) which found at superficial velocity 0.8739m/s at heat pipe number (3) and at particle bed height 2.5 cm comparing with no particle was used



a-Superficial velocity 0.8739 m/s



b-Superficial velocity 1.1236 m/s



c-Superficial velocity 1.377 m/s

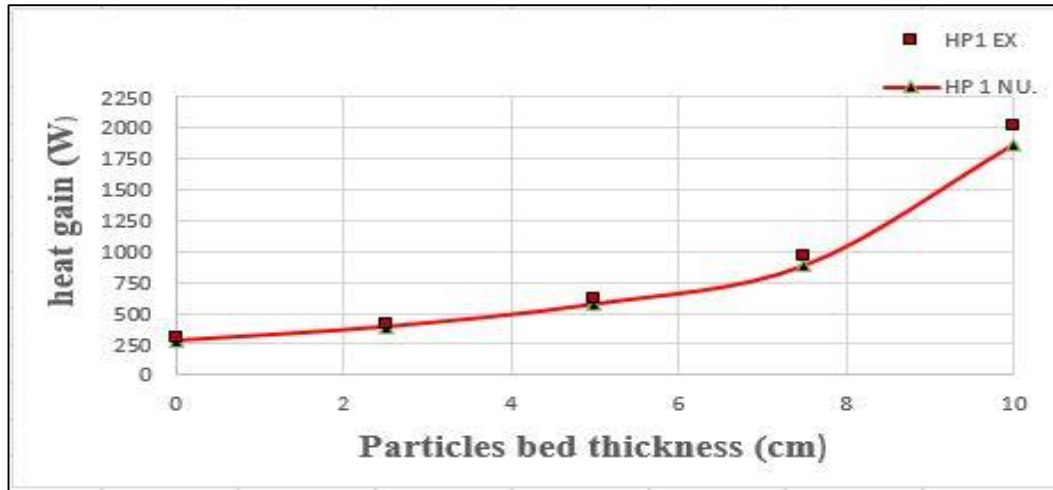
Figure (5.22): Relationship between Nusselt and Reynolds numbers for all heat pipes at different bed thickness and superficial velocities

## **5.4 comparison between experimental numerical results**

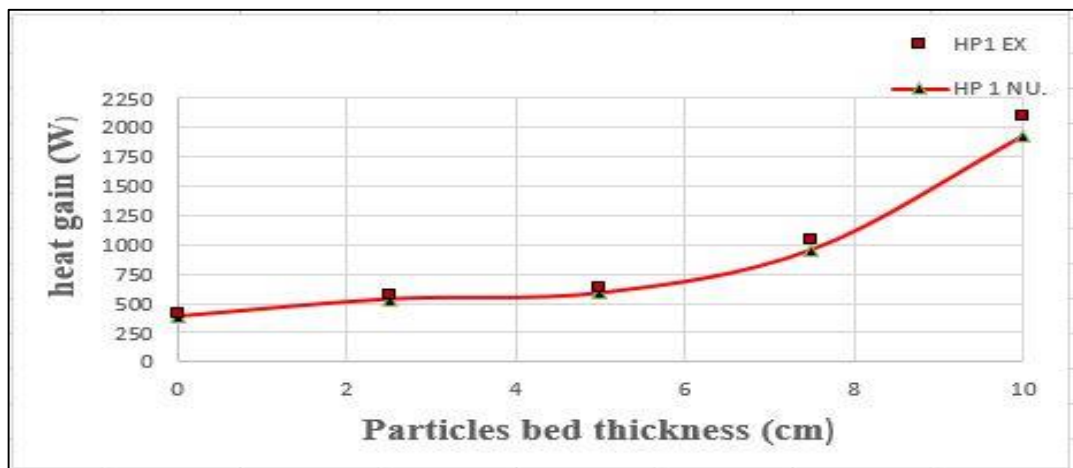
### **5.4.1 heat pipe location**

Figure (5.23 a-c) collects evaporator heat gained for numerical and experimental measured for superficial velocity (0.8739 to 1.377) m/s and particle bed height (0 to 10) cm. for heat pipe number (1). From the lower figure, it could have observed that heat pipe gained was similar behavior at experiment and numerical values. It could be observed that at increasing particle bed thickness increased heat gained for all heat pipes; but with different ratios since the increase of heat transfer coefficient for air- particles mixtures. Also it could be observed that with the increase air velocity heat pipe gained increased because the good commingles take place at high velocity.

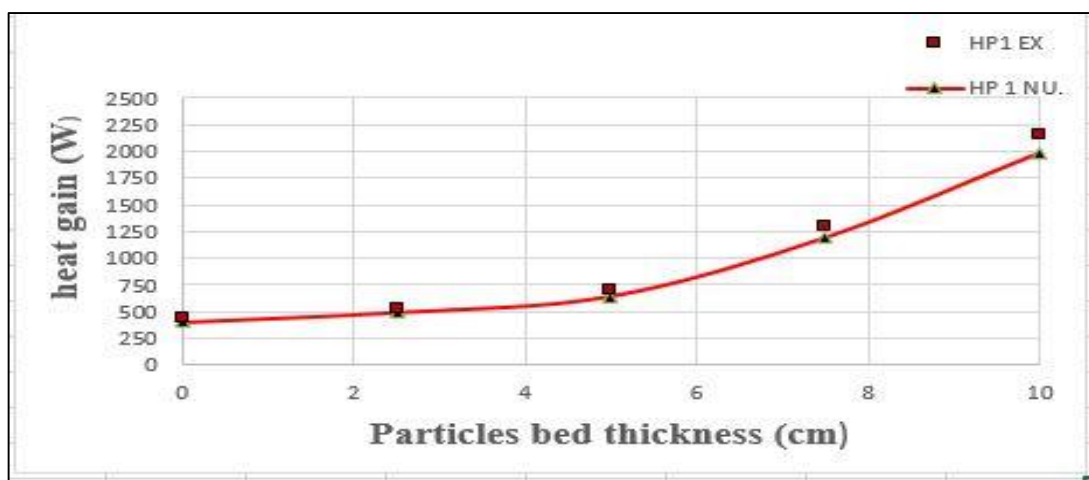
From the same figure, it could be observed that amount of numerical and experimental values were closed together and with maximum deviation between them is (8%) .It could be also observed that numerical less than experimental values due to errors in measurements devices that used to measure heat and air flow rate in experimental part .Another reason was in experimental calculation when mixture properties were taken constant with changing of temperature for domain while, indeed all, the properties were changing with temperature ,also the hypotheses that used in numerical procedure



a- Air velocity 0.8739m/s



b- Air velocity 1.1236 m/s



c- Air velocity 1.377 m/s

Figure (5.23a-c): Numerical and experimental comparison heat gained values for heat pipe (1) in evaporator part at different particle bed thickness and air velocities

### 5.4.2 Influence of particle bed thickness

Figure (5.23 C) shows the particle bed effect on evaporator part heat gained numerically and experimentally for heat pipe number (1) to compare between them. The bed thickness in our consideration was (0, 2.5, 5, 7.5, 10) cm. and superficial velocity was (1.377) m/s. clearly, it could be noted that increasing heat gained with increasing particle thickness.

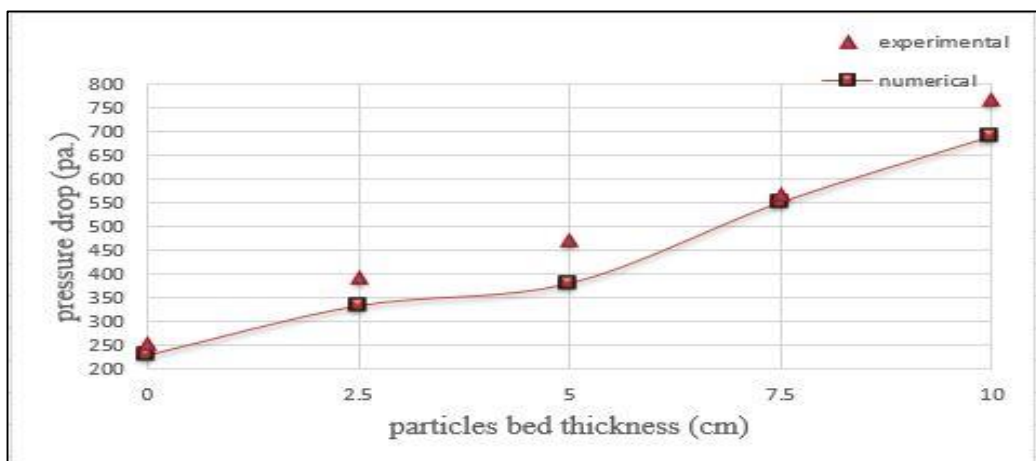
### 5.4.3 Pressure drop comparison

Figure (5.24 a) represents experimental numerical pressure drop comparison at superficial velocity 0.8739 m/s for particle bed (0, 2.5, 5, 7.5 ,10) cm. two curves closed together and with average deviation (11%).

And Figure (5.24 b) represents it at superficial velocity 1.1236 m/s and with average deviation (4%).

At same Figure at(c) with superficial velocity 1.377 m/s and with average deviation (8.6%).

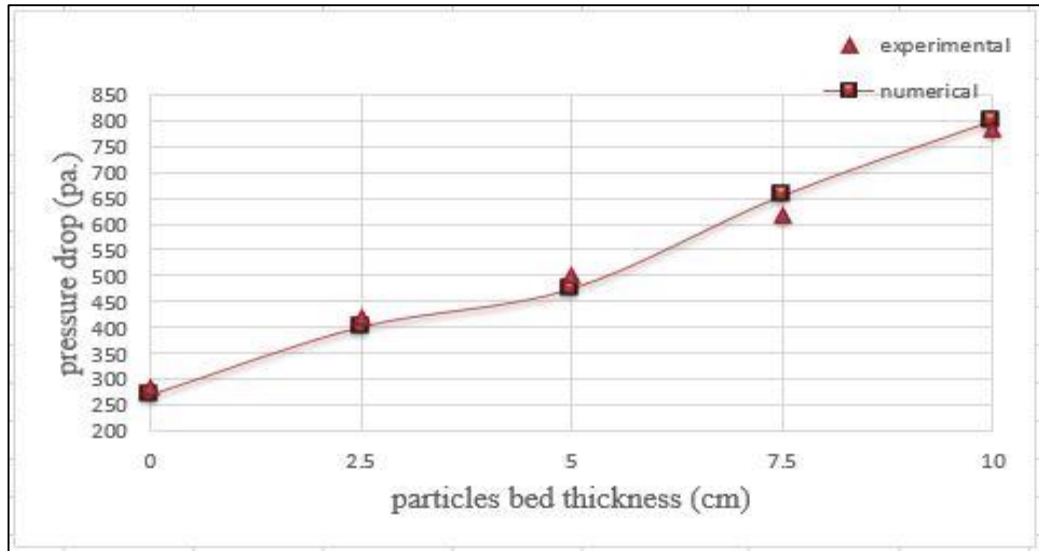
It seems the deviation between numerical and experimental values due to the measuring pressure drop at two-dimension models while at real model there was three dimensions.



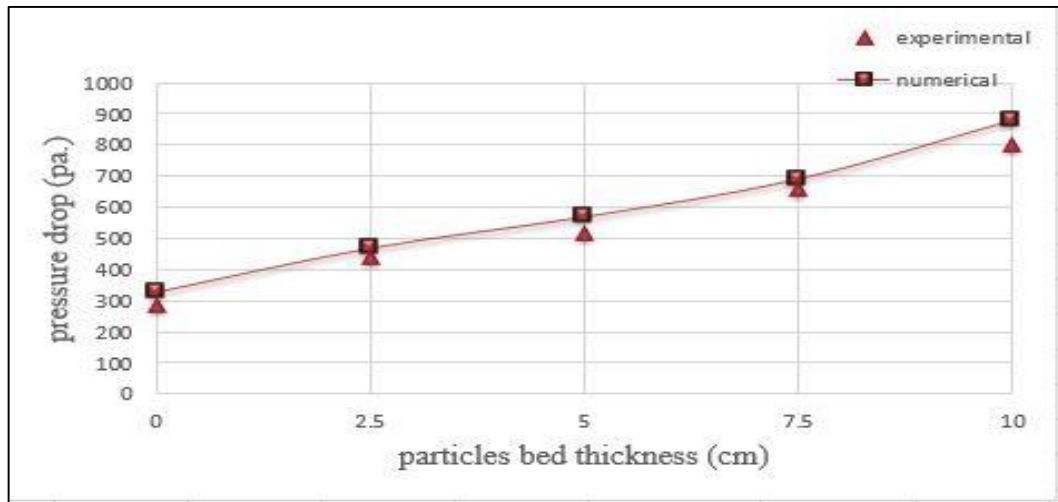
a-Superficial velocity 0.8739 m/s

Figure (5.24): Pressure drop experimental numerical comparison

At different superficial velocity



b-Superficial velocity 1.1236 m/s



c-Superficial velocity 1.377 m/s

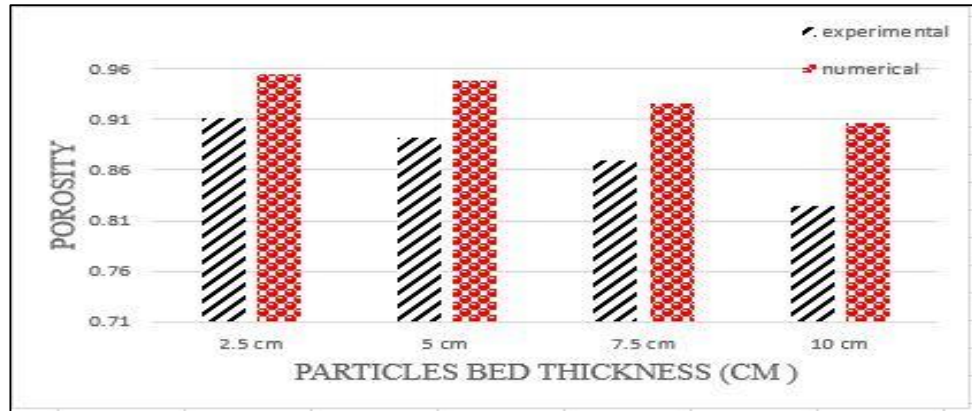
Figure (5.24) continued

#### 5.4.4 Porosity comparison

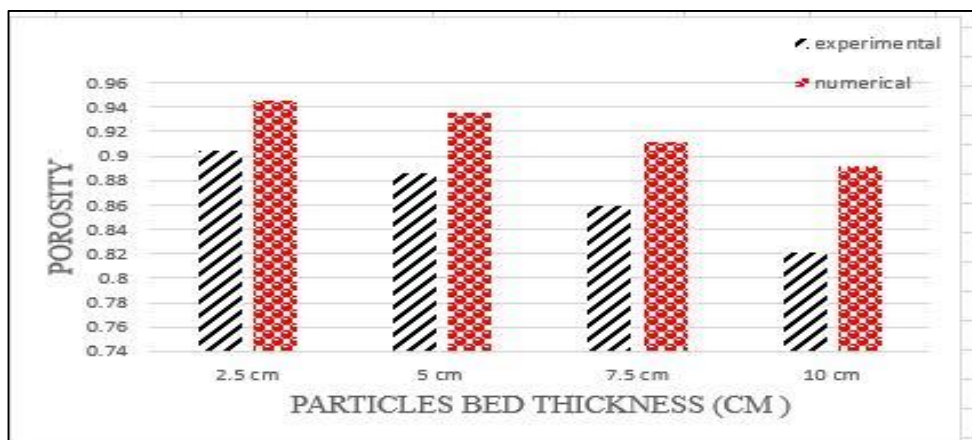
Figure (5.25a) represents experimental numerical porosity comparison at superficial velocity 0.8739 m/s for particle bed (2.5, 5, 7.5 ,10) cm. two column closed together and with average deviation (3.5 %).

Figure (5.25 b) represents porosity at superficial velocity 1.1236 m/s and the average deviation was (5.75 %).

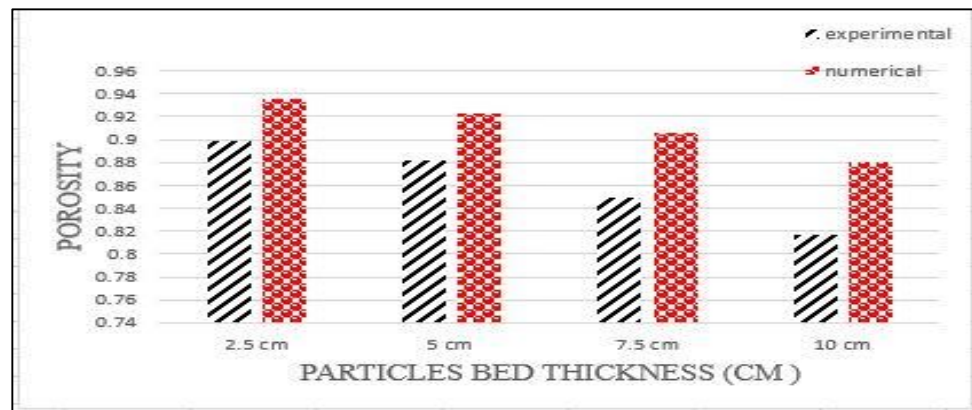
Figure (5.25 c) represents porosity at superficial velocity 1.337 m/s and the average deviation was (5.4 %).



a-Superficial velocity 0.8739 m/s



b-Superficial velocity 1.1236 m/s



c-Superficial velocity 1.377 m/s

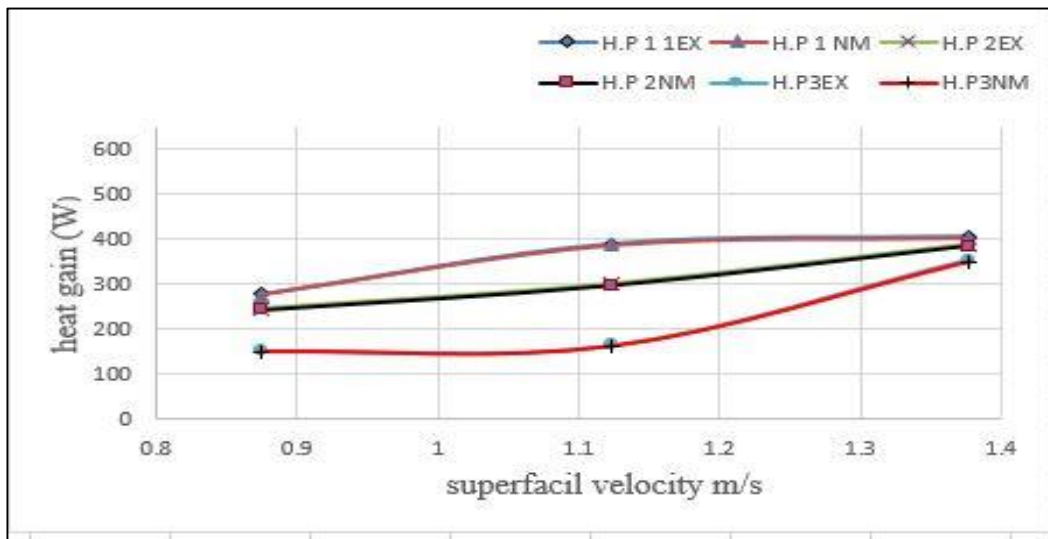
Figure (5.25 a-c): Experimental- numerical porosity comparison at superficial velocity (0.8739-1.377) m/s for particle bed (2.5, 5, 7.5 ,10) cm



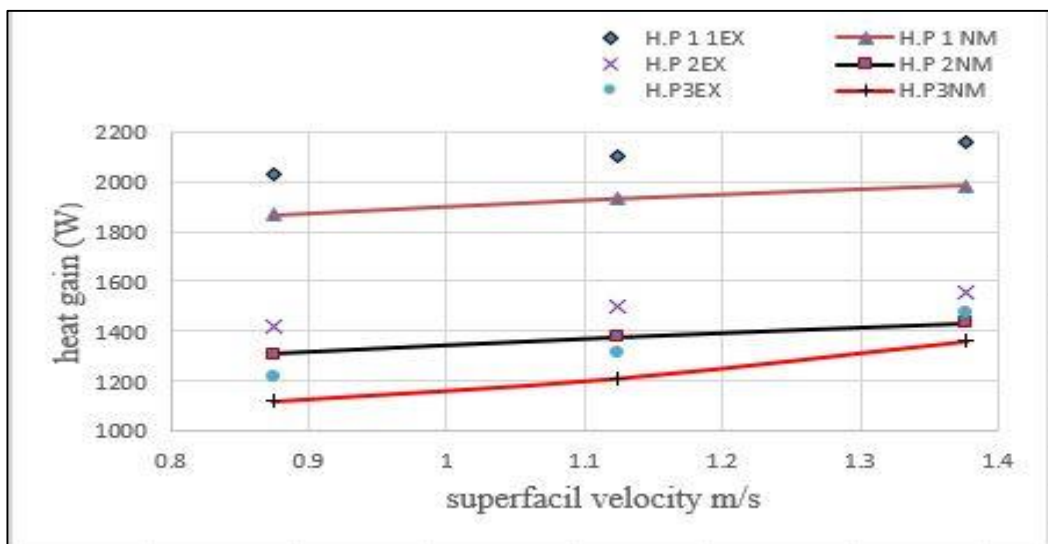
### 5.4.5 Comparison of superficial velocity effect

Figure (5.26 a-b) represent comparison between experimental and numerical values for evaporator heat gained.

It could be noted from chart similar behavior between experimental and numerical values with average deviation about (8.5%). It is also observed that superficial velocity changes have less effect on increasing heat gained in evaporator part with testing operation range.



a-Air only



b- Particle bed thickness 10cm

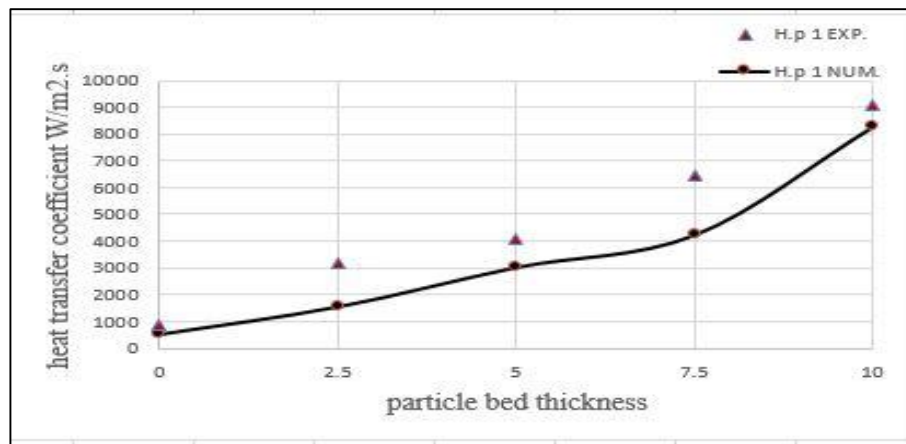
Figure (5.26 a-b): Comparison experimental- numerical heat gained values for different superficial velocity at different bed thickness

### 5.4.6. Comparison of heat transfer coefficient

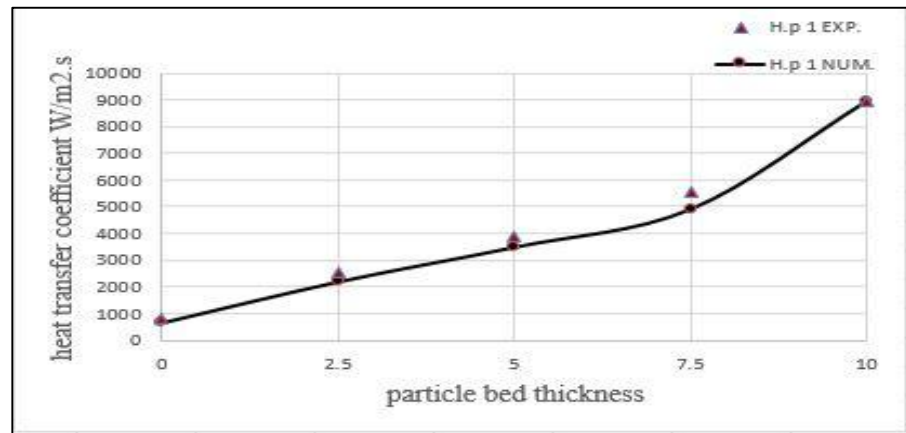
Figure (5.27 a) shows a comparison between heat transfer coefficient values of experimental and numerical procedure at superficial velocity 0.8739m/s and for particle bed height (0,2.5,5,7.5,10) cm. definitely two curves closed together but average deviation between them at that velocity was 11.5 %.

Figure (5.27 b) shows same comparison at superficial velocity 1.1236 m/s with average 9.9 %

Figure (5.27 c) shows same comparison at superficial velocity 1.377m/s with average deviation 9.96 %

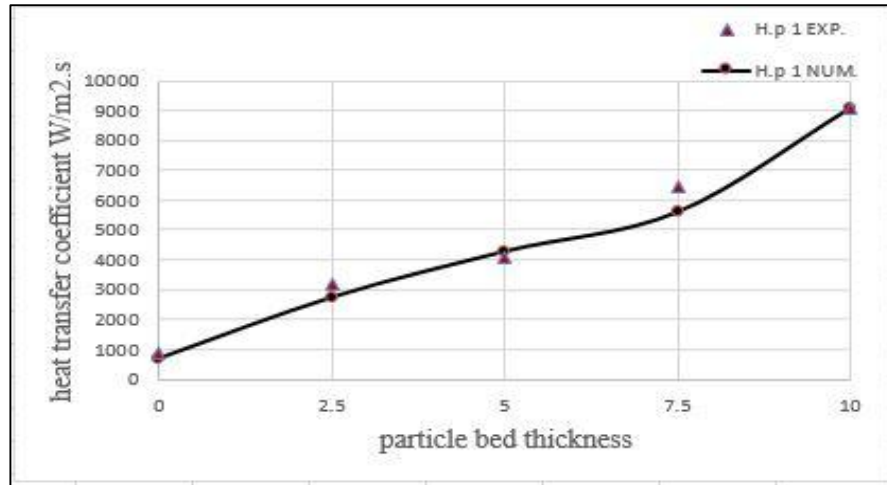


a-Superficial velocity 0.8739 m/s



b-Superficial velocity 1.1236 m/s

Figure (5.27a-c): Heat transfer coefficient comparison for experimental-numerical values for heat pipe number (1)



c-Superficial velocity 1.377 m/s

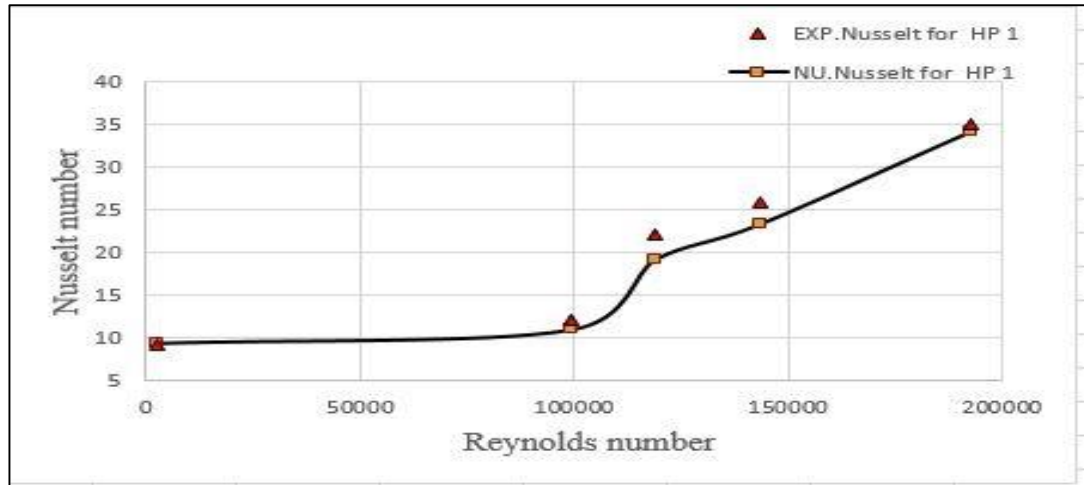
Figure (5.26) continued

#### 5.4.7 Comparison experiential and numerical Nusselt number

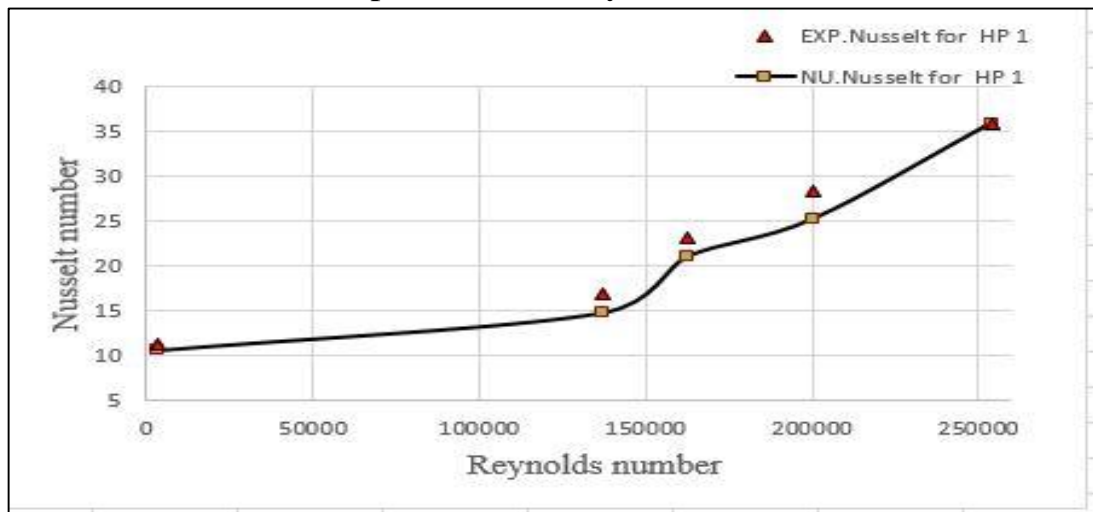
Figure (5.28a) represents comparison between numerical experimental values for Nusselt numbers at heat pipe inside evaporator part for superficial velocity 0.8739m/s. The two curves closed together average deviation for heat pipe no. (1, 2, 3) was 7.28%,7.08%,6.525% respectively.

Figure (5.28b) represents comparison between numerical experimental values for Nusselt numbers at heat pipe inside evaporator part for superficial velocity 1.1236m/s. The two curves closed together average deviation for heat pipe no. (1, 2, 3) was 7.2%,7.14%,7.72% respectively.

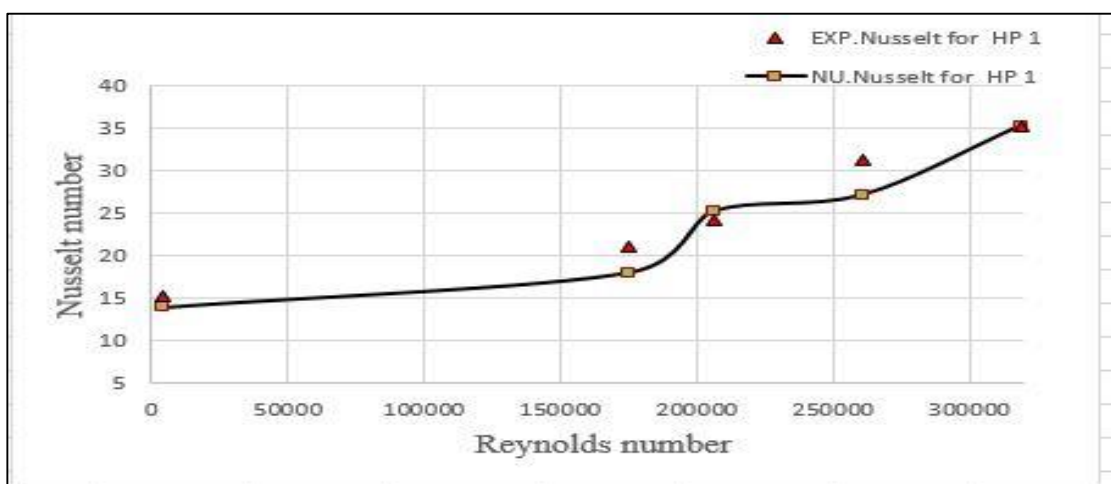
Figure (5.28c) represents comparison between numerical experimental values for Nusselt numbers at heat pipe inside evaporator part for superficial velocity 1.377m/s. The two curves closed together average deviation for heat pipe no. (1, 2, 3) was 8.16%,6.94%,10.76% respectively.



a-Superficial velocity 0.8739 m/s



b-Superficial velocity 1.1236 m/s



c-Superficial velocity 1.377 m/s

Figure (5.28 a-c): Comparison experiential and numerical values of Nusselt Number for heat pipe number (1)

**CHAPTER SIX**

**CONCLUSIONS AND**

**RECOMMENDATIONS**

## Conclusions and Recommendations

### 6.1. Conclusions

The experimental statistics were compared with a CFD simulation data extracted from ANSYS FLUENT 18.0. The following conclusions can be made.

- 1- Heat pipe location have severe effect on heat gained in evaporator part, where pipe heat gained has direct proportional with its location close to heat source. Heat pipe number (1) gained heat greater than heat pipe number (3) with 57%. maximum amount of heat gained in evaporator part achieved at high superficial velocity 1.337 m/s and at high particle bed thickness 10 cm.
- 2- The results show that when the particle bed increased from (2.5 to 10) cm. the porosity decreased by (9%) approximately for all superficial velocities. For increasing superficial velocity from (0.8739 to 1.377) m/s, the porosity decreased by 2%.
- 3- Increasing superficial velocity for (0.8739 to 1.337) m/s increased the heat gained at evaporator part for maximum and minimum values (21 and 8) % respectively.
- 4- When particle bed thickness increased from (0 to 10) cm. pressure drop by 65% increased; while at same particle bed but at different air superficial velocity, the pressure drop does not exceed (13%).
- 5- The heat transfer coefficient at particle bed thickness (10) cm. increased by (70%) if compared with no particle bed case at the same superficial velocity at heat pipe number (1).
- 6- The maximum Nusselt Number was (35.125) which was achieved at maximum particle bed height (10cm) at maximum superficial velocity

(1.377m/s). The maximum enhancement in Nusselt Number was (75.7%).

7- From the comparison of the results, the minimum and maximum difference in Nusselt number was (6.525 and 18.6) %. between the experimental and the numerical results.

## **6.2. Recommendations**

Recommendation can be given in the following points:

- 1- Studying heat gained in heat pipe at same outer condition but for different working fluid type, different wick layer number, different wick type and also at different heat pipe diameter.
- 2- Using other types of particles inside the box. Also heat gained can be calculated with different particles diameter and comparing between the results and previous results.
- 3- Use a wide range of air superficial velocity and note the difference in heat gained at different air velocity.
- 4- Add Nano particles inside heat pipe and study heat pipes heat gain enhancements.
- 5- Studied effect of heat pipes sort on heat gain in evaporator parts and its effect on heat transfer coefficient inside evaporator part.

# **REFERENCES**



## References

- [1] Peterson G. P., "Introduction to Heat Pipes," "Jentung Ku NASA/Goddard flight center" vol.2. p. 356, 2015.
- [2] Reay and P. Kew, "Heat pipe components and materials," Heat pipes Theory, Des. vol.11 Appl., p. 108–110, 114, 122, 126–127, 2006.
- [3] Yang. H., Khandekar., and. Groll. M, "Performance characteristics of pulsating heat pipes as integral thermal spreaders," Int. J. Therm. Sci., vol. 48, No. 4, pp. 815–824, 2009.
- [4] Dunn. P. D. and. Reay D. A., "The heat pipe Advantage by Econotherm," Phys. Technol., vol. 4, pp. 187–201, 1973.
- [5] Chen. T., "Heat pipes and its applications," "Encycl. Two-Phase Heat Transf. Flow II", ., vol. 33, No. 4 pp. 311–353, 2015.
- [6] Vasiliev. L. L., "Heat pipes in modern heat exchangers," "Appl. Therm. Eng.," vol. 25, No. 1, pp. 1–19, 2005.
- [7] Wallin. P., "Heat Pipe , selection of working fluid," "Heat and Mass Transfer, Lund, Sweden," ., vol. 24, No. 12 pp. 1–7, 2012.
- [8] Obeed Majeed. "Mathematical model for predicting the heat transfer coefficient between shallow gas fluidized beds and vertical surface immersed in it," full thesis, Univ. Mosul 2002.
- [9] Meir G. B., "'Basics of Fluid Mechanics', Potto Project, Chicago, Illinois, eMail: genick at potto dot org, Version 0.3.4 July 25, 2013."
- [10] Kunji. O., Daizo and Levenspici, "Fluidization Engineering. ," Florida: Robert E. Krieger Publishing Company," 1984.

- [11] Ergun. S. and Corning. A. A., “Fluid Flow through Randomly Packed Columns and Fluidized Beds,” *Ind. Eng. Chem.*, vol. 41, No. 6, pp. 1179–1184, 1949.
- [12] Xu. B. H. and Yu. a. B., “Numerical simulation of the gas-solid flow in a fluidized bed by combining discrete particle method with computational fluid dynamics,” “*Chem. Eng. Sci.*”, vol. 52, No 16, pp. 2785–2809, 1997.
- [13] Fan L., Grace J., and Epstein N., “CFD Simulation of a Liquid-Fluidized Bed of Binary Particles”, *Engineering Conferences International*, ., vol. 36, No. 46. 2010.
- [14] Ajay M. R., and Karnik A., “Numerical investigation of the effect of bed height on minimum fluidization velocity of cylindrical fluidized bed”, *International Congress on Computational Mechanics and Simulation (ICCMS)*, IIT Hyderabad, 2012.
- [15] Kumar R. and Pandey K. M., “CFD Analysis of Circulating Fluidized Bed Combustion”, *IRACST-Engineering Science and Technology: An International Journal (ESTIJ)*, Vol. 2, No. 1, PP. 163-173, 2012
- [16] Tandon M.P., and Karnik A.U., “Simulation of Rectangular Fluidized Bed with Geldart D Particles”, *10th International Conference on CFD in Oil & Gas, Metallurgical and Process Industries, SINTEF, Trondheim, Norway*, June 2014.
- [17] Mohammad S.Q. Aldabbagh, “Optimum design of a heat pipe,” *College of Basic Education / Mosul /University Al-Rafidain Engineering* Vol.23 No. 2 April 2015 pp. 43–56, 2014

- [18] Hou, Z. Y. Zhou, and A. B. Yu, “Gas-solid flow and heat transfer in fluidized beds with tubes: Effects of material properties and tube array settings,” *Powder Technol.*, vol. 296, pp. 59–71, 2016
- [19] Grewal .N. S. , “A generalized correlation for heat transfer between a gas-solid fluidized bed of small particles and an immersed staggered array of horizontal tubes,” *Powder Technol.*, vol. 30, No. 2, pp. 145–154, 1981.
- [20] Udell. K. S., “Heat Transfer in Porous Media Considering Phase Change and Capillarity - The Heat Pipe Effect,” *Int. J. Heat Mass Transf.*, vol. 28, No. 2, pp. 485–495, 1985.
- [21] Kobro, H. and Brereton, ““Control and Fuel Flexibility of Circulating Fluidized Beds’, ,” “ *Circulating Fluidized Bed Technology*, ed. P Basu, ,” pp.263-272, Pergamon Press, Toronto.,” 1986.
- [22] Dry, R. J., White, R. B. and Close, ““The Effect of Gas Inlet Geometry on Gas-Solid Contact Efficiency in a Circulating Fluidized Bed’, *Fluidization VII*, ed. O. E. Potter and P. J. Nicklin, pp. 21 1-2 18, Engineering Foundation, New York.,” 1992.
- [23] Ninad. S, “Incorporation of Heat Pipes Into Engine Air Pre-Cooling:A Feasibility Study”, A thesis Master Department of Mechanical and Nuclear Engineering College of Engineering, B.E., University of Pune. 2003.
- [24] Parise. M. R., “Heat Transfer Coefficient in a Shallow Fluidized Bed Heat Exchanger with a Continuous Flow of Solid Particles,” “*Braz. Soc. Mech. Sci. Eng.*, ,” vol. VIII, No. 3, pp. 253–258, 2006.
- [25] Ahmad. H. H, “Heat Transfer Characteristics in a Heat Pipe Using Water-Hydrocarbon Mixture as a Working Fluid . ( An Experimental

- Study ) Iraqi Academic Sci. J., pp. 128–137, 2011.
- [26] Yang, Y. Y. Yan, and D. Mullen, “Recent developments of lightweight, high performance heat pipes,” *Appl. Therm. Eng.*, vol. 33–34, No. 1, pp. 1–14, 2012.
- [27] Salwe .A. M., “Local heat transfer coefficient around a horizontal heating element in gas-solid fluidized bed,”” *International Journal of Application or Innovation in Engineering & Management*” vol. 2, No. 6, pp. 344–348, 2013
- [28] Asirvatham. L. G., R. Nimmagadda, and S. Wongwises, “Heat transfer performance of screen mesh wick heat pipes using silver-water nanofluid,” *Int. J. Heat Mass Transf.*, vol. 60, No. 1, pp. 201–209, 2013.
- [29] Lechner S. M. Merzsch, and H. J. Krautz, “Heat-transfer from horizontal tube bundles into fluidized beds with Geldart A lignite particles,” “*Powder Technol.*” vol. 253, pp. 14–21, 2014.
- [30] Moslemian, M. M. Chen, and B. T. Chao, “Heat transfer to horizontal tubes in a fluidized bed: The role of superficial gas and local particle velocities,” *Exp. Therm. Fluid Sci.*, vol. 4, No. 1, pp. 76–89, 1991.
- [31] El-baky M. A. A.. and Mohamed. M. M., “Experimental Study of Heat Pipes Heat Exchanger for Heat Recovery in Air,” *Ain Shams University, Faculty of Engineering, Cairo, Egypt, Scientific Bulletin*, vol. 40, No 4, pp. 1119–1136, 2006.
- [32] Hafidh Hassan Mohammed Al-Ghazali, “Investagation Of Heat Transfer in (Gas-Solid) Circulating Fluidized.phD full thesis.submitted to collage of engineering/ baghdad university ” 2011.

- [33] Sahoo. P. and Sahoo. A., "A comparative study on effect of different parameters of CFD modeling for gas-solid fluidized bed," "Part. Sci. Technol. ", vol. 33, No. 3, pp. 273–289, 2015.
- [34] Pakam. Y. and T. Soontorn chainack saeng, "Experimental Investigation of Air-Water HPHE Using Ethanol as the Working Fluid," Contemporary Engineering Sciences vol. No 9, pp. 823–834, 2016.
- [35] Kobayashi, "Heat Pipe Thermodynamic Cycle and its Applications," "Journal of Solar Energy Engineering," vol.No 1. May 1985, 2016.
- [36] Akbarzadeh et al., "Formulation and analysis of the heat pipe turbine for production of power from renewable sources," Appl. Therm. Eng., vol. 21, No. 15, pp. 1551–1563, 2001.
- [37] Tien. C. L., "Fluid Mechanics of Heat Pipes," Annu. Rev. Fluid Mech., Department of Mechanical Engineering, University of California, Berkeley, California vol.NO 7. 1, pp. 167–185, 1975.
- [38] "[https://www.google.com/search?q=working+fluid+move+inside+heat+pipe&source=lnms&tbm=isch&sa=X&ved=0ahUKEwiBqIH3iZ\\_dAhXBCywKHVI5BRUQ\\_AUICygC&biw=1366&bih=650#imgrc=wS8cgWDpTSnxbM:&spf=1535986096177](https://www.google.com/search?q=working+fluid+move+inside+heat+pipe&source=lnms&tbm=isch&sa=X&ved=0ahUKEwiBqIH3iZ_dAhXBCywKHVI5BRUQ_AUICygC&biw=1366&bih=650#imgrc=wS8cgWDpTSnxbM:&spf=1535986096177)."
- [39] Yassir Makkawi, "Particle to Gas Heat Transfer in a Circulating Fluidized Bed Riser" in "10th International Conference on Circulating Fluidized Beds and Fluidization Technology - CFB-10", T. Knowlton, PSRI Eds, ECI Symposium Series, (2013)
- [40] Poolpol. S.. "Experimental Studies of Heat Transfer in Circulating Fluidized Bed" Ph. D. Dissertation, Department of Chemical

- Engineering, University of New Brunswick, “,” 1992.
- [41] Svarovsky. L. •,” Solid—Gas Separation- Chapter 8”, “Gas Fluidization Technology”. Copyright by Johan Wiley and Sone Ltd, 2013.
- [42] Martin Fler,” Heat Recovery from the Exhaust Gas of Aluminum Reduction Cells” School of Science and Engineering/REYST, Master’s thesis, School of Science and Engineering, Reykjavík University, pp. 111. Reykjavík, Iceland, 27 January 2010
- [43] . Raghavan. V. R, “Parametric studies of wall heat transfer in a fluidized bed circulating through a packed bed,” vol. 144, pp. 139–144, 1989.
- [44] Lints. L. . •, M.C. and Glicksman, “Circulating fluidized Bed Technology,” “ AIChE,” Vol.IV, pp 297-304, 1994.
- [45] Eiamsa-ard, S., “Heat transfer enhancement in a tube using delta-winglet twisted tape inserts. ,” “Applied Thermal Engineering,” 30(4): p. 310-318.” 2010.
- [46] “White, F.M., Fluid Mechanics fourth edition, McGraw and Hill. International Edition, Singapore. 1994.”
- [47] “ANSYS FLUENT 12.0 User’s Guide,” *Acta Psychiatr. Scand.*, vol. 123, No. 6, pp. 407–408, 2011.
- [ 48] Brand. S., “Towards an optimal design of heat pipe equipped heat exchangers,” Eindhoven University of Technology Department of Mechanical Engineering Division: Thermo Fluids Engineering Section no. January, 2010
- [49] Lints. L. •, M.C. and Glicksman, “Circulating fluidized Bed

- Technology,” “AICHE,” Vol.IV, pp 297-304, 1994.
- [50] Eiamsa-ard, S., “Heat transfer enhancement in a tube using delta-winglet twisted tape inserts.,” “Applied Thermal Engineering, 30(4): p. 310-318.” 2013.
- [51] Perry M.-H. K. RH Perry, CH Chilton,” Chemical engineering’s handbook”. 1973.
- [52] Fluent Inc. “ANSYS FLUENT 12.0 User’s Guide,” ANSYS, Inc. is certified to ISO 9001:2008 See., vol. 123, No. 6, pp. 407–408, 2011.
- [53] Fluent Inc., “Fluent User’s Guide, ‘Modeling Discrete Phase’, Fluent Inc., September 29, 2006.”
- [54] Fluent Inc., “Fluent User’s Guide, ‘Modeling Discrete Phase’, Fluent Inc., ,” “Chapter 18,”, pp. 1–52. 2014
- [55] Smith. C., “A Solution for Every Multiphase Challenge,” Ansys, pp. 1–55, 2012.
- [56], “Modeling Multiphase Flows,” Fluent User’s Guid., Chapter23 pp. 1–186, 2006.
- [57] Bakker A., “Applied Computational Fluid Dynamics, Mesh Generation”, Computational fluid dynamics lectures, [www.bakker.org](http://www.bakker.org), 2002-2006.
- [58] Mahdi, Q.S.,and S.A. Fattah, “Numerical Investigation to Evaluate the Performance of Helical Coiled Tube Heat Exchanger With and Without Nano fluid.,” ASME 2013 Int. Mech. Eng. Congr. Expo., 2013.
- [59] Hassanain Ghani and Abudl-Muhsin, “Numerical Investigation of the

- Effect of Wire Screen Mesh Specification and Evaporator Length on Thermal Performance of Cylindrical Heat Pipe,” pp. 240–254, 2014.
- [60] Hada. S. S. and P. K. Jain, “Influence of Different Parameters on Heat Pipe Performance,” “Int. J. Eng. Res. Appl. .”, vol. 5, no. 10, pp. 93–98, 2015.
- [61] Ali. Aref. Hatim, “Evaluation of Fluidized bed Heat Pipe Heat Exchanger,” “full thesis Submitted to the Department of Mechanical Engineering University of Technology” 2003.,”
- [62] Nemec. P., Čaja. A., and Malcho. M., “Mathematical model for heat transfer limitations of heat pipe,” Math. Comput. Model., vol. 57, no. 1–2, pp. 126–136, 2013.
- [63] Hameed. H. G. and. Rageb A. M. A., “Experimental investigation of thermal performance of variable conductance cylindrical heat pipe using nanofluid,” Int. J. Mech. Mechatronics Eng., vol. 14, no. 6, pp. 27–32, 2014
- [64] Figliola. R. and Beasley D., Theory and Design for Mechanical Measurements.third edition . 2011.
- [65] Jia. D., Lim, S, Sokhansanj, and Tsutsumi A., “Heat Transfer in a Pulsed Fluidized Bed of Biomass Particles,” “Ind. Eng. Chem. Res.,” vol. 56, No. 13, pp. 3740–3756, 2017.



## **Appendix-A**

---

### **1. effective of Capillary radius $r_c$**

$$r_c = \frac{1}{2N} \quad \dots(A-1)$$

Where N is the number of pores at wick for one meter

### **2. Porosity $\epsilon_p$**

$$\epsilon_p = 1 - \frac{\pi * S * N * DW}{4} \quad \dots(A-2)$$

S = crimping factor for wick structure = 1.05

### **3. Permeability K**

$$K = \frac{DW^2 * \epsilon^2}{122(1-\epsilon)^2} \quad \dots(A-3)$$

### **4. Screen Mesh Effective Thermal conductivity $K_{eff}$**

$$K_{eff} = K_l * \left[ \frac{(K_l + K_w) - ((1-\epsilon) * (K_l - K_w))}{(K_l + K_w) + ((1-\epsilon) * (K_l - K_w))} \right] \quad \dots(A-4)$$

$K_l$  = thermal conductivity for liquid

$K_w$  = thermal conductivity for the wick

### **5. Effective heat pipe length $L_{eff}$**

$$L_{eff} = 0.5L_e + L_{ad} + 0.5L_c \quad \dots (A-5)$$

### **6. Vapor core temperature**

The equation that calculation heat pipe limit getting from

$$T_v = \frac{T_{se}L_e + T_{sc}L_c}{L_e + L_c} \quad \dots(A-6)$$

Where  $T_v$  vapor gap temperature,  $T_{se}$  heat temperature at the evaporator part surface,  $T_{sc}$  heat temperature at condenser part surface,  $L_e$  evaporator part length,  $L_c$  condenser part length.

## 7. limitation of heat transfer in the heat pipe[62]

The heat pipe transfer heat from evaporating side to condenser side by working fluid movement inside it, if the amount of heat exceeds limit range the liquid-vapor cycle may be disturbed and that lead to evaporate dry and at that time the heat pipe stop work. That limits was calculate from previous equation.

### 7.1 Capillary limit.

The movement of working fluid inside the heat pipe depends on pressure differential and that includes liquid and vapor phase, so that amount of that pressure difference should be more than pressure losses inside heat pipe  $\Delta P$  max

$$Q_{c,max} = \left[ \frac{\rho_l \times \sigma_l \times h_{fg}}{\mu_l} \right] \left[ \frac{A_w \times K}{l_{eff}} \right] \left[ \left[ \frac{2}{r_{eff}} \right] - \left[ \frac{\rho_l}{\sigma_l} \right] g L t \cos \theta \right] \quad \dots(A-7)$$

### 7.2 Viscous limit

That limit depends on losses in pressure because of viscosity The general expression represents that limit calculation was.

$$Q_{v,max} = \frac{\pi \times r_v^4 \times h_{fg} \times \rho_{v,e} \times P_{v,e}}{12 \times \mu_{v,e} \times L_{eff}} \quad \dots(A-8)$$

### 7.3 Entrainment limit

Inside heat pipe, there is tow phase flow liquid and vapor at the same time, if that amount of shear force becomes larger than surface tension of liquid at that time particle of liquid was leave its path (the wick) and travel with vapor

$$Q_{e,max} = A v \times h_{fg} \left[ \frac{\rho v \times \sigma_l}{2 r_{c,aver}} \right]^{0.5} \quad \dots(A-9)$$

## 7.4 Sonic limit

Liquid converted to vapor in evaporator part and since vapor mass increased gradually until it reaches to a maximum value at the end of evaporator so the vapor velocity becomes very high, and when the vapor velocity equal to sonic velocity then choked flow was occurring.

$$Q_{s, \max} = 0.474 * A_v * h_{fg} * (\rho_v * P_v)^{0.5} \quad \dots(A-10)$$

### 3.3.5 Boiling limit

This type of limit was concern with the evaporator part of heat pipe that at high operation temperature the bubble was created inside wick structure in evaporator part, that bubble becomes like a film inside wick prevented heat transfer axially from heat source to working fluid to heated it and also prevent more liquid to back from condenser to evaporator and that caused evaporator dry.

$$Q_{b, \max} = \left( \frac{4 * \pi * l_{eff} * T_v * \sigma v}{h_{fg} * \rho_l * \ln\left(\frac{r_i}{r_v}\right)} \right) * \left( \frac{1}{r_n} + \frac{1}{r_{ce}} \right) \quad \dots(A-11)$$

### 3.4 Falling ratio

Studied the exact amount of working fluid that should be but inside heat pipe was Avery important matter because a small amount of working fluid means dry may happen in the evaporator and large amount mean water has plugged the condenser and to calculate it there is a theoretical equation to calculate it as shown below.

$$m = A_v * L * \rho_v + A_w * L * \varepsilon * \rho_l \quad \dots(A-12)$$

Where all that working fluid properties at 200 C°

And there is an experimental equation

$$\phi = V_1 / V_w \quad \dots(A-13)$$

Where:

$\phi$ : working fluid falling ratio

$V_1$ : working fluid volume

$V_w$ : volume of wick space

## Heat pipe calculation

### 1-Vapor core temperature

$$T_V = \frac{T_{Se}L_e + T_{Sc}L_c}{L_e + L_c} = \frac{81.6*64.5 + 34.5*42.3}{64.5 + 42.3} = 63^{\circ}\text{C}$$

### 2- effective Capillary radius $r_c$

$$r_c = \frac{1}{2N} = \frac{1}{2*7086.614} = 7.0555 * 10^{-5}$$

### 3- heat pipe porosity

$$\varepsilon_p = 1 - \frac{\pi*S*N*Dw}{4} = 1 - \frac{\pi*1.05*5*0.055}{4} = 0.773$$

### 4- Permeability

$$K = \frac{Dw^2*\varepsilon^2}{122(1-\varepsilon)^2} = \frac{0.055^2*0.773^2}{122(1-0.773)^2} = 2.87523*10^{-4}$$

### 5- Screen Mesh Effective Thermal conductivity $K_{eff}$

$$K_{eff} = Kl * \left[ \frac{(Kl+Kw) - ((1-\varepsilon)*(Kl-Kw))}{(Kl+Kw) + ((1-\varepsilon)*(Kl-Kw))} \right]$$

$$Kl = 0.654 \text{ w/m.k} \quad \text{at } 60^{\circ}\text{C}$$

$$Kw = 16.35 \text{ w/m.k for stainless steel} \quad \text{at } 60^{\circ}\text{C}$$

$$= 0.654 * \left[ \frac{(0.654+16.35) - ((1-0.773)*(0.654-16.35))}{(0.654+16.35) + ((1-0.773)*(0.654-16.35))} \right] = 0.94915 \text{ w/m.k}$$

### 6-Effective heat pipe length $L_{eff}$

$$L_{eff} = 0.5L_e + L_{ad} + 0.5L_c = 0.5*(64.5 + 2*1 + 34.5) = 0.505 \text{ m}$$

Properties at  $60^{\circ}\text{C}$  and wick properties wanted in heat pipe limitation calculation listed below

$$h_{fg} = 2358.6$$

$$\beta_l = 0.06619$$

$$\rho_l = \frac{1}{v_f} = 983 \text{ kg/m}^3 \quad \mu_l = 0.4673 \cdot 10^{-3} \text{ N.S/m}^2 \quad \mu_{ve} = 1.05 \cdot 10^{-5}$$

$$r_i = 9.9 \cdot 10^{-3} \text{ m} \quad \text{and} \quad r_v = 9.35 \cdot 10^{-3} \text{ m}$$

$$r_n = 2 \cdot 10^{-6} \text{ constant value}$$


---

### 7- Sonic limit

$$\begin{aligned} Q_{s, \max} &= 0.474 \cdot A_v \cdot h_{fg} \cdot (\rho_v \cdot p_v)^{0.5} \\ &= 0.474 \cdot \pi \cdot (9.35 \cdot 10^{-3})^2 \cdot 2358.6 \cdot 10^3 \left( \frac{1}{7.68} \cdot 19.92 \cdot 10^3 \right)^{0.5} \\ &= 15637 \text{ watt} \end{aligned}$$

### 8- Viscous limit

$Q_{v, \max} = \frac{\pi \cdot r_v^4 \cdot h_{fg} \cdot \rho_v \cdot p_v}{12 \cdot \mu_{ve} \cdot L_{eff}}$  for getting case average temperature in evaporator surface was  $T_{ve} = 81.5 \text{ }^\circ\text{C}$  at that temperature calculate density and pressure

$$= \frac{\pi \cdot (9.35 \cdot 10^{-3})^4 \cdot 2358.6 \cdot 10^3 \cdot \left( \frac{1}{7.68} \right) \cdot 19.92 \cdot 10^3}{12 \cdot 1.05 \cdot 10^{-5} \cdot 0.505} = 23.08 \cdot 10^5 \text{ watt.}$$

### 9- Entrainment limit

$$\begin{aligned} Q_{e, \max} &= A_v \cdot h_{fg} \left[ \frac{\rho_v \cdot \sigma l}{2rc_{aver}} \right]^{0.5} \\ &= \pi \cdot (9.35 \cdot 10^{-3})^2 \cdot 2358.6 \cdot 10^3 \cdot \left[ \frac{\left( \frac{1}{7.68} \right) \cdot 0.06619}{2 \cdot 7.05555 \cdot 10^{-5}} \right]^{0.5} \\ &= 17013 \text{ watt} \end{aligned}$$

### 10- Capillary limit

$$Q_{c, \max} = \left[ \frac{\rho_l \sigma l h_{fg}}{\mu_l} \right] \left[ \frac{A_w \cdot K}{l_{eff}} \right] \left[ \left[ \frac{2}{r_{eff}} \right] - \left[ \frac{\rho_l}{\sigma l} \right] g L t \cos \theta \right]$$

When evaporator is down and condenser above then  $\theta = 180$

If Condenser is down and evaporator above then  $\theta = 0$

If horizontally  $\theta = 90$

$A_w = \text{cross section area for wick} = \pi * D_i = \pi * 19.8 \text{ mm} = 62.2 \text{ mm}$

$$= 62.2 * 5 * 0.11 = 34.2119 \text{ mm}^2 = 34.2119 * 10^{-6} \text{ m}^2$$

$$= \left[ \frac{983 * 0.06619 * 2358.6 * 10^3 *}{0.4673 * 10^{-3}} \right] * \left[ \frac{34.2119 * 10^{-6} * 2.87523 * 10^{-4}}{0.505} \right] * \left[ \left( \frac{2}{7.05555 * 10^{-5}} \right) - \left( \frac{983}{0.06619} \right) * 9.81 * 1 * \cos 90 \right]$$

$$= 3.1813 * 10^4 \text{ watt}$$

### Calculation for working fluid

$$r_i = 19.8/2 \text{ mm} = 9.9 \text{ mm}$$

$$r_v = r_i - (\text{number of wick layer} * \text{layer thickness})$$

$$= 9.9 - (5 * 0.11) = 9.35 \text{ mm}$$

$$A_w = \pi * (r_i^2 - r_v^2) = 33.2616 \text{ mm}^2 \text{ wick cross section area}$$

$$A_v = \pi * r_v^2 = 2.746 * 10^{-4} \text{ m}^2$$

$$\rho_f = \frac{1}{v_f} = 969 \text{ kg/m}^3 \quad \text{from steam table at } 60^\circ\text{C}$$

$$\rho_v = \frac{1}{v_v} = 0.3378 \text{ kg/m}^3$$

$$m = A_v * L * \rho_v + A_w * L * \epsilon * \rho_l$$

$$= 2.746 * 10^{-4} * 1 * 0.3378 + 33.2616 * 10^{-6} * 1 * 0.773 * 969$$

$$= 0.025 \text{ kg} = 25 \text{ CC}$$

That's theoretical value and bay mutably by 2.55 that many searchers recommend

$$= 25 * 2.55 = 63.75 \text{ cc fulling amount for each pipe}$$

OR

$$\phi = V_l / V_w$$

$$V_w = \pi * (r_i^2 - r_v^2) * l = \pi * (9.9^2 - 9.35^2) * 1 = 33.26 * 10^{-6} \text{m}^3$$

$$V_{w \text{ new}} = V_w * \epsilon_p = 33.26 * 10^{-6} * 0.773 = 25.711 * 10^{-6} \text{m}^3$$

considered that best ratio was 2.55 as recommended

$$V_1 = 25.711 * 10^{-6} * 2.55 = 65.56 \text{ CC}$$

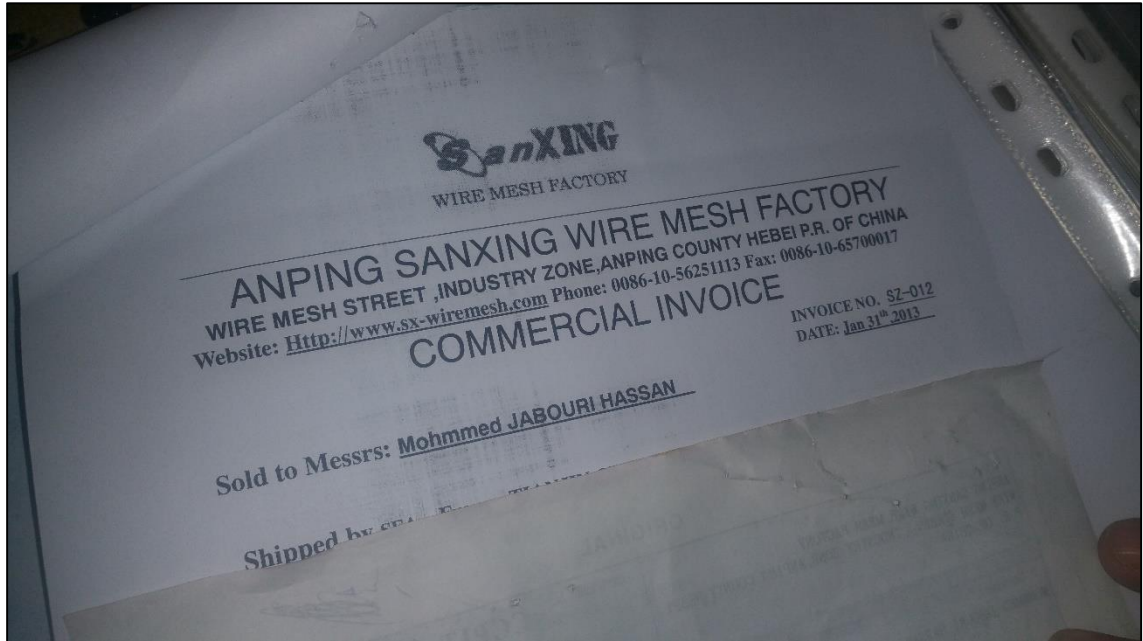


Figure (A-1) wire screen mesh originality certificate

Table A-1 compatibility data[5]

Wick material	Working fluids					
	Water	Acetone	Ammonia	Methanol	Dow-A	Dow-E
Copper	RU	RU	NU	RU	RU	RU
Aluminium	GNC	RL	RU	NR	UK	NR
Stainless steel	GNT	PC	RU	GNT	RU	RU
Nickel	PC	PC	RU	RL	RU	RL
Refrasil fibre	RU	RU	RU	RU	RU	RU

RU, recommended by past successful usage; RL, recommended by literature; PC, probably compatible; NR, not recommended; UK, unknown; GNC, generation of gas at all temperatures; GNT, generation of gas at elevated temperatures, when oxide present.

Table A-2 different types of working fluid with useful temp.  
Range[2]

Medium	Melting point (°C)	Boiling point at atmos. press. (°C)	Useful range (°C)
Helium	-271	-261	-271 to -269
Nitrogen	-210	-196	-203 to -160
Ammonia	-78	-33	-60 to 100
Pentane	-130	28	-20 to 120
Acetone	-95	57	0 to 120
Methanol	-98	64	10 to 130
Flutec PP2 <sup>1</sup>	-50	76	10 to 160
Ethanol	-112	78	0 to 130
Heptane	-90	98	0 to 150
Water	0	100	30 to 200
Toluene	-95	110	50 to 200
Flutec PP9 <sup>1</sup>	-70	160	0 to 225
Thermex <sup>2</sup>	12	257	150 to 350
Mercury	-39	361	250 to 650
Caesium	29	670	450 to 900
Potassium	62	774	500 to 1000
Sodium	98	892	600 to 1200
Lithium	179	1340	1000 to 1800
Silver	960	2212	1800 to 2300



## ***Appendix-B***

---

### **(Calibration Values of Thermocouple and Temperature Recorder)**

In the present work thermocouple with K type manufacture from kormaed +aluminum used and chosen that type of thermocouple because of high working range for operation temperature (190 – 1260) K. Used in present work 28 thermocouple, five in evaporator surface of each one of three heat pipe and one at condenser part, one before heater and one above of it in evaporator part, two above of distributed plate and one after each pipe in evaporator part and three after each pipe in condensers part

Each one of thermocouples calibration process was taken place to it and the calibration procedure was.

Exposing each thermocouple to a fixed point setting (distilled water, boiling temperature, at 100C° and ice point at 0 C°at, atmospheric pressure). Also exposed to acetone with boiling point (56.1C°). Figure (B 1) show the data plan of the thermocouple, reading temperature degree for that test compared with the real temperatures that take by used mercuric manometer. The average calibration line fits the spread data points, and line equation represent correction equation for reading value, that procedure applied for all (28) thermocouple.

$Y = 0.9989x + 0.0581$  correction equation for thermocouple reading

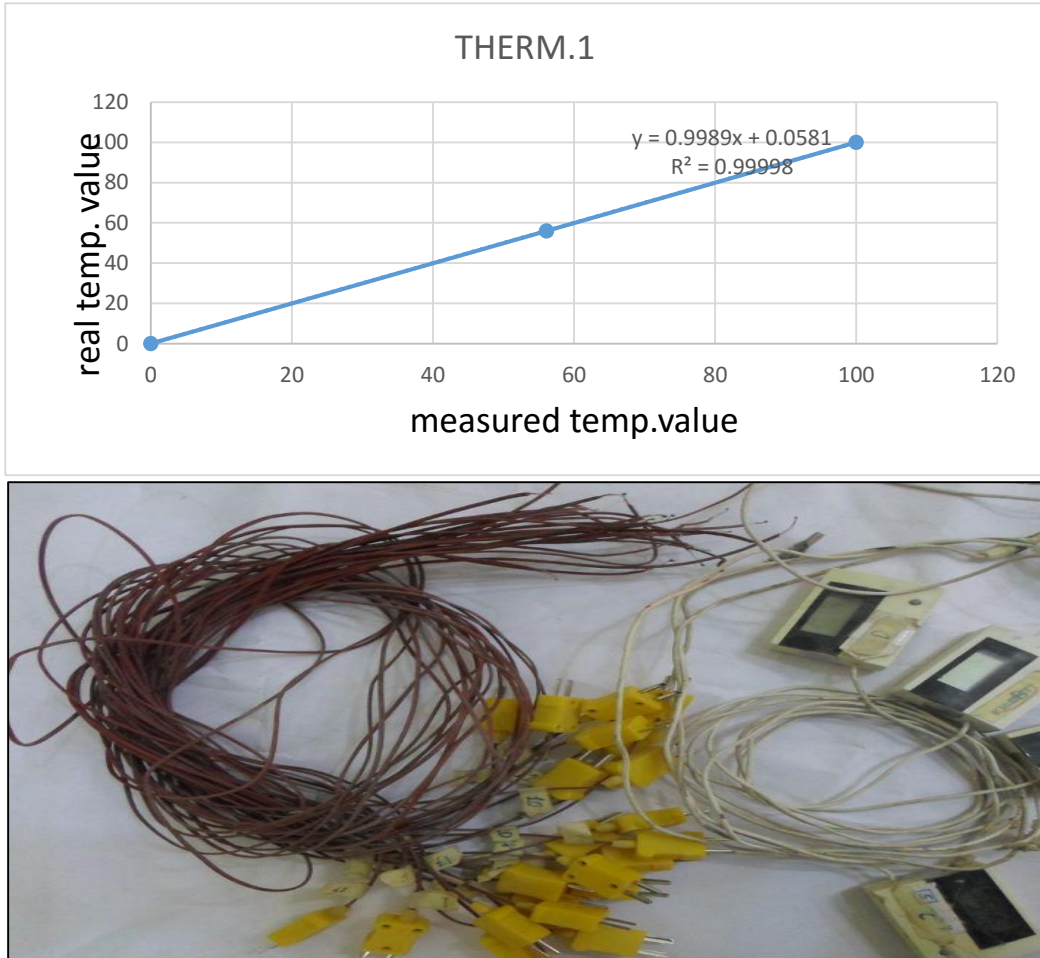


Figure (B 1): Thermocouple photo and its calibration for one of them

	Measuring Range	Resolution	Accuracy
<b>Air Flow</b>	0.1 to 30.0 m/s	0.01 m/s	±3% of reading ±1%FS
	0.2 to 110 km/hr	0.1 km/hr	
	0 to 600 ft/min	1 ft/min	
	0.1 to 59 knots	0.01 knots	
	0.12 to 68 MPH	0.01 MPH	
<b>Air Flow Volume</b>	0 to 999900 CFM	0.001 CFM	
	0 to 999900 CMM	0.001 CMM	
<b>Response time</b>	1 second		
<b>Manual Memory Capacity</b>	5 x 99 sets. (Direct reading from LCD display)		
<b>Operating Conditions</b>	0°C ~ 50°C (32°F ~ 122°F), ≤80% R.H.		
<b>Power Source</b>	6 pcs size AAA Battery		
<b>Battery Life</b>	Approx. 10 hours		
<b>Size</b>	150(L) x 72(W) x 35(H)mm		
<b>Weight</b>	Approx. 400g (including Probe)		
<b>Accessories</b>	Instruction manual, Battery, Carrying case		

Figure (B 2): Hot wire properties



**Calibration certificate for data recorder**



**Calibration certificate for velocity meter**

## Appendix-C

---

### Uncertainty Calculation

For calculate error analysis, repeated the reading for all thermocouples for four times, take water boiling point as reference. Standard and main standard deviation was calculate as following:

$$\sigma = \sqrt{\frac{\sum_1^n (x_i - \bar{x})^2}{n - 1}} \quad , \quad \sigma_m = \frac{\sigma}{\sqrt{n}}$$

Where  $\sigma$  is the standard deviation

$\sigma_m$  is the mean standard deviation

$x_i$  is the values of temperature reading

$\bar{x}$  is the mean of values temperature reading

$n$  is the number of reading of temperature.

As the true value ( $x$ ) was also calculated by

$$x = \bar{x} \pm \sigma_m$$

For thermocouple no. (1), the reading values were (101.1,99.1,98.2,99.3) °C.

The average for that's values was (99.425)

standard deviation calculates:

$$= \sqrt{\frac{(101.1-99.425)^2 + (99.1-99.425)^2 + (98.2-99.425)^2 + (99.3-99.425)^2}{4-1}}$$

$$= 1.551$$

$$\sigma_m = \frac{1.551}{\sqrt{4}} = 0.7755$$

And the true value ( $x$ ) =  $99.425 \pm 0.7755 = 100.2005, 98.6495$

$$\text{The percentage uncertainty} = \frac{100.2005 - 99.425}{100.2005} * 100\% = 0.773 \%$$

=


$$\frac{98.6495 - 99.425}{98.6495} * 100\% = -0.786\%$$


As well as with other sensors. The Table below displays the shows the percentage uncertainty values of each of the four pressure sensors.


THER.NO	HEAT READING VALUES										Average	$\sigma$	$\sigma_m$	X1	X2	percentage uncertainty %	
	101.1	99.1	98.2	99.3	99.425	1.55107	0.77554	100.201	98.6495	0.773985318						-0.786154763	
THER.1	101.1	99.1	98.2	99.3	99.425	1.55107	0.77554	100.201	98.6495	0.773985318	-0.786154763						
THER.2	102.3	101.3	98.6	99	100.3	1.99081	0.99541	101.295	99.3046	0.982676464	-1.002376704						
THER.3	101.5	99.1	98.4	97.5	99.125	1.98389	0.99195	100.117	98.1331	0.990788045	-1.010818176						
THER.4	100.8	101.8	97.5	97.9	99.5	2.05508	1.02754	100.528	98.4725	1.02214531	-1.043477012						
THER.5	101.6	97.8	98.3	97.9	98.9	2.3202	1.1601	100.06	97.7399	1.159403762	-1.186926298						
THER.6	98.1	97.3	102.3	98.3	99	2.26569	1.13284	100.133	97.8672	1.131340125	-1.157531358						
THER.7	102.3	101.3	98.6	99	100.3	1.99081	0.99541	101.295	99.3046	0.982676464	-1.002376704						
THER.8	101.1	99.1	98.2	99.3	99.425	1.55107	0.77554	100.201	98.6495	0.773985318	-0.786154763						
THER.9	98.1	97.3	102.3	98.3	99	2.26569	1.13284	100.133	97.8672	1.131340125	-1.157531358						
THER.10	101.5	99.1	98.4	97.5	99.125	1.98389	0.99195	100.117	98.1331	0.990788045	-1.010818176						
THER.11	100.8	101.8	97.5	97.9	99.5	2.05508	1.02754	100.528	98.4725	1.02214531	-1.043477012						
THER.12	101.3	97.8	101.5	97.5	99.525	2.09583	1.04791	100.573	98.4771	1.04194514	-1.064120238						
THER.13	102.1	98.3	97.4	98.3	99.025	2.71278	1.35639	100.381	97.6686	1.351235735	-1.38876676						
THER.14	98.3	101.3	98.3	101.6	99.875	1.77694	0.88847	100.763	98.9855	0.881736012	-0.897564307						
THER.15	101.3	98.3	97.1	98.1	98.7	2.32666	1.16333	99.8633	97.5367	1.164920672	-1.192708897						
THER.16	101.6	98.3	98.3	99.5	99.425	1.99937	0.99969	100.425	98.4253	0.995459858	-1.015681256						
THER.17	98.3	101.3	98.3	101.6	99.875	1.77694	0.88847	100.763	98.9855	0.881736012	-0.897564307						
THER.18	102.1	98.3	97.4	98.3	99.025	2.71278	1.35639	100.381	97.6686	1.351235735	-1.38876676						
THER.19	101.6	98.3	98.3	99.5	99.425	1.99937	0.99969	100.425	98.4253	0.995459858	-1.015681256						
THER.20	102.1	98.3	97.4	98.3	99.025	2.71278	1.35639	100.381	97.6686	1.351235735	-1.38876676						
THER.21	101.1	99.1	98.2	99.3	99.425	1.55107	0.77554	100.201	98.6495	0.773985318	-0.786154763						
THER.22	101.5	99.1	98.4	97.5	99.125	1.98389	0.99195	100.117	98.1331	0.990788045	-1.010818176						
THER.23	101.5	99.1	98.4	97.5	99.125	1.98389	0.99195	100.117	98.1331	0.990788045	-1.010818176						
THER.24	101.6	97.8	98.3	97.9	98.9	2.3202	1.1601	100.06	97.7399	1.159403762	-1.186926298						
THER.25	98.1	97.3	102.3	98.3	99	2.26569	1.13284	100.133	97.8672	1.131340125	-1.157531358						
THER.26	102.3	101.3	98.6	99	100.3	1.99081	0.99541	101.295	99.3046	0.982676464	-1.002376704						
THER.27	101.3	98.3	97.1	98.1	98.7	2.32666	1.16333	99.8633	97.5367	1.164920672	-1.192708897						
THER.28	102.1	98.3	97.4	98.3	99.025	2.71278	1.35639	100.381	97.6686	1.351235735	-1.38876676						

## Appendix-D

### Published Papers

  
**Journal of Engineering and Applied Sciences**  
Scopus coverage years: from 2009 to Present  
Publisher: Medwell Journals  
ISSN: 1816-949X E-ISSN: 1818-7803  
Subject area: Engineering  
[View all documents >](#) [Set document alert](#) [Journal Homepage](#)



  
**Web Page Alert**  
2018  
0.35  
2017  
0.145  
2016  
0.555

<http://www.scimagoir.com/journalsearch.php?c=21100231100&tip=sid&clean=0>  
<https://www.medwelljournals.com/journalhome.php?jid=1816-949x>

August 17, 2018

**Dear Author(s)**

**Dr./Mr(s). Mohammed W. Aljibory/ University of Kerbala /Iraq**  
**Dr./Mr(s). Hafidh HassanAl-Ghazali/ University of kufa /Iraq**  
**Dr./Mr(s). Taher Habeeb Alkharasani/ University of Kerbala /Iraq**

Based on reviewer's recommendations, I am delighted to inform you that your following manuscript (Medwell ALKAIM WQ4) has been accepted for the publication in (Journal of Engineering and Applied Sciences ISSN: 1816-949X).

**Title:** Experimental investigation the effect of fluidize bed concentration on heat pipe performance

Received on: July 14, 2018  
Accepted on: August 17, 2018  
Plagiarism %: 9 %  
Date of publication: Vol:14 (No.03-04) to get release in February 2019.

Thank you very much for submitting your article to "Journal of Engineering and Applied Sciences"

International Editorial Board  
Dr. Ayad Alkaim

Thanks,  
Regards  
International Editorial Board  
Dr. Ayad Alkaim  
Babylon University/ College of science for women  
Please do not hesitate to contact me for further information  
[alkaimayad@gmail.com](mailto:alkaimayad@gmail.com)  
Mobil and Viber: 00964-7801324986  
Whats App: 00964-7801324986

.....

BABYLON INTERNATIONAL CONFERENCE FOR ENGINEERING AND  
INFORMATION TECHNOLOGY (BICEIT2018)



Notification of Acceptance of the BICEIT2018



October 11-12, 2018

<http://www.biceit.org>

Dear Hafidh Hassan Al-Ghazali, Mohammed Wahhab. Aljbory and Taher Habeeb Alkharasani,

Paper ID: 44

Paper Title: Numerical and experimental study the effect of solid partides flow on heat pipe performance

**Congratulations!** The review processes for **Babylon International Conference for Engineering and Information Technology (BICEIT2018)** have been completed. We are pleased to inform you that your paper identified above has been accepted for publication and oral presentation. You are cordially invited to present the paper orally at **BICEIT2018** to be held on, October 11-12, 2018. All accepted papers will be published in **Scopus** index **International Journal of Engineering and Technology (UAE)**, ISSN: 2227-524X.

The Conference Program will be available at the website in <http://www.biceit.org>.

Finally, we would like to further extend our congratulations to you and we are looking forward to meeting you at the conference activities.

Yours sincerely,

**The Conference Scientific Committee**

<http://www.biceit.org>



## الخلاصة

في هذا البحث، تم إجراء دراسة عملية وعددية لتحسين قيم معامل أداء الأنبوب الحراري باستخدام الطبقة المتميعة. استخدم دقائق الغبار المتطاير من مدخنة معمل الأسمنت كجزيئات متميعة حيث سخنت لمحاكاة مدخنة المعمل، الهواء الداخل الى النموذج الذي تم صنعه. سخن بواسطة مسخن كهربائي، وكانت سرعة الهواء الداخل للنموذج  $(0.8739, 1.1236, \text{ and } 1.377) \text{ m/s}$  وتم وضع غبار الأسمنت في جزء المبخر بأرتفاعات مختلفة  $(2.5, 5, 7.5 \text{ and } 10) \text{ cm}$ .

الجانب العملي تضمن إنشاء منظومة اختبار تحتوي على اجهزه قياس ومعدات ضروريه لحساب مقدار التحسين بقيمه الكسب الحراري، ومن أجزاء المنظومه (مقياس سرعة لجريان، متحسسات الحرارة، صمامات، مانوميتر، أنابيب حرارية، صندوق خشبي، أنابيب توصيل الهواء وعازل الجزيئات)، جزء تصنيع الانابيب الحراريه شمل اختيار انابيب من النحاس بقطر خارجي  $22.22 \text{ mm}$  وداخلي  $19.8 \text{ mm}$ ، وضعت داخل كل انبوب 5 طبقات من ستنلس ستيل، وأستخدم الماء المقطر كمائع تشغيل بمقادير  $65.5 \text{ ml}$  لكل انبوب.

أجريت الاختبارات ضمن مدى عدد رينولدز  $(Re = 2400 - 318728)$  وبسرعه هواء متجانسه، كما وشملت الدراسة العملية تحضير الجزيئات ودراسه خواصها مختبريا مثل (الكثافه، الموصليه الحراريه، قطر الجزيئات)، كما وتم حساب معدل الجريان ودرجه حراره سطح الانبوب الحراري وأنخفاض الضغط لكل حاله.

أستخدم برنامج  $(18.0)$ -ANSYS FLUENT bundle لحل المعادلات التفاضليه الحاكمه عند البعدين وعند الابعاد الثلاث لدراسة تأثير الجزيئات على تحسين انتقال الحراره وكذلك دراسة تصرفها بالحيز، وبينت النتائج ان اكبر قيمه لعدد نسلت  $(35.2)$  تم الحصول عليها في جزء المبخر عند الانبوب الحراري (1) وعند أرتفاع جزيئات  $10 \text{ cm}$  وعند سرعه هواء  $1.337 \text{ m/s}$  ( $Re = 318728$ )، كما وبينت النتائج ان زياده عدد رينولدز من  $2400$  الى  $318728$  يزيد الكسب الحراري للأنبوب الحراري بجزء المبخر بمقدار  $72.5\%$ ، ومن خلال إجراء المقارنه بين النتائج العمليه والنظريه لعدد نسلت لوحظ تطابق مقبول بين النتائج وبأقل وأعلى نسبه أختلاف  $(4, 18.6)$  % على التوالي.



جمهورية العراق  
وزارة التعليم العالي والبحث العلمي  
جامعة كربلاء - كلية الهندسة  
قسم الهندسة الميكانيكية

## دراسة تأثير الجريان المتميع (غاز - صلب ) على أداء الانبوب الحراري

رسالة مقدمة الى كلية الهندسة - جامعة كربلاء كجزء من  
متطلبات نيل درجة ماجستير علوم في الهندسة الميكانيكية

من قبل

ظاهر حبيب حسين

(بكالوريوس هندسة ميكانيك 1997 )

بأشراف

أ.م.د. محمد وهاب كاظم الجبوري

أ.م.د.حافظ حسن محمد الغزالي